STUDY OF TRACE GASES IN THE TROPICAL REGION

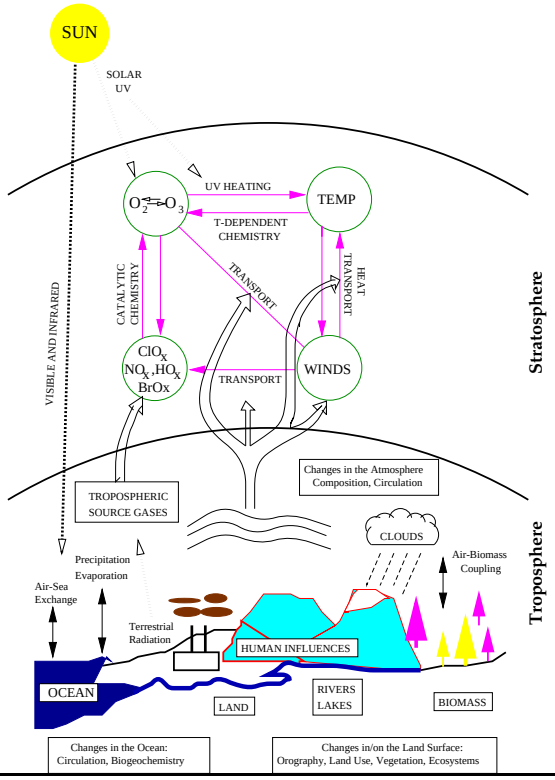

Prabir kumar Patra

STUDY OF TRACE GASES IN THE TROPICAL REGION

Prabir kumar Patra

Ph. D. Thesis
August 1997

PHYSICAL RESEARCH LABORATORY,
AHMEDABAD 380 009
INDIA

STUDY OF TRACE GASES IN THE TROPICAL REGION

A Thesis Submitted
To
Gujarat University
For
The Degree of Doctor of Philosophy
In Physics

by
PRABIR KUMAR PATRA

PHYSICAL RESEARCH LABORATORY
AHMEDABAD 380 009
INDIA

August 1997

CERTIFICATE

I hereby declare that the work presented in this thesis is original and has not formed basis for the award of any degree or diploma by any University or Institution.

Prabir K. Patra
(Author)

Certified by:

Dr. Shyam Lal
(Thesis Supervisor)
Physical Research Laboratory
Ahmedabad 380 009, India

You have spread out the heavens like a tent
and built your home on the waters above.
You use the clouds as your chariot
and ride on the wings of the wind.
You use the winds as your messengers
and flashes of lightning as your servants.

PSALM 104, vv. 2-4 (*Good News Bible)*

Dedicated
to
my parents

Contents

Acknowledgements

I would like to express my deepest gratitude and thanks to Dr. Shyam Lal for his meticulous guidance, his enormous enthusiasm and his endless encouragement shown during the whole period of work. His friendly attitude has always kept me lively at work.

I extend my grateful acknowledgements to Prof. B.H. Subbaraya who has shown deep interest in my work and provided time from his busy schedule for valuable advice. He has thus become a mentor and friend in the course of this work. I am indebted to Mr. Y.B. Achyara for his support throughout the balloon experiments; from fabrication of the mechanical and electronic modules of the cyrosampler payload to the launch. His cheerful presence and aesthetic sense of living have always motivated me.

I am extremely fortunate to have the assistance of Mr. S. Venkataramani and Mr. T.K. Sunil at PRL and during the field measurements, at Hyderabad and in the Arabian Sea with a fantastic team spirit. Mrs. S. Desai has been helpful in preliminary data analysis. Manish, one of my close associates, has helped me at every step during my stay at PRL. I thank them all for maintaining a healthy working atmosphere, and for fruitful and stimulating discussions.

I would like to express my sincere thanks to Dr. A. Jayaraman, Dr. D.K. Chakrabarty, Prof. S.K. Bhattacharya, Prof. H. Chandra, and Prof. R. Sridharan. Their comments have always been helpful at various stages of my work.

The thesis comprises of work supported by several fellow members from various institutions in a number of ways, to whom I am extremely grateful: Mr. M.N. Joshi, Mr. S. Sreenivasan, Mr. Surpali and the team members at balloon facility, Hyderabad for rendering help in successful balloon launches; Mr. P. Rajaratnam and Mr. G.N. Dutta (ISRO-HQ, Bangalore) for their relentless efforts during balloon expeditions; Dr. R. Borchers and Dr. J. Harnisch (MPAE, Lindau), and Prof. P. Fabian (now at Universitat Munchen, Freising Weihenstephan) for providing the vertical profiles obtained from Hyderabad in 1987 and 1990 and GAP/France both published and unpublished data; Prof. P.J. Crutzen and Dr. C. Brühl (MPIC, Mainz) for permitting some of us to use the MPIC 2D chemistry transport model; Dr. C.H. Jackman (GSFC/NASA, Maryland) has been prompt to give his 2D

model results and other relevant information as and when required; Dr. M. Maiss (now at MPIC, Mainz) and his colleagues at University of Heidelberg were very helpful in making absolute calibration of "*PRL* working standards" for SF_6. Discussions with all of them have provided a great insight into this work and have improved my understanding of this field to a great extent.

I appreciate the support and enthusiasm exhibited by Dr. M.M. Sarin and Prof. S. Krishnaswami to take up the project on oceanic studies under JGOFS (India) programme and for useful discussions. I thank Mr. Manish Dixit for his help in analysis during the cruises. I have also enjoyed the company and discussions with several people from NIO during the JGOFS expeditions to the Arabian Sea: Dr. M. Dileep kumar (also have taught me marine biogeochemistry), Dr. S. Prasanna Kumar, Dr. M. Madhupratap, Dr. S.W.A. Naqvi, to name a few. I sincerely thank all the participants (particularly Mangesh Gauns, V.V.S.S Sarma) captains and crew members of all the JGOFS cruises for their variety of help on board.

Various facilities of PRL have been extensively utilized during my work. I am thankful to all of them, particularly the liquid nitrogen plant, mechanical workshop, glass blowing facility, photography and documentation etc. It is also a pleasure to acknowledge the support of the Library staff members and people associated with the computer center.

I express my heartiest regards and love to my sisters (khuku and Rinku), brothers (Harihar, Sudhamay, and Tapan) and other family members for their encouragements and supports provided throughout my life. I sincerely thank them all for simply being there and being themselves. I can only name a few of my PRL friends here: Devashis, Joyti, Poulose, Raju, Ramachandran (also for critically going through an initial draft of my thesis), Ratan, Ravibhushan, Santhanam, Shikha, Sivakumaran, Tarun, however, I acknowledge the company of all other prlites for making these years of staying in PRL a wonderful experience.

Abstract

It is only a few decades since we realized that the minor constituents play significant role in characterizing the chemical, dynamical, and radiative behaviour of the Earth's atmosphere. The minor constituents, fairly well mixed in the troposphere, are transported to the global stratosphere mainly by the strong upwelling through the tropical tropopause. In addition, due to availability of intense solar radiation resulting in larger abundances of reactive radicals, like O^1D and OH, the tropical region offers many interesting phenomena to study. The tropical region is also recognized to have largest interaction during the troposphere-stratosphere exchange. However, the measurements of trace gases involved in these atmospheric processes are scarce in the tropical region. Therefore, to study the vertical distributions of trace gases in the troposphere and stratosphere, a cryogenic air sampler has been developed indigenously and successfully flight tested using high altitude balloon on April 16, 1994 from the national balloon launch facility at Hyderabad (17.5^0N, 78.6^0E). Fourteen air samples were collected in the 8-37 km altitude range during the ascent as well as descent of the balloon.

This thesis presents a study of several trace gases which play important role in ozone chemistry particularly in the stratosphere, and greenhouse warming of the Earth's surface. Their vertical profiles are also used to study various atmospheric processes. The thesis consists of six chapters:

- A brief description of the Earth's atmosphere and its various processes (chemical, radiative, and dynamical) controlled by the minor constituents, particularly in the troposphere and the stratosphere, influencing the climate near the ground is given in **Chapter 1** (Introduction).
- The study begins (**Chapter 2**) with a brief description of the techniques, *in situ* as well as remote, used for measuring the vertical distributions of the minor constituents in the lower atmosphere. The average tropospheric concentrations of individual species measured over a period of time have been used to estimate their tropospheric growth rates. The distributions of the long-lived gases are compared with those measured earlier on March 27, 1987 and April 9, 1990 from the same site and using similar techniques, jointly with MPAE. These measurements are compared with the MPIC 2D model results to identify normal/disturbed stratospheric conditions.

- **Chapter 3** discusses various dynamical parameters which are related to the distribution of trace gases such as 1) vertical eddy diffusivity, responsible for the upward transport of trace gases, deduced from the distributions of N_2O and CFC-12 and its variations in the stratosphere. 2) 'Age', a parameter which is a diagnostic of stratospheric transport time, using the vertical distributions of long-lived species (SF_6), bearing imprints of atmospheric dynamics. 3) Stratospheric mixing processes which can disturb the vertical profiles from their normal behaviour using the "age" distributions and correlations of simultaneous measurements of trace gases.
- Source gases for the ozone depleting radicals are inert in the troposphere, and ozone is vulnerable to the catalytic loss processes due to halogens produced during dissociation of these gases by the solar UV radiation and chemical reactions in the stratosphere. It is, therefore, necessary to estimate the reactive and unreactive components of the halogen containing gases. **Chapter 4,** comprises of information on the vertical distributions of halocarbons and estimated "age" of air which have been calculated using SF_6 vertical distributions to compute the chlorine and bromine loadings into the stratosphere and their subsequent stratospheric partitioning into organic and inorganic forms.
- Atmospheric budgets (balancing source and sinks) of solely man-made constituents are fairly well estimated, whereas, due to large uncertainty in estimating the sources and sinks of biogenic gases, their accurate assessments still remain poor. **Chapter 5** presents a discussion on the natural sources of two important biogenic gases (N_2O and CH_4) from the Arabian Sea which acts as a natural chimney for some of these gases due to its unique biogeochemistry leading to their larger *in situ* production and the circulation pattern which brings the water, rich in dissolved gases, from the sub-surface layers to the air-sea interface.
- **Chapter 6** summarizes these results and discusses the future scope in this field of atmospheric research.

Acronyms and Abbreviations

AASE	Airborne Arctic Stratospheric Expeditions
ALE	Atmospheric Lifetime Experiment
CFC	Chlorofluorocarbon
ClO_x	ClO + 2[Cl_2O_2] + Cl + 2[Cl_2] + HOCl + $ClONO_2$
Cl_x	ClO_x + HCl
CMDL	Climate Monitoring and Diagnostics Laboratory
CTM	Chemistry-Transport Model
GC	Gas Chromatography
GAGE	Global Atmospheric Gases Experiment
GBP	Geosphere Biosphere Programme
GSFC	Goddard Space Flight Center (Maryland, USA)
HCFC	Hydrochlorofluorocarbon
IPCC	Intergovernmental Panel on Climate Change
ISRO	Indian Space Research Organisation (Bangalore, India)
JGOFS	Joint Global Ocean Flux Study
MPAE	Max Planck Institüt für Aeronomie (Lindau, Germany)
MPIC	Max Planck Institüt für Chemie (Mainz, Germany)
MST	Mesosphere-Stratosphere-Troposphere (radar)
NCAR	National Centre for Atmospheric Research (Boulder, USA)
NOAA	National Oceanic and Atmospheric Administration (Boulder, USA)
NO_x	NO + NO_2
PRL	Physical Research Laboratory (Ahmedabad, India)
STE	Troposphere-Stratosphere Exchange
UNEP	UN Environment Programme
UV	Ultra violet
UV-B	Ultra violet-B radiation (ca. 280 to 310 nm)
VMR	Volume Mixing Ratio
WMO	World Meteorological Organisation (UN)

Chapter 1

Introduction

The composition of the present Earth's atmosphere has evolved over the years under the influence of various natural and anthropogenical processes which are relatively well understood near the ground. It is incessantly dynamic and active, and still maintains a fairly steady state. The constituents of the atmosphere can be divided in the following categories (Table 1.1): 1) major constituents of fairly constant abundances, mainly nitrogen (N_2), oxygen (O_2), and argon (Ar); together constitute more than 99.96% of the total atmospheric gases. 2) remaining trace amount of gases, often referred to as minor constituents, of variable concentrations with respect to time and space which will be the main focus of this thesis. 3) there also exists solid and liquid particles with largest space-time variation, such as aerosols, water droplets etc. The altitude region from surface to about 100 km, where the distributions of permanent gases are in nearly uniform proportion, is known as *homosphere,* and the region above it is called as *heterosphere* due to rapid change in their distributions with increasing altitude. However, it is also important to note that the mixing and transport of these constituents are mainly controlled by random movements and turbulent mixing by large eddies below about 100 km and the atmosphere attains the convective equilibrium. Above this region these processes are dominantly associated with molecular diffusion, each molecular species achieves a distribution defined by its own scale height. These two regions are separated by an ill-defined boundary, called *turbopause.*

Table 1.1: *Composition of the terrestrial atmosphere*[a].

Major constituents		Minor/trace constituents (contd.)	
Constituent	% by volume	Constituent	% by volume
nitrogen (N_2)	78.084	methane (CH_4)	1.5×10^{-4}
oxygen (O_2)	20.948	nitrous oxide (N_2O)	0.27×10^{-4}
argon (Ar)	0.934	carbon monoxide (CO)	0.19×10^{-4}
Minor/trace constituents		water vapor (H_2O)	$\leq$0.04
carbon dioxide (CO_2)	0.033	ozone (O_3)	$\leq 12 \times 10^{-4}$
neon (Ne)	18.18×10^{-4}	sulfur dioxide (SO_2)[b]	0.001×10^{-4}
helium (He)	5.24×10^{-4}	nitrogen oxides (NO_x)[b]	0.001×10^{-4}
krypton (Kr)	1.14×10^{-4}	ammonia (NH_3)[b]	0.004×10^{-4}
xenon (Xe)	0.089×10^{-4}	cloud and precipitation	$\leq$0.01
hydrogen (H_2)	0.5×10^{-4}	aerosol[b]	$\leq 10^{-7}$

[a] After US Standard atmosphere 1976.

[b] concentrations near the Earth's surface.

1.1 Mean Structure of the Atmosphere

On the basis of the vertical temperature structure of the atmosphere, it is again described in a series of *layers (Figure 1.1).* These *layers,* surrounding the Earth's surface, are represented by *spheres*, viz. the *troposphere, stratosphere, mesosphere, thermosphere, exosphere,* separated by well defined boundaries (*pause*) - the *tropopause, stratopause, mesopause,* and *thermopause,* respectively. Inside a *sphere* the temperature gradient with respect to height remains fairly constant and at the *pause* the temperature gradient appears to cease. The *troposphere* is characterized by a negative temperature gradient with increasing altitude at a typical lapse rate of 6.5^0K/km between ground and the tropopause. The *tropopause* height and temperature varies with latitude, season, and meteorological conditions, and in the tropical region its temperature is typically less than 200^0K at around 17 km. In the layer on its top, the *stratosphere,* temperature increases with increasing height to a maximum value of about 270^0K at the level of *stratopause* ($\sim$50 km). These two layers play key roles in determining weather and climate of the lower atmosphere, and have largest direct influence on the life on Earth. Above the *stratopause,* temperature decreases again with respect to height like in the *troposphere.* The *mesosphere* lies between the stratopause the *mesopause* attaining a minimum temperature of about 180^0K. In the *thermosphere* temperature increases with increasing altitude up to about 250 km, attaining a temperature in the range of 500^0K to 2000^0K (not shown in Figure

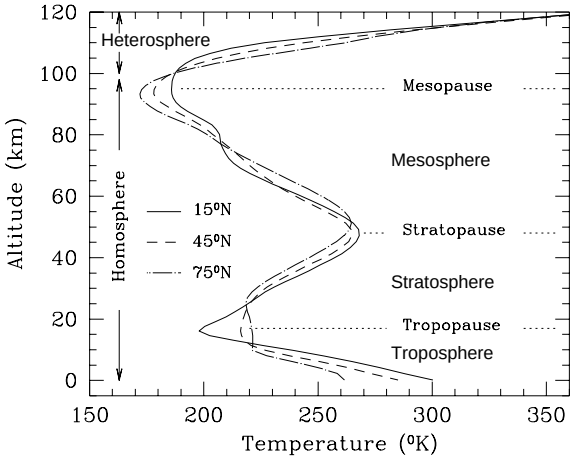

Figure 1.1: *Vertical temperature structure of the Earth's atmosphere (COSPAR International Reference Atmosphere 1986) showing various 'spheres' and average positions of the 'pauses' at three latitudes representing tropical (15^0), midlatitude (45^0), and polar (75^0) regions.*

1.1). The outermost region of our atmosphere, extends up to the interplanetary medium, known as *exosphere.* In this thesis, we will deal mainly with the stratospheric system, and to some extent with the tropospheric forcings through ocean-atmosphere interaction.

1.2 Minor constituents in the Earth's atmosphere

Ozone (O_3), one of the most important minor constituents, absorbs the biologically harmful incoming solar ultraviolet (UV) radiation and plays a pivotal role in setting up the thermal structure of the atmosphere through the heating/cooling balance, particularly in the stratosphere and mesosphere. However, other minor species are important in regard to perturbing the photochemical behaviour of the stratosphere and radiative equilibrium of the troposphere. Atmospheric distributions of some of these gases and their role mainly in the troposphere and the stratosphere are discussed in the following sections.

1.2.1 Ozone

Bulk of its amount is present in the stratosphere (∼90% of the total atmospheric O_3[1]) forming a concentration peak at about 27 km in the tropics [*Subbaraya,* 1987] which lowers at higher latitudes as shown in Figure 1.2. Its peak altitude is located at ∼20 km in the polar region. Ozone is pro-

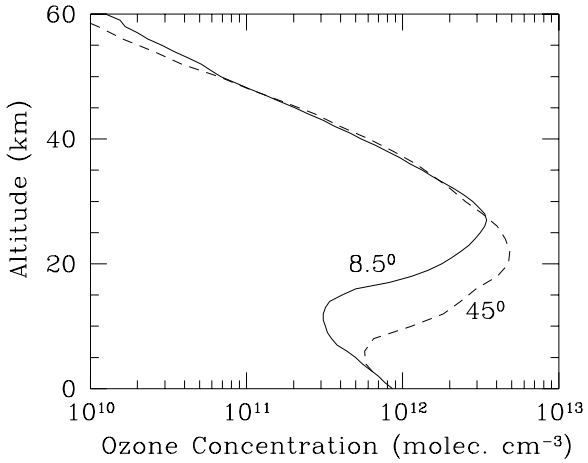

Figure 1.2: *Vertical distributions of O_3: Reference profile for the tropics (8.5^0) [Subbaraya, 1987] and midlatitudes (45^0) [Krueger and Minzner, 1976]. Total ozone amount calculated from the tropical profile is 270 DU and from the midlatitude profiles is 345 DU. The total ozone amount can be as high as 460 DU in the high latitude spring.*

duced mainly in the tropical upper stratosphere through the pure oxygen photochemistry, i.e. by combining an oxygen molecule with an oxygen atom, released by the photolysis of O_2 by UV radiation.

$$\begin{aligned} O_2 + h\nu &\overset{\lambda \leq 242.4nm}{\longrightarrow} O + O \\ O_2 + O + M &\longrightarrow O_3 + M \end{aligned} \tag{1.1}$$

where $h\nu$ represents a photon, and M is any air molecule. The balance of its atmospheric abundances is primarily maintained by the following loss processes involving pure oxygen photochemistry [*Chapman,* 1930]:

$$O_3 + h\nu \overset{\lambda \leq 1100nm}{\longrightarrow} O_2 + O$$

[1]The term "total ozone" is defined as the amount of ozone molecules per unit area integrated over the air column. 1 DU (Dobson units) = 10^{-3} atm cm.

$$\begin{aligned} O_3 + O &\longrightarrow 2O_2 \\ O + O &\longrightarrow O_2 \end{aligned} \tag{1.2}$$

It was recognized later, from a preliminary analysis of photochemical equilibrium conditions for the upper stratosphere and the measurements of ozone vertical profiles from series of rocket soundings, that these destruction mechanisms for a pure oxygen atmosphere alone cannot lead to adequate ozone destruction for maintaining a steady state ozone concentration and also to explain the observed ozone distributions in the stratosphere, respectively [*Nicolet,* 1975]. Distribution of atmospheric ozone is dominated by photochemistry in the middle stratosphere and above (shorter photochemical lifetime), whereas its distribution is largely determined by transport in the lower and polar stratosphere, and in the upper troposphere (longer photochemical lifetime), causing the inter-hemispheric or seasonal differences and also explains the latitudinal anomaly in the measured total ozone distribution. Despite the fact that the production rate of O_3 is largest in the tropics, anomalously high columnar ozone is measured towards the poles during late spring in the normal atmospheric condition (without the influence of catalytic halogen chemistry). These features are caused by the transport of ozone by the stratospheric meridional circulation from the tropics to mid- and high latitudes with higher intensity in the winter hemisphere.

1.2.2 Other minor constituents

Most of the other trace gases that are chemically and radiatively active in the atmosphere, especially playing deleterious roles such as ozone depletion and global warming are solely forced from the troposphere. Trace gases, such as chlorofluorocarbons (CFCs), brominated compounds, nitrous oxide (N_2O) etc. are released at the Earth's surface. These gases are sparingly soluble in water and have insignificant photochemical loss in the troposphere. Due to sufficiently long atmospheric lifetimes, large fraction of these gases reach the stratosphere where they are dissociated in the presence of solar UV radiation and chemical reactions leading to production of ozone depleting radicals. For example, CFCs, brominated compounds, N_2O produce chlorine (Cl), bromine (Br), nitric oxide (NO), respectively, which take part in the catalytic O_3 destruction. The radiative forcing of the troposphere is mainly controlled by carbon dioxide (CO_2), water vapour (H_2O), methane (CH_4), O_3, N_2O, halocarbons (includes all the gases containing at least one of the halogen species

F, Cl, Br, or I) etc. Another group of species which are particularly short-lived by the virtue of their high reactivity, involved in regulating the life-time and transportation of many trace species from the troposphere to the stratosphere, e.g., hydroxyl radicals (OH) being one of the most important constituents which play a key role in removing many of the harmful species (sometimes it is also called as *detergent* of the atmosphere). These gases, in addition, actively participate in the tropospheric O_3 production chemistry such as carbon monoxide (CO), nitrogen oxides (NO_x), non-methane hydro-carbons (NMHCs) etc. [*Crutzen,* 1988]. The discussion on this group of species is beyond the scope of this thesis. Also the chemistry of tropospheric ozone, in itself, is a separate topic of research.

1.3 Role of Minor Constituents

In the homosphere, permanent gases (mainly N_2 and O_2) are chemically rather inert, and their concentrations neither alter significantly with time nor play any considerable role in the climatic processes. On the contrary, minor constituents in the Earth's atmosphere play important roles in controlling various chemical, dynamical and radiative processes, particularly in the tro-posphere and stratosphere. Due to their well defined photolysis rates and distinguished chemical properties, distributions of these trace species have been exploited to characterize many chemical and dynamical atmospheric processes [see for extensive review *Brasseur and Solomon,* 1986; *Andrews et al.,* 1987].

1.3.1 Chemistry of the stratospheric ozone

It is now established that the thickness of columnar ozone in the atmosphere is reducing due to various anthropogenical activities on the Earth's surface [*World Meteorological Organization* (WMO), 1995]. The extent of ozone loss varies significantly with latitude and the seasons - largest loss can be found in the polar region during the spring. It is now more than a decade since the large depletion of ozone was first discovered in the Antarctic region [*Farman et al.,* 1985]. Such depletions of ozone are attributed to the coupled chemical, dynamical, and radiative processes based on the knowledge gathered from numerous measurement programmes, remote as well as *in situ,* conducted in the Antarctic and Arctic regions. With the help of this understanding, depletion of ozone at different latitudes have also been simulated using two

and three dimensional coupled models by a few groups. In the stratosphere, where the ozone layer is formed, O_3 is found to be destroyed mainly through the following catalytic reactions

$$\begin{aligned} O_3 + X &\rightarrow XO + O_2 \\ XO + O &\rightarrow X + O_2 \\ \hline net: O_3 + O &\rightarrow X + 2O_2 \end{aligned} \tag{1.3}$$

where X ≡ H, OH, NO, Cl, Br, I etc. Such a catalytic cycle involving H and *odd oxygen* (O and/or O_3) is the most efficient destruction mechanism above about 50 km [*Bates and Nicolet,* 1950]. The chain reaction involving OH and O_3 was first introduced by *McGrath and Norrish* [1958]. The depletion of odd oxygen due to catalytic cycle of NO is one of the main mechanisms through which ozone is destroyed in the stratosphere, particularly in the altitude region of 35-45 km [*Crutzen,* 1970]. The depletion of stratospheric ozone can also be influenced by Cl radicals [*Stolarski and Cicerone,* 1974] and can play a significant role in net columnar ozone loss in the presence of enhanced supply of its source gases from the troposphere [*Molina and Rowland,* 1974]. Other catalytic cycle that involves Br [*Wofsy et al.,* 1975] are most efficient in ozone destruction, particularly in the lower stratosphere [*Wennberg et al.,* 1994] and in tropospheric polluted air mass [*Sander and Crutzen,* 1996]. More recently, *Solomon et al.* [1994] have indicated much larger ozone depletion efficiency of I radicals; about 1000 times greater compared to Cl if released in 15-20 km height range. Introduction of the chain reactions by the former two radicals (H and OH) were found necessary to explain partly the observed vertical profiles of ozone, however, ozone destructions due to later three radicals (namely NO, Cl, and Br) were envisaged mainly to study the impact of human activities on the ozone layer. Sources of the reactive radicals, e.g., OH, NO, Cl, Br in the stratosphere are primarily due to the reactions of H_2O, and N_2O with O^1D and photolysis of chlorocarbons, and bromocarbons by UV radiation, respectively. These gases are commonly referred to as *source gases.*

However, explanation of the larger ozone loss in the midlatitude lower stratosphere required introduction of additional loss process through the synergistic reactions of chlorine, bromine, and hydroxyl radicals which can be represented as:

$$\begin{aligned} Z + O_3 &\rightarrow ZO + O_2 \\ OH + O_3 &\rightarrow HO_2 + O_2 \end{aligned}$$

$$\begin{aligned} HO_2 + ZO &\rightarrow HOZ + O_2 \\ HOZ + h\nu &\rightarrow OH + Z \\ \hline net: 2O_3 &\rightarrow 3O_2 \end{aligned} \tag{1.4}$$

where Z ≡ Cl and Br. In spite of very low abundance of bromine radicals compared to that of chlorine in the atmosphere the relative importance of this cycle in destroying ozone due to Cl and Br are nearly the same [*Wennberg et al.,* 1994]. The combined effect of chlorine and bromine in ozone depletion is more significant in absence of oxygen atom, particularly during the polar winter (dark) and spring (twilight) through the cycle [*McElroy et al.,* 1986; *Solomon,* 1990].

$$\begin{aligned} Cl + O_3 &\rightarrow ClO + O_2 \\ Br + O_3 &\rightarrow BrO + O_2 \\ ClO + BrO &\rightarrow Cl + Br + O_2 \\ \hline net: 2O_3 &\rightarrow 3O_2 \end{aligned} \tag{1.5}$$

Largest ozone loss has been observed in the polar stratosphere during the spring while a circumpolar vortex is formed by the polar night westerly jets in each hemisphere [*Schoeberl et al.,* 1992]. Whilst the dynamical features of the vortex are determining the chemical composition of air, temperature inside decides the amount of halogen activation. A loss of about 60-70% of total ozone during September at the South Pole is being repeatedly observed with ozone concentrations approaching near zero values in the altitude region of 14-19 km [*Hofmann,* 1996]. The severity and sustenance of this ozone hole is associated with the amount of halogen species transported to the polar stratosphere and its temperature which controls the formation of polar stratospheric clouds (PSCs), mostly composed of hydrated sulfuric acid. Role of PSCs in dehydrating and denitrifying the stratosphere, in turn, activating the reactive chlorine and bromine partitioning can be described through this reaction scheme based on *Crutzen and Arnold* [1986] and *Hanson et al.* [1994].

$$\begin{aligned} N_2O_5(g) + H_2O(s) &\rightarrow 2HNO_3(s) \\ ClONO_2(g) + H_2O(s) &\rightarrow HOCl(g) + HNO_3(s) \\ ClONO_2(g) + HCl(s) &\rightarrow Cl_2(g) + HNO_3(s) \\ HOCl(g) + HCl(s) &\rightarrow Cl_2(g) + H_2O(s) \end{aligned} \tag{1.6}$$

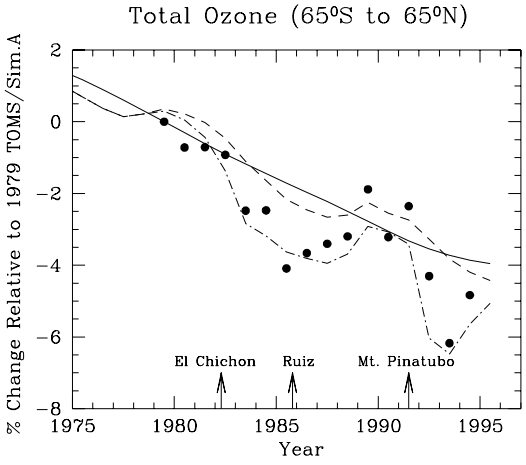

Figure 1.3: *Percentage total ozone changes in the latitude band 65^0S to 65^0N for TOMS version 7 relative to the 1979 TOMS value (•). The lines are ozone change obtained from GSFC 2D model relative to the 1979 simulation-A value; simulation-A (solid line): for chlorine and bromine increase only, simulation-B (dashed line): for chlorine and bromine increase and solar UV flux variations, and simulation-C (dash-dot line): due to chlorine and bromine increase, solar UV flux variations, and stratospheric sulfate aerosol surface area variation [see Jackman et al., 1996 for details]. The major volcanic eruptions during this period are also indicated.*

Where *s* is the solid phase and *g* represents the gas phase. This set of reactions removes nitrogen oxides and water molecules from the stratosphere and deactivate the reservoir chlorine species such as HCl, $ClONO_2$ into reactive chlorine (Cl_2, HOCl). An analogous cycle with $BrONO_2$ and HOBr has also been included in the more recent two-dimensional models.

In general a positive correlation of O_3 loss with increasing halogen abundance has been established (Figure 1.3) with certain degree of modulation by the variation in solar irradiance due to 11 year solar cycle. Increased aerosol loading into the stratosphere provides larger surface area, conducive for active heterogeneous chemistry thus leading to larger ozone loss due to major volcanic eruptions (e.g. El Chichon, Ruiz, Mount Pinatubo).

1.3.2 Radiative forcing of the trace gases in the troposphere

Most of the trace gases are important absorbers of the outgoing thermal (terrestrial) radiation, emitted by the Earth, in the troposphere. CH_4, N_2O, Halocarbons (CFCs, HCFCs, Halons etc), in particular, consist of several strong IR absorption bands in the atmospheric *window region* (8-12 μm) which is nearly unattenuated by the absorption bands of H_2O, CO_2, and O_3, which are the major contributors to the increased surface temperature of the Earth (Figure 1.4). Present estimates (assuming 1992 concentration levels of the

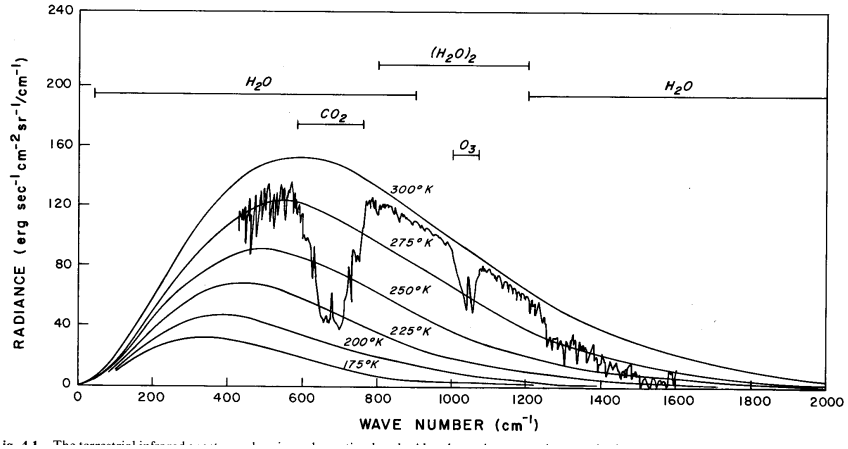

Figure 1.4: *The terrestrial infrared radiation spectrum observed by the IRIS instrument on board Nimbus 4 satellite near Guam (15.1^0N, 215.3^0W) on April 27, 1970. The black-body emission spectra at different temperatures and the absorption bands of various molecules are also shown (adapted from Liou, [1980]).*

radiatively active gases) show that while CO_2 is by far the most important of these gases, it is alarming to note that other gases which are in much lower concentrations such as CH_4, N_2O, and halocarbons play a very important role in trapping the terrestrial radiation and thereby contributing significantly to the greenhouse warming [*Intergovernmental Panel on Climate Change* (IPCC), 1996]. Increase in the Earth's surface temperature caused by these radiatively active gases is partly compensated by the negative radiative forcing by the aerosols and results in a net increase of about 0.2^0C per decade.

1.3.3 Radiative balance and dynamics of the middle atmosphere

The net heating/cooling balance in the stratosphere is controlled by heating due to absorption of solar UV radiation mainly by ozone with miniscule contribution from CO_2, O_2 and nitrogen dioxide (NO_2), and infrared (IR) radiative cooling due to CO_2, O_3 and H_2O [*London,* 1980]. The lower and middle stratosphere is approximately in radiative equilibrium and its circulation, a net upward flux acting in the tropics, is forced from below which is driven by energy generated in association with the formation of clouds and precipitation in the troposphere. The tropical tropopause is the most important region for transporting the tropospheric constituents into the stratosphere during this strong *upwelling* motion. Present understanding of various troposphere-

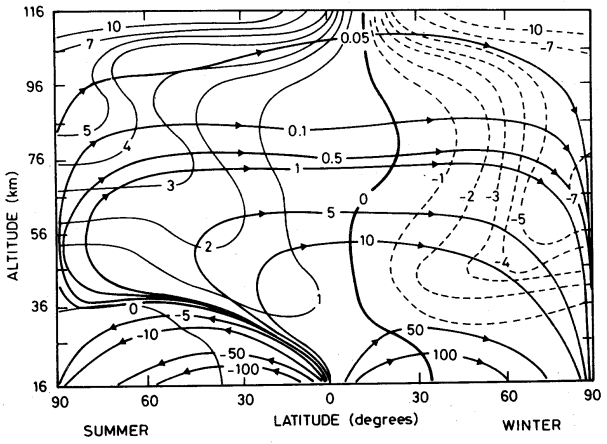

Figure 1.5: *Mean meridional circulation derived from the radiative heating and cooling balance by the minor constituents in the stratosphere [Garcia and Solomon, 1983].*

stratosphere exchange processes is discussed in *Holton et al.* [1995]. The Eulerian streamlines governed by the net adiabatic heating and cooling can be theoretically generated as shown in Figure 1.5. The upper stratosphere and mesosphere exhibit a strong radiative imbalance that results in upward transport where the net adiabatic heating is positive (in the summer pole) and downward transport in the region of net cooling (in the winter pole). This radiative imbalance also helps in maintaining a quasi-horizontal circulation from the summer to winter hemisphere in the meridional plane. It is, therefore, apparent that any change occurring in the abundances of these trace gases or deviation from their characteristic vertical profiles (ozone in

particular) will induce a large imbalance in the atmospheric radiation equilibrium/circulation system [*Ramaswamy et al.,* 1992].

1.4 Tropospheric trends and climatological importance of trace gases

In recent years, it has been observed that the increased atmospheric burden of most of these trace gases has approached a critical level due to industrialization of the human society. Although the sources of these trace gases are located near the Earth's surface and are released to the atmosphere mainly by the anthropogenical activities; biogenic gases like CO_2, N_2O, CH_4, methyl halides are also produced during natural processes. Various important role and potential utilities of the anthropogenically produced gases will be discussed in Chapters 2, 3, and 4. Among the natural sources, oceans are found to control atmospheric abundances of some of these gases which is discussed in Chapter 5.

To assess the relative importance of these trace gases and also to identify the critical abundance levels, several evaluation studies have been carried out so that precautionary measures can be undertaken to control their emissions [see for details *WMO,* 1995; *IPCC,* 1996 etc]. Two separate indices have been assigned to each gas indicating the effectiveness in ozone depletion and global warming, namely, the ozone depletion potential (ODP) and global warming potential (GWP), respectively. Both these parameters are generally proportional to the atmospheric lifetime of the gas under study and its tropospheric concentration. Various parameters of importance associated with the selected trace gases are given in Table 1.2.

1.5 Troposphere-stratosphere coupling

With the advent of various measurement techniques and theoretical modeling capabilities, the tropospheric and stratospheric regions are fairly well understood in terms of their basic characteristics. However, processes involved in the understanding of the lower atmosphere as a closely connected system, through troposphere-stratosphere coupling, are poorly known. A

Table 1.2: *Detailed information on various trace gases related to ozone depletion and global warming (compiled from WMO, 1995; IPCC, 1996; Montzka et al., 1996).*

Chemical Species		Lifetime	Concentration		Current*	RF**	ODP
Name	Formula		(ppbv)		Growth	w.r.t	w.r.t
		(Year)	pre-ind	1992	ppbv/yr	CO_2	CFC-11
Natural and anthropogenically influenced gases							
carbon dioxide	CO_2	variable	278,000	356,000	1,000	1	-
methane	CH_4	12.2	700	1714	8	20	-
nitrous oxide	N_2O	120	275	311	0.8	200	-
methyl chloride	CH_3Cl	1.5	$\sim$0.6	$\sim$0.6	0	-	0.02
methyl bromide	CH_3Br	1.2	$<$0.01	$\sim$0.01	0	-	0.64
Gases to be phased out before 2000 following the Montreal Protocol and its amendments							
carbon tetrachloride	CCl_4	42	0	0.132	-0.0005	5555	1.2
CFC-11	CCl_3F	50	0	0.268	0	12222	1
CFC-12	CCl_2F_2	102	0	0.503	0.007	15555	0.8
Halon-1301	$CBrF_3$	65	0	0.002	0.0002	15555	12
Halon-1211	$CBrClF_2$	20	0	0.003	0.00015	-	5.1
Other gases of present and future interest							
HCFC-22	$CHClF_2$	12.1	0	0.100	0.005	10555	0.04
HCFC-141b	CH_3CFCl_2	9.4	0	0.002	0.001	7777	0.10
HCFC-142b	CH_3CF_2Cl	18.4	0	0.006	0.001	10000	0.05
sulfur hexafluoride	SF_6	3200	0	0.0032	0.0002	35555	-

* rate of change in abundances from 1990 to 1992 (contd.).

** radiative forcing (RF), an index assigned to quantify the effectiveness of any gas in global warming and is defined as the net heating induced by each molecule of the gas in question relative to that provided by each CO_2 molecule.

simplified atmospheric model can be separated in two parts: 1) the stratospheric interplay of chemical, dynamical, and radiative processes dominated by the minor constituents, and 2) the tropospheric forcings into the stratosphere such as transport of the source gases mainly through the tropical tropopause and downward transport of many chemical species (e.g. O_3, NO_x) from the stratosphere during various exchange processes. These processes are schematically depicted in Figure 1.6. Many other processes interacting with various parts of the climate system, regarded as internal forcings, also include the exchange of biogenic gases from the ocean-to-atmosphere across the interface.

Any constituent (molecule, atom, ion, aerosol etc.) found in the lower atmosphere necessarily originates from the Earth's surface, either due to anthropogenical and natural processes on the land or from the ocean surface (also includes lakes and rivers) due to natural activities in the water column.

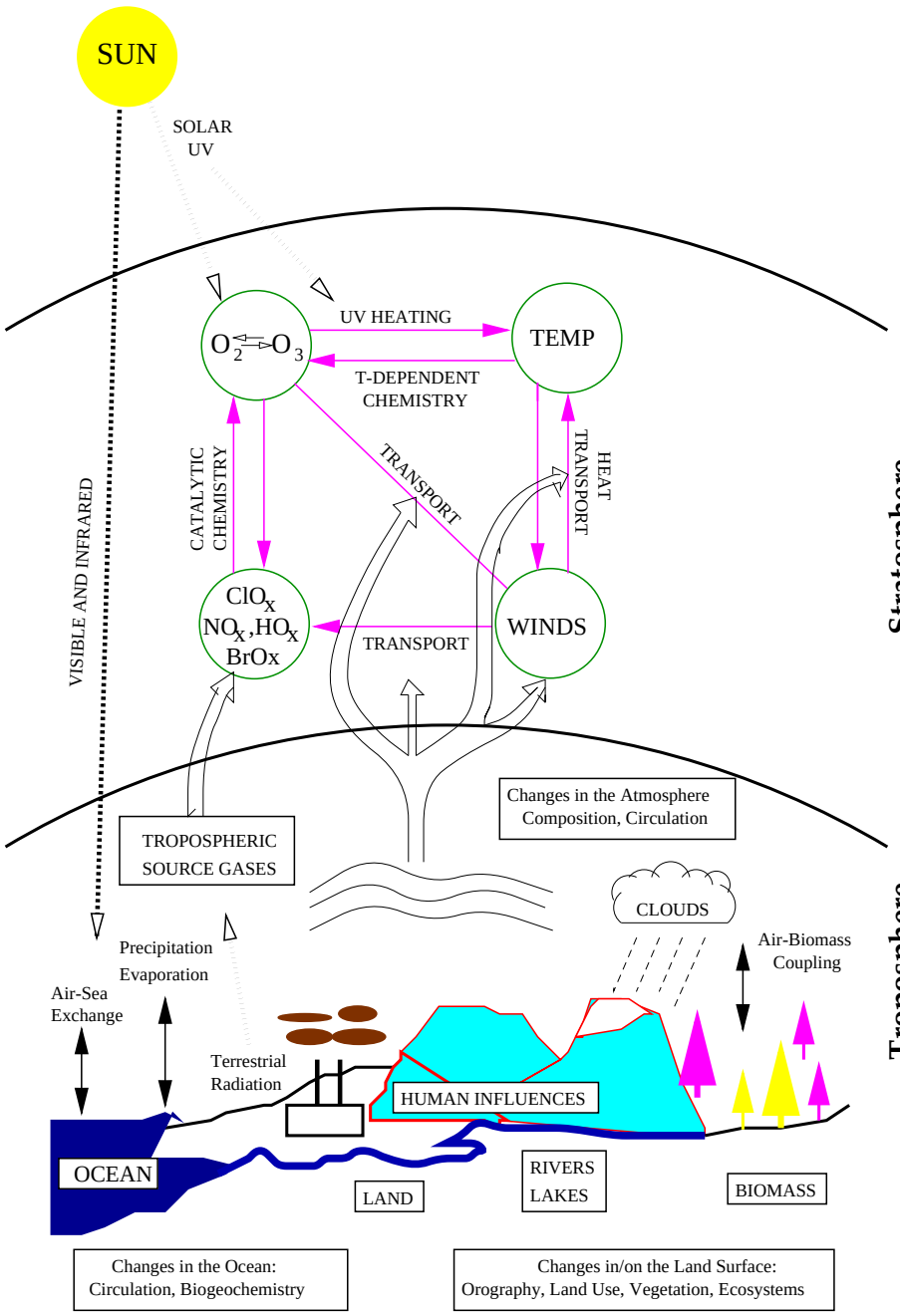

Figure 1.6: *Schematic diagram of the troposphere-stratosphere model showing the various coupling processes. Adapted from WMO [1985] and IPCC [1996] with appropriate modifications.*

Recently, the study of the influences of human activities on the oceanic biogeochemistry, especially in the coastal zone, are receiving attention.

Immediately after these constituents, gaseous or particulate, are released into the atmosphere, they participate in the chemical (e.g. tropospheric ozone, hydroxyl radicals etc.) and radiative (heating and cooling) budgets near the ground. Many of these processes are mostly localized and fairly restricted to the atmospheric boundary layer - the layer of the atmosphere that exchanges various physical parameters (mass, energy, momentum) and chemical constituents between the Earth's surface and the atmosphere through turbulent mixing (above this layer lies the free troposphere). Within a few kilometers from the ground, fate of the particulate materials is decided by scavenging due to washout, and faster coagulation/sedimentation rates. The residence time of the tropospheric aerosols is typically of the order of a week. Stratospheric aerosols, which exists in the stratified layer above the tropopause extending up to about 30 km, are formed after major volcanic eruptions and/or diffusion of sulfur bearing gases such as H_2S, COS, CS_2, SO_2 from the troposphere in a small fraction. The background stratospheric aerosol layer has about a few particles per cm^3, but immediately after major volcanic eruption their number can go beyond one order of magnitude higher [see for example *Ramachandran et al.,* 1994].

In the troposphere, atmospheric lifetime of various chemical constituents, such as methane, non-methane hydrocarbons, methyl halides, hydrogenated halocarbons are decided by the reactions mainly with OH. However, chemical constituents with atmospheric lifetime more than few months are fairly well mixed in the free troposphere due to larger convective mixing and can significantly be transported to the stratosphere, such as CH_3Br [see for example, *Lal et al.,* 1994]. Constituents with even shorter lifetime (order of days to month) such as methyl iodide (CH_3I) and dimethyl sulfide (CH_3-S-CH_3) can only be injected to the upper troposphere and lower stratosphere through the deep convective turrets (e.g. inter-tropical convergence zone, thunderclouds) from the boundary layer [*Wang et al.,* 1995]. From the above, it is clear that, these two adjacent *spheres* cannot be treated separately, in order to understand the interplay of various chemical and physical processes of the lower atmosphere.

Chapter 2

Vertical Distribution of Trace Gases

2.1 Introduction

Only limited number of techniques are available for comprehensive measurement of distributions of trace gases. For example, satellite based remote atmospheric sensors can make measurements of a few gaseous species like O_3, H_2O, CO_2, N_2O, NO_2, CH_4, CF_2Cl_2, $ClONO_2$, HCl etc. [*J. Geophys. Res., special issue on Evaluation of the UARS data, Vol. 101, No. D6,* 1996] in certain altitude ranges but with poor altitude resolution. In recent years, this technique has proved satisfactory to map the global distributions of trace species [see for example *Russell et al.,* 1993; *Roche et al.,* 1996], to determine long term trends of minor constituents such as O_3 [*Jackman et al.,* 1996 and references therein], to study the large scale atmospheric dynamical processes [*Rundell et al.,* 1993]. Vertical mixing ratio profiles for certain gases can also be deduced from the column abundances measured using space-borne and ground based IR observations [*Rinsland et al.,* 1993; *Zander et al.,* 1994]. This technique, however, is restrictively applicable to the compounds having strong and well isolated infrared absorption bands. On the other hand, employing *in situ* techniques e.g. analysis of collected ambient air samples for trace gases, resonance fluorescence for radical measurements have been more reliable and also have built the basis of validating remote observations. For example, measurements using aircraft in the lower stratosphere and troposphere have provided many crucial information about the time evolution

of the lower stratospheric chemical and physical processes [*Anderson et al.,* 1989; *Wennberg et al.,* 1994]. The balloon-borne cryosampling technique can provide adequate whole air samples for simultaneous measurements of vertical distributions of a large number of source gases in the troposphere as well as in the stratosphere (up to about 35 km). A general overview of whole air sampling techniques, widely used for tropospheric and stratospheric measurements, has been elaborated by various authors [e.g. *Lueb et al,* 1975; *Ehhalt,* 1980, *Fabian*, 1981].

Surface measurement of trace gases provides detailed information on their trends in tropospheric concentration, thereby the total atmospheric loading, which play a key role in determining the physical and chemical behaviour of the atmosphere. By virtue of the convective equilibrium (i.e. larger mixing) in the troposphere, these gases are fairly uniformly distributed in this region, but the overlying stably stratified layer (the stratosphere), which is also sometimes referred as *sphere of ignorance* due to its inaccessibility for measurement of the atmospheric parameters, exhibits extremely slow mixing across the isentropes and asymmetric horizontal circulation. Therefore, it is often difficult to assess the influence of any change in tropospheric constituents on the stratospheric processes. For example, the halocarbon measurements made at different environments in both the hemispheres on the Earth's surface are used to study the loading of halogen species (equivalent/effective equivalent) from the troposphere to the stratosphere and their probable impact on the stratospheric ozone [*Montazka et al.,* 1996]. However, this approach suffers from lack of required information on the transport time of an air parcel to travel from the troposphere to the various stratospheric altitude at any corresponding latitudes. More realistic estimations have been made for the abundances of reactive halogens in the lower stratosphere [see *Woodbridge et al.,* 1995; *Daniel et al.,* 1996] with the help of *in situ* measurements using aircrafts. Hence, the simultaneous measurement of vertical distributions of minor constituents those are established to be potential dynamical tracers and chemically active using *in situ* techniques covering more height and latitude would be extremely useful for more accurate study of such atmospheric processes. Most recent reports indicate that a number of vertical profile measurements of the trace gases are available at mid- and high latitude regions, on the other hand, measurements over tropical regions are scarce [*Fraser et al.,* 1994; *Fabian et al.,* 1996], even though tropical regions play vital role in transporting these trace gases into the global stratosphere due to the strong upwelling motions prevailing there. A programme has been initiated at PRL to study the vertical distributions of

various trace gases, especially over the tropical region, as a part of the *Indian Space Research Organisation (ISRO)'s Geosphere Biosphere Programme (GBP).* A balloon-borne cryosampler has been developed in India and successfully flight tested from Hyderabad on April 16, 1994. Description of the cryosampler instrument and its operation, field experiment carried out, and the subsequent laboratory analysis of collected ambient air samples (in the altitude range of 8 to 37 km) are discussed in this chapter.

2.2 Balloon-borne Cryosampler Experiment

2.2.1 A brief outline of the cryosampler

The cryosampler consists of sixteen electropolished, vacuum baked, stainless steel tubes of volume 400 ml each. Since concentration levels of trace gases are very low in the atmosphere (as low as parts per trillion by volume, pptv), the quality of tubes plays an important role. Each tube was vacuum baked several times to remove impurities at trace levels. All the sampling tubes with bellow-sealed stainless steel Nupro valves are assembled on a common manifold with the help of $\frac{1}{2}$ inch Swagelok fittings (Figure 2.1). The manifold is also connected to a 10 feet long air intake tube to avoid sample contamination due to degassing of the balloon gondola. Each valve is driven by a motor (GR 32.0 with gear ratio 288:1, ITT make) through a clutch which ensures proper torque for leak tight closure. Gear boxes in the motors were cleaned carefully and lubricated with low temperature grease. The manifold is kept on an interface which is attached to a cryotherm so that tubes are immersed in liquefied Neon (-246^{0}C). Capacity of the cryotherm is about 25 liters. A vapour pressure of 1.5 bar inside the cryotherm is maintained using a safety release valve. Liquid Ne is preferred due to its higher thermal capacity than that of liquid He with a lower boiling point (-268.9^{0}C). The motor valve assembly is enclosed in a thermally insulated, double walled chamber and is covered with an insulating transparent Pyrex plate on top with O-rings to avoid the ambient cool air circulation. A hermetically sealed 50 pin connector is mounted on the top plate, which carries power for all the sixteen motors and thermistor (used to monitor temperature) connections. Cryosampler is completely enclosed in a specially designed light weight aluminum cage. This arrangement prevents any damage to the cryosampler during parachute landing and also makes it convenient to handle during transportation and integration with the balloon gondola. The cryosampler valves are operated (opening or closing) by using a cryo-control unit through

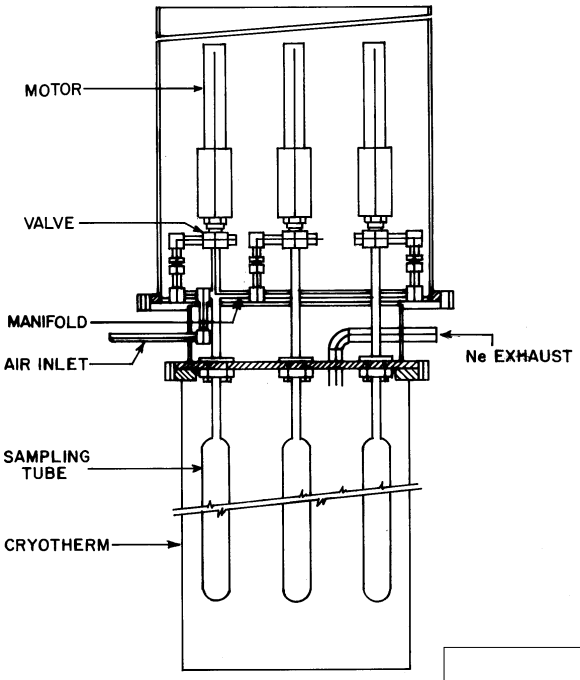

Photograph of the Cryo-Sampler here

Figure 2.1: *Plate shows a picture of the cryosampler developed in India and used during the balloon experiment conducted on April 16, 1994 (courtesy: D.R. Ranpura). A line drawing (courtesy: S.C. Bhavsar) of the Cryosampler shows its various mechanical sections (top).*

telecommands as discussed in the next section.

2.2.2 Cryo-Control Unit (CCU) and its operation

The electronic cryo-control unit basically is an interface between the telemetry unit and the cryosampler. The block diagram of the cryo-control unit (CCU) is shown in Figure 2.2. Four bits of one data commands are used to address 16 valves. Six ON/OFF commands, namely, arm, safe, open, close, high current, normal current are used to control the entire unit. High current option to motors is kept as standby for normal current, in case motor does not operate due to larger friction, which increases the normal operating current of the motors, especially at low temperatures. The unit generates status information for open/close, arm/safe, high current/normal current, motor address numbers, motor ON/OFF, and motor current value in analog (0-9 V) as well as in digital form (12 bits). The CCU was qualified for environmental specifications needed for space-borne applications.

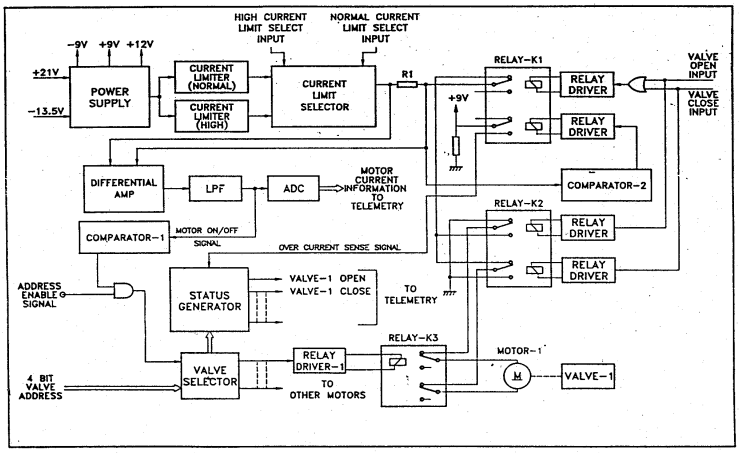

Figure 2.2: *Block diagram of the electronic cryo-control module showing various components and operations.*

Initially the instrument is kept in safe and normal current condition. The operation of the instrument starts with arm command. After receipt of this command by CCU, the arm output status becomes logical one and safe status becomes logical zero. The desired sampling tube to be opened or closed is selected through a data command which is decoded by the valve address demultiplexer circuit. This is confirmed by the 4 bit valve address in the telemetry output. The evacuated sampling tubes are kept closed before

the launch of the balloon. The valve of the sampling tube is then opened with the help of open command at a desired altitude. The valve opening duration depends on the altitude, more precisely on the ambient pressure; sampling duration increases as pressure decreases. The status of the valve and motor are confirmed through the status information. After collecting the air sample for a predetermined period, the valve is closed and necessary status information are verified. This process is repeated for all the sampling tubes. After completing the sampling in all the tubes the instrument is put in the safe mode.

2.2.3 Balloon gondola

A 146,000 m^3 size balloon made out of low density polythelene was launched from Hyderabad, carrying the cryosampler payload which consists of mainly cryosampler, cryo-control unit, telemetry/telecommand, a radio frequency link etc. (Figure 2.3). A brief overview of the operations during the balloon flight will be given here. Further technical details on balloon flights can be found in *Damle et al.* [1983] and *Joshi* [1991]. Electrical signals corresponding to various mechanical & electrical parameters regarding the status of valves and motors, and a number of house keeping parameters such as pressure, temperature were transmitted through PCM/FM *telemetry* system. A *Radio Frequency link* having a carrier frequency of 136 MHz was used. The RF link consists of the transmitter, generally a frequency/pulse modulated energy source, and its antenna at the data source on the balloon. These signals were received at the control room using a suitable receiving antenna. The *telecommand* system provided a number of ON/OFF commands required for cryosampling process as well as for balloon flight operations which include command channels for ballasting, valving, and flight termination. The carrier frequency used for the telecommand system was 148 MHz. Ballasting is an essential process to control the ascent of the balloon (especially to speed up at the tropopause level to avoid breaking of the film at low temperature), whereas a gas releasing apex valve actuated by an electric motor was used for controlled descent of the balloon. The flight was terminated by separating the parachute and its payload from the balloon. A *rip chord* built into the balloon and attached to the parachute rips a hole in the balloon allowing it to fall to the Earth. The balloon gondola along with its loadline has been picturized in Figure 2.3.

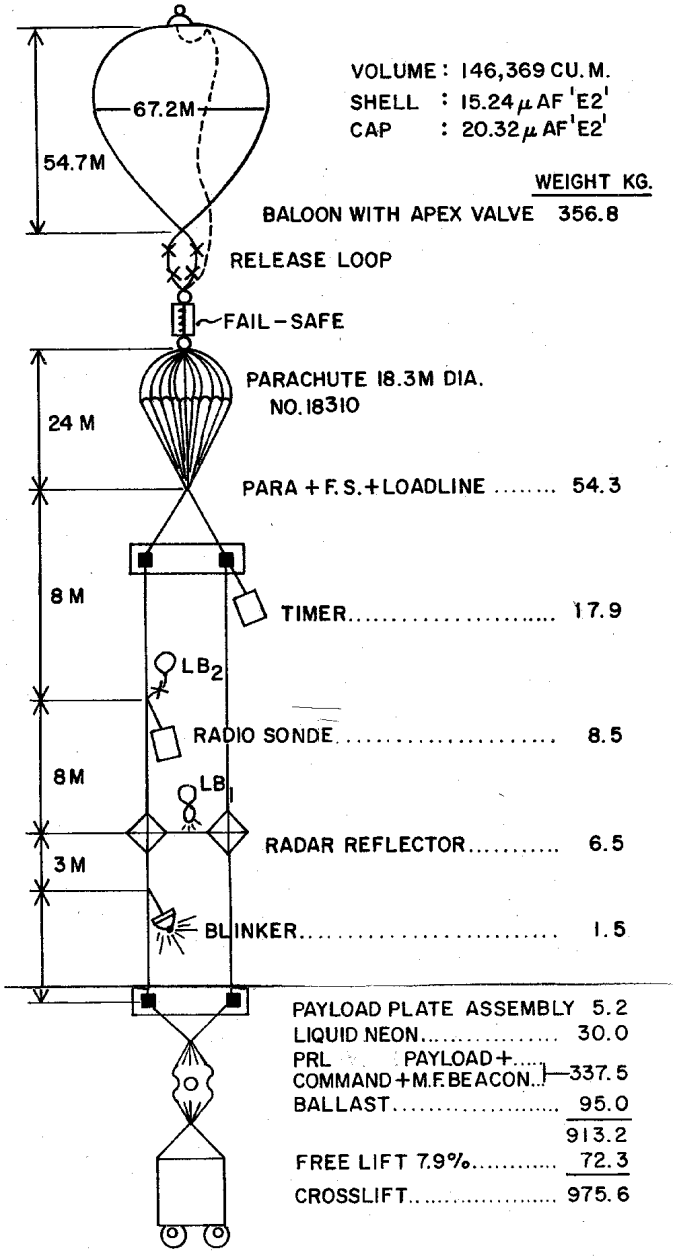

Figure 2.3: *Loadline of the balloon gondola consisting of the cryosampler payload, associated electronic packages, and mechanical equipments (not to scale). Prepared at National balloon facility, Hyderabad.*

2.2.4 Collection of air samples

The balloon flight was conducted from the national balloon facility at Hyderabad on April 16, 1994. The sampling tubes were maintained at a vacuum of about 10^{-6} Torr using a turbo molecular pump for more than a week and all the valves were closed just before the filling of liquid neon in the cryotherm prior to flight. The balloon was launched at 0530 IST. The balloon take off was normal and intake tube was deployed immediately using a telecommand. Air samples were collected at desired altitudes by opening and closing the valves through telecommands for certain duration which was decided prior to flight depending on the altitude, during both ascent and apex valve controlled descent of the balloon. The air inside the manifold and intake tube was flushed with *in situ* air by opening a spare tube (# 16) before collecting sample in each tube. Seven samples were collected during the ascent. The balloon reached the highest (ceiling) altitude of 37 km. It was then kept floating at the same altitude for about an hour. The balloon was then controlled to descent slowly by releasing the lift gas through an apex valve. Eight air samples were to be collected during the controlled descent down to an altitude of 20 km. However, the flight was terminated at 25 km altitude at

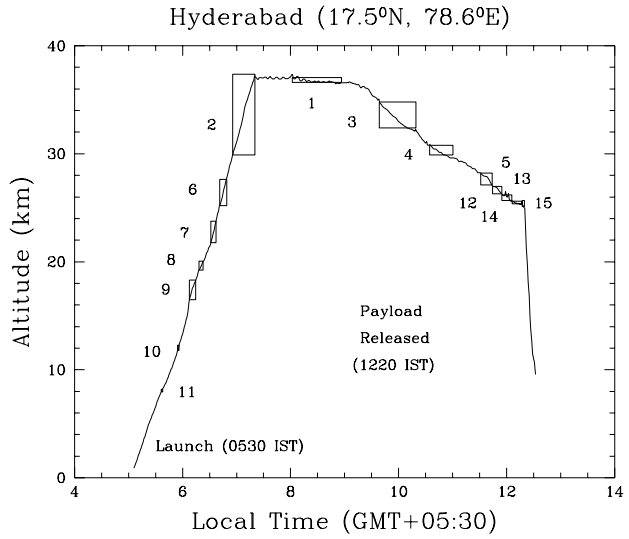

Figure 2.4: *Trajectory of the balloon, carrying the cryosampler on April 16, 1994, showing the altitude attained as a function of local time (IST). The boxes drawn on the trajectory indicate the valve opening time span and the height range of air sampling. The numbers adjacent to the boxes are denoting the values assigned to each sampling tubes during the flight operation.*

1220 IST due to high wind speeds prevalent there, which could have caused balloon drifting beyond the allowed corridor. As a result only four air samples could be collected at predetermined heights and the remaining sampling tubes were filled in the altitude range of 27-25 km. The trajectory of the balloon and altitude ranges in which the samples were collected are depicted in Figure 2.4. The valve opening time varies from about 0.5 min at around 8 km to about an hour at the ceiling altitude of 37 km (Figure 2.4). The details of these data are given in Table 4 (see next page). The cryosampler, telemetry, telecommand units and apex valve were successfully recovered after the termination of the flight. The cryosampler was brought back to PRL for gas chromatographic analysis as described in next sections.

Table 2.1: *Details of air sampling during the balloon-borne cryo-sampler experiment on April 16, 1994 from Hyderabad.*

Valve opening and closing Time (IST)	Atmospheric Pressure Range (mb)	Height Range (km)	Tube Number
05:37:27 - 05:37:50	358 - 341	7.96 - 8.21	11
05:54:33 - 05:56:02	201 - 186	11.79 - 12.26	10
06:07:36 - 06:14:29	105. - 72.08	16.48 - 18.30	9
06:18:20 - 06:22:58	62.34 - 54.97	19.24 - 20.05	8
06:31:34 - 06:37:00	42.13 - 31.03	21.77 - 23.77	7
06:41:15 - 06:49:16	24.91 - 17.11	25.18 - 27.64	6
06:55:48 - 07:20:14	12.1 - 4.13	29.91 - 37.37	2
08:01:45 - 08:56:45	4.33 - 4.39	37.06 - 36.96	1
09:38:23 - 10:19:27	5.97 - 8.41	34.78 - 32.39	3
10:34:39 - 11:00:26	10.65 - 12.15	30.78 - 29.88	4
11:31:10 - 11:44:10	15.65 - 18.52	28.22 - 27.11	5
11:44:22 - 11:54:42	18.93 - 20.97	26.97 - 26.30	12
11:54:52 - 12:05:46	21.34 - 23.09	26.18 - 25.67	13
12:06:05 - 12:16:59	23.26 - 24.18	25.62 - 25.36	14
12:17:10 - 12:19:46	23.09 - 25.18	25.67 - 25.11	15

2.3 Vertical Profiles of Trace Gases

These air samples have been analyzed at PRL using various Gas Chromatographic (GC) techniques. Different GC column materials and detectors are selected based on the physical and chemical properties of the gases under study. In this section, measurement procedure followed for N_2O and various halocarbons and their distributions will be discussed.

The vertical profiles of trace gases have also been simulated using the Max Planck Institüt of Chemie (MPIC), Mainz, Germany two dimensional chemistry-transport model (CTM). Only a brief account of the schemes used in the model will be given here; detailed description of this CTM can be found in several publications [*Gidel et al.*, 1983; *Brühl and Crutzen*, 1988 and 1989]. The model has 18 equally spaced latitudinal grids of 10^0 centered from 85^0S to 85^0N and 34 vertical spacing of about 2 km covering an approximate altitude from 0 to 60 km with closer spacing near the ground. Solar fluxes are computed using a two-stream method and photolysis rates are calculated every 15 days. Only the long-lived species are transported using an Eulerian mean circulation. The chemistry is treated for different groups of species such as odd oxygen, HO_x, NO_x, ClO_x, BrO_x etc. including about 130 species.

2.3.1 Measurement and distribution of nitrous oxide

Separation of N_2O in the sample air is obtained using a GC column packed with Porapak-Q and maintained isothermally at 40^0C. N_2O is detected with the help of an Electron Capture Detector (ECD) by injecting about 4 ml of air sample. Absolute calibration of N_2O is made with respect to the PRL working standards, outside air collected in 50 liters gas cylinders at high pressure. The laboratory working standards are calibrated using synthetic mixtures of known concentrations prepared using in-house static dilution system. Effect of ECD non-linearity for widely varied N_2O concentration ranges ($\sim$313 ppbv at surface to about 40 ppbv in stratosphere) as discussed by *Butler and Elkins* [1991] does not seem to introduce any measurable error while estimating N_2O mixing ratios at various altitudes as well as in the oceanic surface water which will be discussed in Chapter 5. The linearities of ECDs which are used in this work have been checked by using 8 diluted mixtures of N_2O in the concentration range of 77 to 417 ppbv which nearly covers the range of N_2O mixing ratios in the working standard, middle-upper stratospheric air samples, and sea surface water samples. The GC responses corresponding

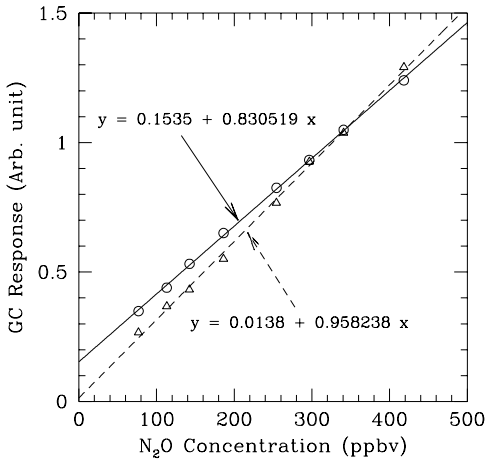

Figure 2.5: *Response curves (△: for Varian ECD; ○: HP ECD) of the gas chromatographs used for measuring N_2O. GC responses are shown as the peak areas normalized with respect to that obtained due to the standard air used for absolute calibrations. Synthetic mixtures were made by diluting a parent N_2O gas mixture of 370 ppmv supplied by Linde gas (UK).*

to N_2O concentrations in the prepared gas mixtures are shown in Figure 2.5. The linear fits (coefficient of correlation, r^2=0.99 for both the cases) matches well with the observational data and do not significantly deviate from the second order quadratic fits (not shown) in this particular concentration range.

Vertical profile of N_2O obtained from these analyses is shown in Figure 2.6. Its average tropospheric concentration is calculated to be about 313 ppbv on April 16, 1994. A comparison of the vertical profiles is made with the earlier measurements available from the same location on March 27, 1987 and April 9, 1990 during a collaborative programme of PRL with Max Planck Institüt for Aeronomie (MPAE), Lindau, Germany. Results of these earlier balloon flights are taken from *Borchers et al.* [1989] and *Lal et al.,* [1994a], respectively. Mixing ratio of N_2O remains constant in the troposphere (∼0-17 km) because of its very long lifetime, with no known considerable loss process and slow growth rate (0.25% year^{-1}). Such constituents of tropospheric origin are subsequently transported to the stratosphere very efficiently where they are mostly being dissociated by the available solar UV radiation (mainly in the atmospheric window region: wavelength ∼190-210 nm) or chemical reactions in the stratosphere, e.g.

$$\begin{aligned} N_2O + h\nu &\rightarrow N_2 + O\ (\sim 90\%) \\ N_2O + O^1D &\rightarrow 2NO\ (\sim 10\%) \end{aligned} \qquad (2.1)$$

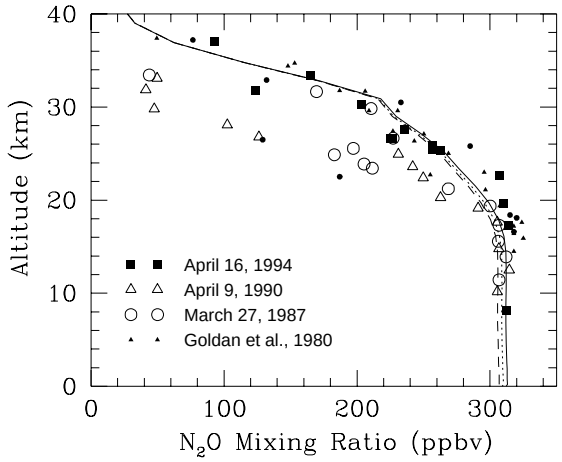

Figure 2.6: *Vertical distribution of N_2O observed on April, 16, 1994 shown along with the previous balloon measurements conducted from Hyderabad (17.5^0N, 78.6^0E), India. Lines indicate the MPIC 2D model simulated profiles at 15^0N for March 27, 1987 (dashed line), for April 9, 1990 (dotted line), and for April 16, 1994 (continuous line). Small symbols represent the measurements made by Goldan et al. [1980] using similar technique from Brazil (5^0S: filled triangle) and Panama (9^0N: filled circle) during the period of 1977-1979.*

These losses are responsible for the observed usual decrease in the mixing ratio profiles in the stratosphere, and later yield NO, providing the major (∼90%) input to the stratosphere and in part influencing even the tropospheric NO_x abundance in the upper troposphere. The atmospheric lifetime of N_2O is best estimated to be ∼120 years [*WMO,* 1995]. A comparison of the stratospheric distributions on March 27, 1987 and April 16, 1994 shows large variations particularly above 20 km apart from the prominent kink seen at around 25 km during 1987, but the 1990 profile shows much faster decrease in the altitude region of 20-32 km with a marginal increase at 33 km. The 2D model results obtained on the balloon flight days, compare well with the 1994 profile. The deviations from the normal profiles (model results with average stratospheric dynamics) on March 27, 1987 and April 9, 1990 cannot be generated by introducing the possible perturbations in the solar irradiance arising due to the 11 year solar cycle variation. For instance, the previous balloon-borne measurements during 1977-1979 from other tropical stations [*Goldan et al.,* 1980] agree fairly well with the profile obtained on April 16, 1994 and 2d model results. Higher tropospheric concentrations during 1977-1979 are probably arising due to inaccuracy in absolute calibration. Only other source constituents measured are CFC-12 and CFC-11 [see

Goldan et al., 1980], however, due to large differences in their tropospheric abundances caused by high growth rates during two periods of experiments, those results have not been used in this study for comparison. Therefore, it is suggested, at this point, that the discrepancies observed in the N_2O profiles over Hyderabad are influenced by the large scale changes occurring in the stratospheric dynamical conditions since its tropospheric growth rate is quite small ($\sim$0.25% per year). The possible dynamical perturbation will be discussed later in details (§3.3).

2.3.2 Measurements of halocarbons

The chloroflourocarbons (popularly known as CFCs; trade name - freons) were invented in the beginning of this century (1920s), particularly CFC-11 and CFC-12, were known to be inert, low boiling point, odourless, colorless, non-flammable chemicals. Due to these properties, CFCs were found suitable for a variety of industrial applications such as aerosols, refrigeration, air conditioning, foam blowing agent, solvents etc. However, large scale usage of these *wonder* chemicals came into force in late 1960s because of rapid industrialization in the United States and Europe. Measurement of halocarbons in the atmosphere was first started by J. E. Lovelock in early 1970s with his newly invented electron capture detector (ECD) for the analysis of trace compounds based on their electronegativity; who then rather bluntly stated "The presence of stable sulphur and carbon fluorides in the atmosphere is not in any sense a hazard, and ..." [*Lovelock*, 1971]. But in the following couple of years *Stolarski and Cicerone* [1974] investigated that the Cl atoms can also participate in ozone destruction reactions, likewise those were already known for HO_x and NO_x catalytic cycles but with greater efficiency, however, stratosphere was then believed to be devoid of free Cl atoms. In the same year *Molina and Rowland* [1974] pointed out that CFCs due to their inertness can reside sufficiently longer in the troposphere and can be transported to the stratosphere without any significant loss where they are dissociated by the intense solar UV radiation producing free Cl atoms which readily react with O_3. In the subsequent year, similar loss mechanism is suggested for Br radicals [*Wofsy et al.,* 1975] which are now realized to be about 40-100 times more effective in depleting the stratospheric ozone [*Solomon,* 1990]. With these understanding, stratospheric O_3 distribution was fairly explained, in spite of a probable threat due to alarmingly high growth rates of halocarbon abundances in the atmosphere caused by the rapid increase in industrial activities.

Stratospheric ozone research received further recognition when J.C. Farman and his coworkers of British Antarctic Survey team reported large and rapid loss in high latitude columnar ozone during the southern hemispheric (Antarctic) spring since the beginning of 1980s using their long time series data base starting from 1957 (as a part of International Geophysical Year, IGY). Hence, the total abundance of reactive halogen species, which are confirmed as culprits for this depletion of ozone, inferred during 1980 is considered to be the "safe level" ($\sim$2 ppbv threshold - at which "ozone hole" first appeared) as far as the maintenance of stratospheric ozone is concerned. Immediately after this report [*Farman et al.,* 1985], several theories of O_3 destruction were evolved: 1) synergistic loss of O_3 by OH, Cl, and Br radicals, 2) heterogeneous reactions which dehydrate and denitrify, particularly the polar stratosphere, and deactivate the reactive halogen species causing large depletion in O_3 at the heights of its peak concentration. Simultaneous *in situ* measurements in the midlatitude and polar regions using aircrafts have also revealed the cause-effect relations of ClO_x activation and enhanced O_3 destruction [*Anderson et al.,* 1989]. In the earlier part of this decade many convincing observations (*in situ* as well as remote) have been carried out in this natural space laboratory. An additional opportunity was provided by the Mount Pinatubo volcanic eruption in Philippines (June 1991) to study the mass release in the troposphere, their dispersion and injection into the stratosphere, and the stratospheric transformations of gases into aerosols those are involved in heterogeneous O_3 chemistry [*WMO,* 1995].

Various halogenated compounds, the sources of reactive halogens in the stratosphere, have been measured using electron capture gas chromatographs (GC-ECDs: Varian VISTA series and HP 5890 Series II) and a GC coupled with quadrupole mass spectrometer (GC-MS) operating in selective ion mode (SIM). Aliquot of about 100 ml of air sample, collected in a glass bead filled 20 cm long $\times$ 0.64 cm OD stainless steel loop cooled at liquid nitrogen temperature (-196^{0}C) and by pumping out the major and unwanted components like N_2, O_2, Ar etc., is injected onto the GC column. Such sample enrichment is essential for analyses of constituents which are in extremely low concentration (as low as a few pptv) in the atmosphere. A 6 m long of 0.32 OD stainless steel column packed with Porasil-L with a carrier gas flow of about 30 ml min^{-1} is used for separation of the species as shown in the chromatogram (Figure 2.7a : upper panel). A mixture of 90% Ar and 10% CH_4 is used as carrier gas for ECD for better stability and higher linearity range compared to that offered by N_2. The GC oven temperature is varied initially from -10^{0}C with a isothermal hold for 1 min to 80^{0}C at a rate of 8^{0}C min^{-1} maintained there for 3 mins (see top-right panel of Figure

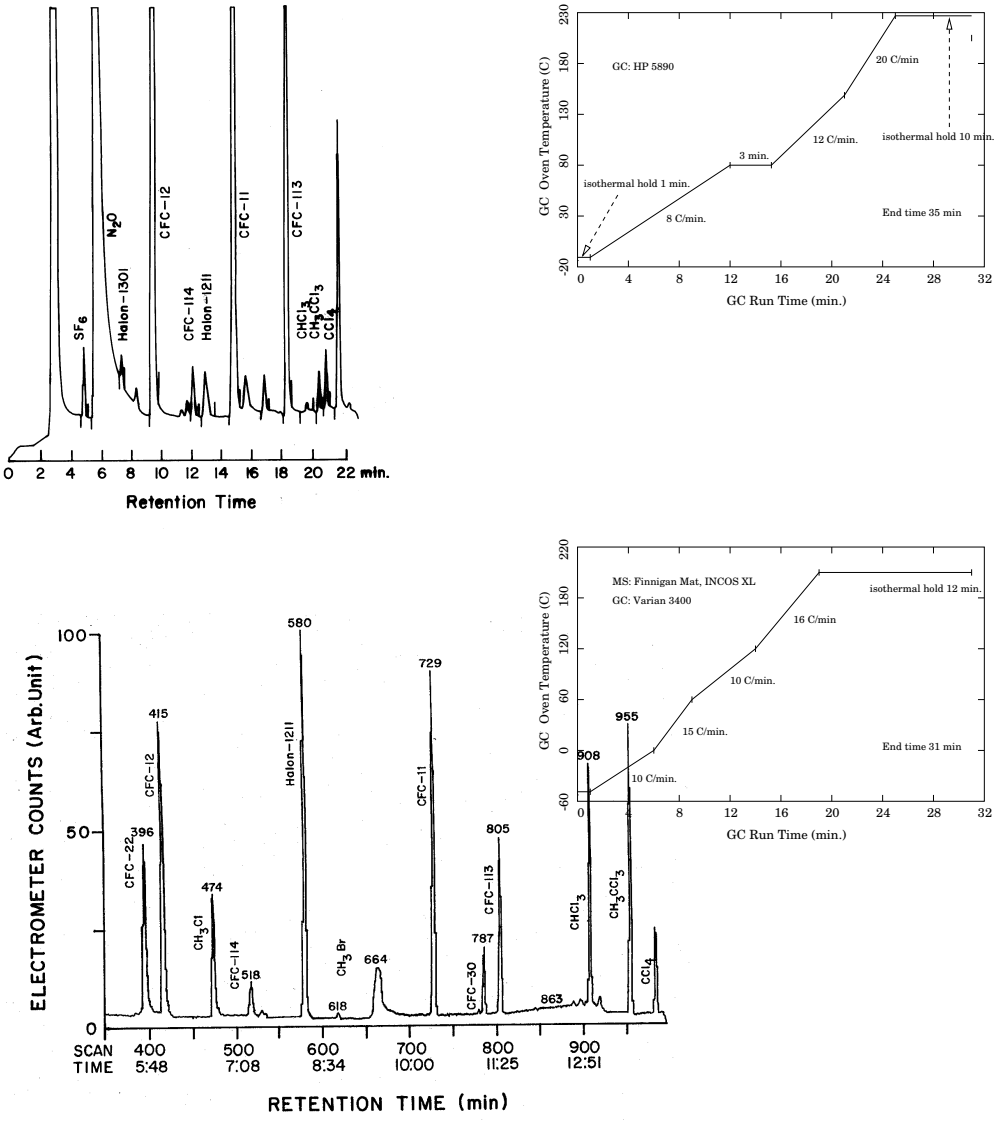

Figure 2.7: *Gas chromatograms (sketch: S.C. Bhavsar) showing separation of various halogenated species such as (a) sulfur hexafluoride (SF_6), various CFCs, halon-1301 and 1211, chloroform ($CHCl_3$), methyl chloroform (CH_3CCl_3), carbon tetrachloride (CCl_4) etc. using GC-ECD (upper panel), and (b) GC-MS detection of a few species those are insensitive to the electron capture detection, e.g. HCFCs, methyl chloride (CH_3Cl), methyl bromide (CH_3Br) etc. (lower panel). In principle this system is versatile and capable of measuring any atmospheric constituents. Insets show the variations of the oven temperature during the analyses.*

2.7). In the next step the temperature was raised to 150^0C at a rate of 12^0C min^{-1} and finally to 225^0C at 20^0C min^{-1} rate. The oven temperature was isothermally maintained there for 12 mins to ensure the complete elution of injected sample, otherwise, the residing components normally disturb the baseline affecting the stability of the ECDs. Repeatability of these analyses are found to be about 1% (1 σ) or better for many of the species.

Figure 2.7b (lower panel) depicts the separations of many other species, in addition, obtained using a capillary column connected to the GC-MS system. A similar preconcentration system is also adopted for sample preparation, however, switching valves (one six port and one eight port VICCI valves) at various steps involved in this process are controlled with the help of GC time-relays during the analysis. The amount of sample required for GC-MS analysis is somewhat larger compared to the GC-ECD analysis to detect many other species which cannot be detected with ECDs, aliquot of about 500 ml to 1000 ml air sample is usually injected onto the capillary column head to achieve better precision. A 60 m long capillary column (JW Scientific, USA) of 0.32 mm OD having DB-1 non-polar coating on fused silica with a carrier flow of 3 ml min^{-1} He is used for separating various components. GC oven temperature is varied from -50^0C to 225^0C in a number of steps to optimize the separation and analysis time (see bottom-right panel of Figure 2.7). To obtain better signal-to-noise ratio for all the peaks selective ion monitoring mode is used with suitable m/z^+ fragments of various species. For example, m/z^+ = 51 is used for HCFC-22 (CHF_2Cl), m/z^+ = 52 is used for CH_3Cl, m/z^+ = 94 is used for CH_3Br detection. The precision of these analyses for the tropospheric samples are calculated to be approximately 5% (1 σ). The absolute calibrations for some of the CFCs (CFC-12, CFC-11, CFC-114 etc.), and halons are made by analyzing the tropospheric samples collected during April 9, 1990 which are calibrated using the static dilution technique at MPAE, Germany. Concentrations of a few other halocarbons (such as CFC-113, HCFCC-22) are adjusted to the surface observations at tropical stations in the northern hemisphere [*Montazka et al.,* 1996].

2.3.3 Vertical distributions of CFCs

The vertical distributions of two important chlorine containing species CFC-12 and CFC-11 measured on April 16, 1994 are shown in Figure 2.8a and 2.8b, respectively. These two CFCs together constitute about 50% of the free Cl radicals in the stratosphere where they play the most significant role in depleting the ozone layer through the catalytic cycles discussed in §1.3. Their

loss processes are similar to N_2O in the stratosphere.

$$\begin{aligned} CF_2Cl_2 + h\nu &\rightarrow 2Cl + products \\ +O^1D &\rightarrow 2Cl + products \\ CFCl_3 + h\nu &\rightarrow 3Cl + products \\ +O^1D &\rightarrow 3Cl + products \end{aligned} \tag{2.2}$$

Dissociation of each CFC-12 and CFC-11 molecule releases 2 and 3 readily reactive Cl atoms, respectively, in the stratosphere. A comparison of the vertical profiles of CFC-12 and CFC-11 measured on April 16, 1994 with those on March 27, 1987 and April 9, 1990 [*Borchers et al.,* 1989; *Borchers, private communication,* 1995) suggests a few distinct features. In the troposphere, as their concentrations do not show appreciable change with altitude, growth rates are calculated with greater caution from the average tropospheric concentrations on the flight days. Estimated growth rates during 1987-1990 are apparently much higher, 4% and 6% per year for CFC-12 and CFC-11, respectively, compared to that of 1.6% per year for both the species, during 1990-1994 showing the effect of phasing out of CFCs as per the Montreal Protocol[1] in 1987.

In the stratosphere, CFC-12 also shows the influence of the dynamical perturbations in an identical manner as discussed for the N_2O distribution, however, the CFC-11 profiles do not show any such discrepancies due to its much shorter *in situ* photochemical lifetime when compared to the dynamical lifetime at the stratospheric altitudes. Stratospheric distribution of CFC-11 is dominantly controlled by the local photochemistry. The stratospheric distributions of these gases also clearly indicate an increase in the loading of CFCs, particularly in the lower stratosphere.

Although the production and industrial applications of CFCs were familiar long before, their faster increase in atmospheric concentrations has been observed during the past three decades, coinciding with the period of rapid industrial growth all over the world. In the present atmosphere, only a small fraction of halocarbons which reaches the stratosphere are naturally produced (see Table 1.2). High precision time series measurements for a number of trace constituents at various stations around the globe are being made to monitor their tropospheric trends [see for example *Fraser et al.,* 1994]. Surface measurements of trace gases [*Cunnold et al.,* 1997] have

[1]A protocol signed by the member countries in order to the restrict the production and release of ozone depleting substances

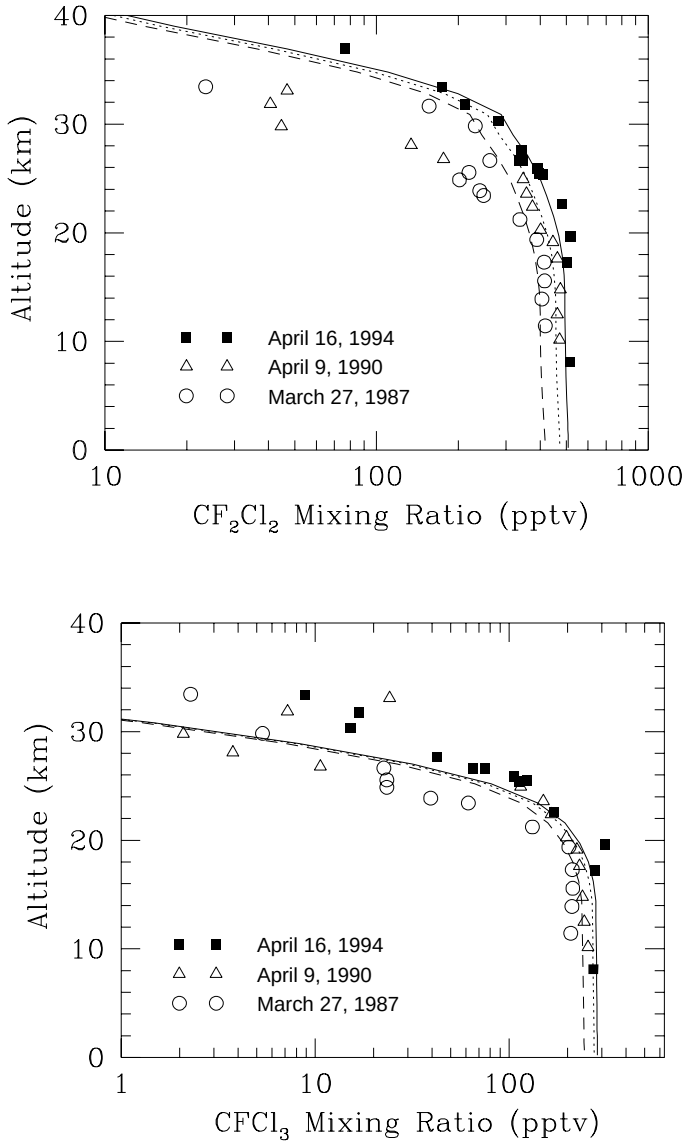

Figure 2.8: *Vertical profiles of (a) CF_2Cl_2 (upper panel) and (b) $CFCl_3$ (lower panel) measured at Hyderabad on April 16, 1994 in comparison with the previous measurements from the same location and 2D model results.*

shown CFC-12 and CFC-11 concentrations to be fairly steadily increasing in the atmosphere at the rates of about 17 and 9 pptv/year, respectively, in the period of 1979 to 1984 which are in good agreement with those estimated from *Elkins et al.* [1993]. These are the highest atmospheric growth rates of CFC-12 and CFC-11 just before halocarbon (more generally the ozone depleting substances) phase out agreement received wide acceptance in a meeting at Montreal (the so called *Montreal Protocol*) which has been subsequently adjusted and amended several times (the revised Montreal Protocol). Decrease in growth rates have been observed to be dramatic since 1987 for CFC-11 and since 1988 for CFC-12.

The average tropospheric growth rates have been estimated from the tropospheric average concentrations (from Figure 2.8) of these gases, which are found to be about 12 and 19 pptv/year for CFC-11 and CFC-12, respectively during 1987 to 1990. The increase rate is quite higher for CFC-11 than those calculated using surface measurements (8.6 and 18 pptv/year for for CFC-11 and CFC-12, respectively) discussed in *Cunnold et al.* [1997]. Similar estimates of tropospheric increase rates using balloon measurements are found to be about 6 and 11 pptv/year for CFC-11 and CFC-12, respectively, between 1990 and 1994 which are again higher compared to those which have been estimated from the surface measurements for the same period - about 2.5 and 9 pptv/year for CFC-11 and CFC-12, respectively. It is, however, noteworthy that the average increase rates in tropospheric concentrations which are estimated using another set of global tropospheric measurements [*Elkins et al.,* 1993; *Montazka et al.,* 1996] to be about 10 and 18 pptv/year for CFC-11 and CFC-12, respectively, during 1987-1990 and they are about 4.5 and 12 pptv/year, respectively, during 1990-1994. These growth rates are apparently in better agreement with the balloon measurements. These disagreements/agreements seem to arise from the delayed response, recorded at the stations operated by NOAA/CMDL stations, of the global consumption constraints of the revised Montreal Protocol by about one year compared to the observations made by the ALE/AGAGE stations [*Cunnold et al.,* 1997]. The delayed response in the balloon measurements is caused by the transport time taken by an air parcel to reach the tropical free upper troposphere from the midlatitudes of the northern hemisphere. Since the NH midlatitude is the region of highest production/usage, the effect of consumption constraints due to Montreal Protocol is also observed earliest in that region of the atmosphere.

As these CFCs are being phased out in compliance with the Montreal

Protocol and its amendments, new substitutes are being introduced to fulfill the industrial requirements. One such compound is HCFC-22 (CHF_2Cl) which is being increasingly used in place of some of the CFCs. One Cl atom is replaced by a hydrogen atom in CFC-12 molecule to make it react with OH in the troposphere and on the other hand its photoabsorption cross-sections decreases significantly (≈250 times lower than CFC-12) in the wavelength range of solar UV radiation penetrating to the stratosphere, especially in the atmospheric window region, thereby reducing its stratospheric loss (*DeMoore et al.,* 1992]. Hence, it is considered to be a minor source of reactive Cl in the stratosphere compared to CFC-12. Its ozone depletion potential is less than that of CFC-12 by about a factor of 7 (Table 1.2). The vertical distribution of HCFC-22 is measured using GC-MS (Figure 2.9). Large devi-

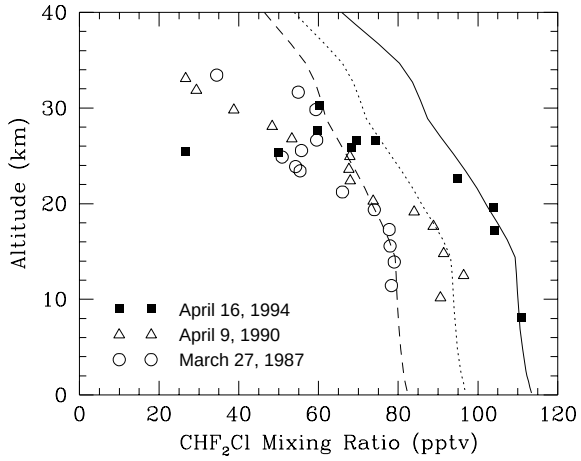

Figure 2.9: *Vertical profiles of HCFC-22 (CHF_2Cl) measured on April 16, 1994 from Hyderabad are compared with previous measurements [Fabian et al., 1994; Borchers, personal communication, 1995] from the same location, and MPIC 2D model simulations.*

ations are found for a few stratospheric samples which are probably arising due to sample contamination. However, the profile shows less decrease in the stratosphere (see March 1987 and April 1990 distributions also) due to lower photochemical loss compared to that of N_2O or CFC-12, the decrease in the lower stratosphere is partly caused by sluggish renewal of the air mass which can be better understood from the vertical profiles of SF_6 (§3.3). Very large growth can be seen in the troposphere due to their enhanced usage as replacements in place of CFCs. Most of the hydrogenated halocarbons such as CH_3Cl, CH_3Br, CH_3CCl_3 were found to be contaminated. Therefore, these profiles are not used in this study.

In the modern atmosphere, a few more HCFCs such as HCFC-141b and HCFC-142b are exhibiting extremely high growth rates of 22% and 54% per year, respectively during 1995 [calculated from *Montazka et al.,* 1996]. These growth rates were even higher in the beginning of 1990s [*Oram et al.,* 1995]. Although these chemicals are less significant to the stratospheric ozone destruction, they do have very high global warming potentials compared to CO_2 and various other important gases contributing to greenhouse warming. Therefore, enhanced usage of these chemicals would play a significant role in global warming in future, suggesting a requirement of further assessment before their wide spread commercial use.

2.3.4 Bromine containing gases in the stratosphere

The reactive bromine radicals (Br and BrO), in spite of their much lower concentrations compared to their chlorine counterparts, play an important role in the loss of stratospheric ozone. Bromine is estimated to be about 40 to 100 times more effective than chlorine in ozone destruction due to the fact that the removal process of Br through the formation of HBr is not usually favoured in the stratosphere, because its formation by the chemical reactions (analogous to HCl) are mostly endothermic in nature. The reaction schemes of Br (also in combination with Cl and OH) are discussed in section 1.3.1. Loss of ozone due to bromine in the Antarctic region is estimated to be around 30% [*Solomon,* 1990; *Wennberg et al.,* 1994]. Methyl bromide (CH_3Br) is an important source of bromine (Br) radical in the Earth's atmosphere. Oceanic regions are believed to be the major sources of this gas along with its few significant anthropogenic sources [*Khalil et al.,* 1993; *Reeves and Penkett,* 1993], recent measurements also reveal some oceanic parts as net sink of CH_3Br [*Lobert et al.,* 1995]. Methyl bromide is used as a soil, grain and space fumigant. It is also emitted from automobile exhaust and biomass burning. Man made sources of CH_3Br are estimated to be about 35-40% of the total budget [*Reeves and Penkett,* 1993; *Singh and Kanakidou,* 1993]. High concentration of this gas has been observed in urban areas. Also a high positive latitudinal gradient ($\sim$1.3), from the southern hemisphere to the northern hemisphere, has been suggested in mean CH_3Br mixing ratio [*Reeves and Penkett et al.,* 1993]. Recent CH_3Br data shows an increase of 0.3$\pm$0.1 pptv/yr during the last four years [*Khalil et al.,* 1993]. It has a relatively short lifetime ranging from 1.2 to 2 years [*Singh and Kanakidou,* 1993; *Khalil et al.,* 1993]. The loss of this gas is mainly due to the reaction with OH in the troposphere and photolysis in the stratosphere, which produces free Br radicals. These Br radicals react with ozone and form BrO

radicals. Data on the vertical distribution, which is necessary to estimate the Br release from CH_3Br influencing the ozone chemistry, was limited only to a preliminary result by *Fabian et al.* [1981].

Air samples collected during a PRL-MPAE joint balloon flight from Hyderabad at fifteen different levels in the altitude region of 10 to 35 km, during both ascent and slow valve-controlled descent of the balloon on April 9, 1990, were analyzed after about five months using a gas chromatograph (Dani 6800) coupled with a quadrupole mass spectrometer (Balzers QMG511) at MPAE. A 4 meter glass column packed with OV-101 on chromosorb WHP together with mass selection on mass spectrometer was used for separation and detection. Methyl bromide was detected at m/z^+ 94. The sample volume required for detection of these gases ranged from 0.7 liter to 1.5 liter. The detection limit for CH_3Br was about 0.2 pptv with sample volume of 1.5 liter. Repeatability of these measurements was within $\pm$10%. Absolute calibration made at MPAE using a static dilution technique gives a value of 8.0 pptv for tropospheric samples with an uncertainty of $\pm$20%.

Due to large loss of CH_3Br in the troposphere through the reaction with OH and based on the available vertical profile [*Fabian et al.,* 1981], it was believed that this constituent may not provide a significant contribution to stratospheric bromine. However, the vertical profile obtained from Hyderabad on April 9, 1990, shows a nearly constant mixing ratio of about 8 pptv in the upper troposphere and lower stratosphere, altitude up to about 20 km, but above this height it decreases sharply to about 1.5 pptv at 23.6 km and 0.5 pptv at 25 km (Figure 2.10). CH_3Br could not be detected in samples collected above 27 km altitudes due to the sensitivity limitation of the system. The only earlier measurement from Southern France reported by *Fabian et al.* [1981] showed a very sharp fall at a much lower altitude region of 12-15 km. The Hyderabad profile is in reasonably good agreement with the results of the MPIC 2D model. The model mixing ratios are normalized to the average tropospheric value of 8.0 pptv to study the vertical distribution of CH_3Br. The observed fall in the mixing ratio above 20 km is sharper than that calculated by the 2D model.

Other two important bromine containing compounds, namely, halon-1211 (CF_2BrCl) and halon-1301 (CF_3Br), having no significant loss in the troposphere, are released solely by the anthropogenical activities such as fire extinguishing. Tropospheric concentrations of halons have been increasing very rapidly in the 1980s [*Lal et al.,* 1985; *Butler et al.,* 1992; *Lal et al.,* 1996]. Figures 2.11a and 2.11b show the distribution profiles of halon-1211 and

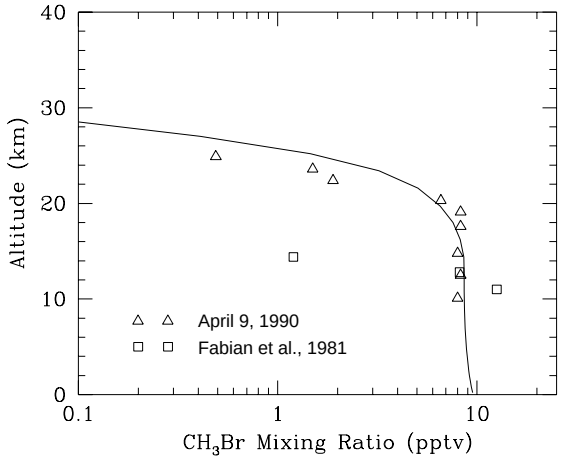

Figure 2.10: *Vertical profiles of CH_3Br measured on April 9, 1990 from Hyderabad and southern France (44^0N) during 1980 [Fabian et al., 1981] compared with the MPIC 2D model results.*

1301 measured at Hyderabad using the technique described in §2.2. Halon-1211 and 1301 profiles show constant mixing ratios in the tropospheric altitude region (up to 17 km). An estimation of the average tropospheric growth rates of these two gases show large increase rates in their concentrations during 1987-1990, 15% and 8% per year for halon-1211 and halon-1301, respectively and a drastic decrease in growth rates to about 4 and 3.6% per year during 1990-1994. Nearly similar trends are estimated for halon-1211 (18%/year during 1987-1990 and 7%/year during 1990-1994 period), and no significant decrease in the growth rates of halon-1301 (about 10%/year) has been observed from the surface measurements during the period of balloon measurements [*Butler at el.,* 1992; *Montazka et al.,* 1996]. This mismatch is probably arising from calibration error involved in this analysis. The production for consumption of halons is assumed to have ceased on December 31, 1993 in developed countries. Due to their long tropospheric lifetimes, these chemical species are transported to stratosphere and release catalytic ozone depleting radicals in the stratosphere on their rapid dissociation by UV radiation and reaction with O^1D. Comparison of the vertical profiles measured during balloon experiments do not show any qualitative difference in the stratosphere (dynamical perturbations are superseded by their high photochemical loss) except a steady increase forced from below. The rate of dissociation of these compounds is the measure of rate of release of the Br radicals. Mixing ratio of halon-1211 and 1301 decreases rapidly from a tropospheric value of 2.15 and 1.97 pptv to 0.07 (no measurable

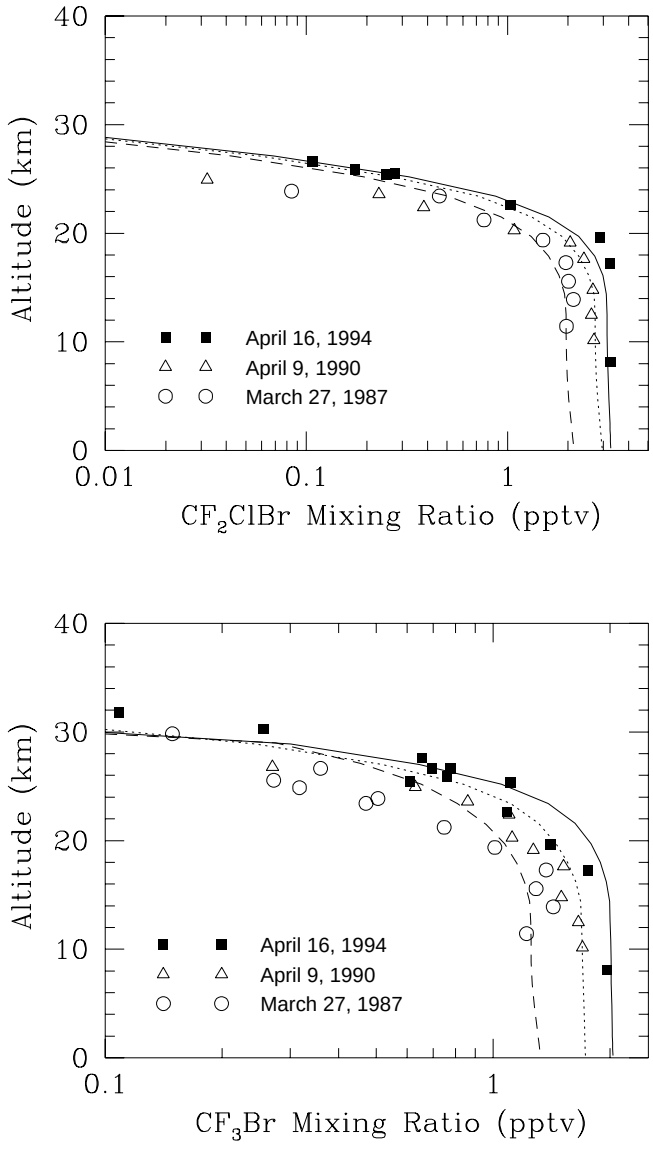

Figure 2.11: *Altitude profiles of two halons: (a) Halon-1211 (CF_2BrCl; upper panel) and (b) Halon-1301 (CF_3Br; lower panel) obtained over Hyderabad using balloon-borne experiments and the MPIC two-dimensional model simulations.*

quantity above) and 0.78 pptv, respectively at 26.4 km height. These species can be dissociated effectively by lower energy solar radiations in the wavelength range of 190-300 nm while compared to that required for N_2O and CFC-12.

2.3.5 Production of Br from CH_3Br and Halons

A calculation has been made to estimate the production of bromine radicals from the three main bromine containing gases which have been measured from the samples of the same balloon flight (on April 9, 1990). Bromoform ($CHBr_3$), with a tropospheric mixing ratio of about 3-6 pptv and lifetime of the order of month [*Cicerone et al.,* 1988], may contribute to the production of Br radicals at lower heights. However, no vertical distribution of $CHBr_3$ extending up to the stratospheric heights is obtained so far. Another Br containing chemical, dibromomethane (CH_2Br_2), is observed to be present in the upper troposphere with an maximum concentration of about 1.7 pptv and may contribute up to about 10% of the total organic bromine at the tropopause, but not detected above 20 km over Hyderabad [*Kourtidis et al.,* 1996]. Hence, CH_2Br_2 is also not included in this calculation. The tropospheric mixing ratio of CH_3Br is the highest (8 pptv), while the mixing ratios of halons 1211 and 1301 are 2.15 pptv and 1.7 pptv respectively during 1990. In the stratosphere CH_3Br decreases most sharply followed by halon-1211. Photodissociation rates are calculated for these three gases for a solar zenith angle of 45^0 using absorption cross-sections given in *DeMoore et al.* [1992]. CH_3Br also reacts with OH, which is the main loss process below about 10 km. The production rate (P_{i^z}) of bromine radicals due to photodissociation at different altitudes (z) for a particular compound (i) is given by the following expression.

$$P_{i^z} = J_{i^z} \cdot n_{i^z} \tag{2.3}$$

Where J_{i^z} is the photodissociation rate at height z and n_{i^z} is the number density of i^{th} gas. Figure 2.12 shows the Br production rates from these three gases. Above 13 km height, photodissociation of CH_3Br produces more free bromine than due to the dissociation of the halons, peaking at around 20 km. The production rate of Br radicals at this peak is 0.6 atom cm^{-3} s^{-1}. Halon-1211 is also a major source of Br in the 10 to 25 km altitude region. However, bromine production from the photodissociation of halon-1211 is lower than that due to CH_3Br photodissociation with a peak value of 0.45 mole cm^{-3} s^{-1} at 20 km. Halon-1301 is the predominant source of free

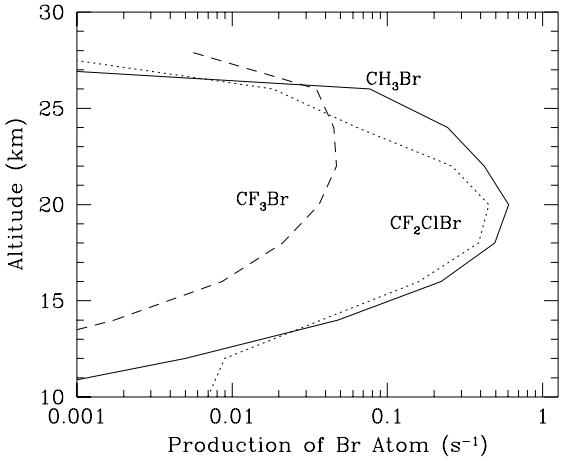

Figure 2.12: *Altitude distributions of bromine production rates from the three major bromine containing compounds.*

bromine only above 25 km. In the stratosphere, production of Br atoms from CH_3Br is equivalent to its production from both the halons.

Due to highest Br production efficiency in the stratosphere, in spite of its low atmospheric abundance near the ground ($\sim$10 pptv, about 10-50 times less than many of the halocarbons), CH_3Br was included as a controlled ozone depleting substance along with CFCs, and halons by the international agreement (United Nations Environmental Program, *Report of the Fourth Meeting of the Parties to the Montreal Protocol on Substances that Deplete Ozone Layer,* Geneva, 1992). Most recent publication on the trends of halogenated compounds [*Montazka et al.,* 1996] indicate that growth rates of halon-1211 and halon-1301 has reduced to 0.11 and 0.07 pptv/year during 1995 from about 0.3 and 0.6 pptv/year, respectively, due to the consumption constraint act imposed by the Montreal Protocol. It is, therefore, fairly apparent that after a few years from now, CH_3Br, with a recent tropospheric growth rate of 0.3 pptv/year [*Khalil et al.,* 1993], will emerge as the only significant source of Br radicals in the stratosphere. Due to the large uncertainties in its biospheric sources and sinks, as a result in the atmospheric lifetime and ODP, no specific phase out plan has been made even in revised versions of the Montreal Protocols. The difficulties associated with the atmospheric budget of CH_3Br are quite different than CFCs and Halons. Its sources are not entirely anthropogenic - important among anthropogenical sources of CH_3Br are emissions from the agricultural fumigants (75% as soil fumigant, 22% as post harvest and 3% as pest control tool), and biomass burning (also include burning of leaded gasoline). Oceans being the largest

natural source of this gas, up to about 40% of the total, it also acts as one of the most important sinks [*Yvon-Lewis and Butler,* 1997]. Other sinks are being the photodissociation and scavenging by the OH reaction (the largest), degradation on the natural soil etc. (see Table 2.2 for details).

Table 2.2: *Present atmospheric budget of methyl bromide (from Yvon-Lewis and Butler* [1997]).

Source type	Emissions (Gg year^{-1})	Sink type	Uptake (Gg year^{-1})
Oceans	56	Hydrolysis and UV	86
Fumigation	46	Oceans	77
Biomass Burning	20	Soils	43
Leaded Gasoline	15	Plants	?
Total	137	Total	206(+)

The lifetime of CH_3Br was debated to vary widely about 1.3 for quite sometime [*Khalil et al.,* 1993] and an ODP of about 0.6 was assigned to this gas [*WMO,* 1995] which is potential to disrupt the natural balance of the atmospheric O_3 causing an increased of hazardous UV radiation reaching the surface of the Earth. However, uncertainties in these estimations of sources and sinks have reduced to a great extent with the availability of recent *in situ* measurements in oceans, soils, biomass burning area etc., and the atmospheric lifetime of CH_3Br using the most recent informations is estimated to be about 0.8 year [*Yvon-Lewis and Butler,* 1997]. This revised lifetime reduced its ODP to about 0.3 and it is quite unlikely that this value would decline any more.

Further research to delineate the atmospheric budget of CH_3Br (a discrepancy in global mass balance of about 70 Gg year^{-1} still persists - missing source) would improve our understanding of different processes controlling the evolution of our atmosphere which also include a better characterization of the stratospheric processes.

This Chapter is restricted only to an overview of the major advantages of cryogenic whole air sampling technique and restricted to discussion on some potential usages of the *in situ* measurements of large numbers of trace gases. A few more vertical distributions, in particular that of CH_4 and SF_6, are described in the next chapters along with their distinct usages especially due to the availability of simultaneous measurements of a large numbers of trace gases which enable us to understand various dynamical and chemical processes acting in the stratosphere.

Chapter 3

Estimation of Dynamical Parameters

Direct measurements of stratospheric dynamical parameters such as vertical transport, transport time of an air parcel from the ground to upper altitudes, perturbations from the mean flows derived from the heating/cooling balance remained elusive for long time. Only recently, comprehensive measurements of horizontal and vertical winds, estimations of large scale mixing due to eddies etc. are made with the advent of high resolution radar, lidar and satellite based remote sensing techniques as well as using high altitude balloon- and rocket-borne *in situ* techniques. The distributions of minor constituents of sufficiently long photochemical lifetimes, compared to their residence time arising due to the stratospheric dynamics, critically depend on their local photochemistry and the transport processes. Therefore, the measurements of trace gases have often been utilized as active or passive tracers to understand the dynamics of the stratosphere; for example, dryness of the tropical stratosphere indicated that the main mass transport from the troposphere to the stratosphere is through the cold tropical tropopause [*Brewer,* 1949], higher amount of observed total ozone over the mid- and high latitudes suggested the mean meridional transport from the tropics to extratropics [*Dobson,* 1956], large scale planetary wave induced mixing in the stratosphere (stronger in the winter hemisphere) is envisaged from the latitude-altitude maps of N_2O [*Rundel et al.,* 1993]. However, the tropical stratosphere appears to be isolated strongly from the extratropical mixing and new stratospheric transport models are suggested only recently [*Plumb,* 1996].

3.1 Vertical Eddy Diffusion Coefficients

3.1.1 Introduction

One-dimensional modeling of the chemistry and composition of planetary atmospheres utilizes a dynamical variable which essentially accounts for vertical fluxes. These fluxes are usually parameterized in terms of the concept of 'eddy diffusion' in turbulent fluids [*Holton,* 1986]. The vertical eddy diffusivity [K_z] originated in studies of sporadically occurring persistent layers of turbulence can be deduced from a radar experiment [*Woodman and Rastogi,* [1984]. Mechanisms of gravity wave saturation induced turbulence causing eddy diffusion have been well documented [*Weinstock,* 1984]. The planetary-wave mixing modulates stratospheric transport processes [*Rundel et al.,* 1993], thereby giving rise to higher diffusion coefficients which will also be reflected in the distributions of long-lived atmospheric constituents.

There have been various attempts to estimate vertical eddy diffusion coefficient in the Earth's atmosphere and a number of theoretical and experimental procedures have been adopted, some of which are enumerated below.

1) Use is made of the atmospheric distribution of radioactive debris of atom bomb, ^{14}C and ^{90}Sr in the stratosphere to estimated K_z [e.g. *Massie and Hunten,* 1981].

2) The vertical distributions of photochemically long-lived atmospheric trace constituents like N_2O, CH_4, O_3 etc. controlled by atmospheric dynamics, are utilized to determine K_z in the stratosphere [*McElroy et al.,* 1974; *Schmeltekopf et al.,* 1977; *Massie and Hunten,* 1981]. However, these are based on sporadic measurements and possible consequences of the seasonal or temporal variability in the mixing ratio profiles of chemical tracers have not been included.

3) A chemical release experiment has been used to measure the instantaneous eddy diffusivity over Hyderabad (17.5^0N, 78.6^0E) [*Chakrabarty et al.,* 1987].

4) Several attempts have been made to study the seasonal variability of eddy diffusivity in the mesosphere and thermosphere using rocket data of mass spectrometric measurements of neutral constituents and also from semi-theoretical calculations of turbulence [*Danilov and Kalgin,* 1992].

5) Radar measurements in the lower stratosphere ($\leq$ 20 km) and

mesosphere (60-90 km) have been used by several workers to study K_z and recently *Fukao et al.* [1994] have shown the existence of large seasonal variability in eddy diffusivity.

The observed seasonal variability and/or the difference between various published results are wide spread and, since there has been no attempt so far to study the possible stratospheric long term variabilities. The vertical eddy diffusion coefficient deduced from the vertical distributions of N_2O and CFC-12 during 1987-1994, are examined from this perspective that these species have long enough atmospheric lifetimes, 120 and 102 years, respectively [*WMO,* 1995], so that their distributions are governed mainly by atmospheric dynamics rather than chemistry. These two atmospheric constituents of nearly equal atmospheric lifetimes are chosen because the transport coefficients substantially vary with their lifetimes; the K_z value increases as lifetime increases in the stratosphere [*Holton,* 1986]. Mixing ratio profiles of N_2O and CFC-12, measured over Hyderabad during March 1987, April 1990, and April 1994 in the altitude range of about 8-37 km using balloon-borne cryogenic air sampler are used to calculate the vertical profiles of the eddy diffusion coefficient.

3.1.2 Mathematical approach

The mixing ratio of any atmospheric constituent varying with space and time can be computed from the well known continuity equation as

$$\frac{dn_i(r,t)}{dt} = P_i(r,t) - L_i(r,t) - \vec{\nabla} \cdot (\vec{\phi}_i\ (r,t)) \tag{3.1}$$

where n_i(r,t) is the concentration of the i^{th} species at position (r) and at given time (t); P_i is the production rate and L_i is the loss rate. For the case of a vertical (z) one-dimensional approximation, the mixing ratio $\left(f_i(z,t) = \frac{n_i(z,t)}{M(z)}\right)$ dependent vertical flux, ϕ_i(z,t), can be defined as

$$\phi_i(z,t) = -K_i(z,t)M(z)\frac{df_i(z,t)}{dz} \tag{3.2}$$

where K_i(z,t) is the vertical eddy diffusion coefficient (K_z), M(z) is the number density of air molecules in ambient air. As the concentrations of N_2O and CFC-12 do not change significantly on short time scales (∼days), a steady state condition is assumed, hence the time dependence of equation (3.1) vanishes. It is well recognized that N_2O and CFC-12 are only produced on

the Earth's surface and are known to have no sources either in the free troposphere or in the stratosphere, so the production term (P) becomes zero. As balloon measurements were possible up to 35-37 km during these flights, vertical profiles are extrapolated up to 40 km without introducing considerable error, to reduce the uncertainty in calculating column integrated values below these heights. Implementing the conditions stated above and integrating equation (3.1) between z and 40 km it gives

$$\left(K_z M(z)\frac{df_i(z)}{dz}\right)_{40\ km} - \left(K_z M(z)\frac{df_i(z)}{dz}\right)_z = \int_z^{40\ km} L(z)dz \tag{3.3}$$

The first term of this equation acts as a virtual zero level of the total loss term (R.H.S.) and conventionally set to zero by shifting this level (z=40 km) to infinity [*Massie and Hunten*, 1981]. Since M(z)$\frac{df_i(z)}{dz}$ decreases very fast in case of N_2O and CFC-12 profiles, especially above 40 km, the first term in equation (3.3) is approximated to zero. Thus equation (3.3) reduces to

$$K_z = \frac{-\int_z^{40\ km} L(z)dz}{M(z) \times [df_i(z)/dz]} \tag{3.4}$$

It is apparent from this expression that the value of K_z is infinite in the altitude range of no mixing ratio gradient (i.e. $\frac{df}{dz}$=0) and simultaneously it is erroneous in the altitude range of low mixing ratio gradient. The loss term basically consists of two parts - photodissociation by solar ultraviolet radiation and reaction with $O(^1D)$. The photochemical schemes formulated for N_2O and CFC-12 are as described in sections §2.3.1 (equation 2.1) and §2.3.3 (equation 2.2).

The reactions with $O(^1D)$ do not contribute much to the loss terms and, even if the concentration of $O(^1D)$ altered by a factor of two, the changes observed in K_z values are not significant (changes of about 4-7% have been seen, depending on the altitude, for both species). This variance is well within the error bars (see for instance Figure 3.5). In order to calculate the photodissociation rates at various altitudes, the intensity of solar radiation is calculated at each altitude adopting a layer-by-layer approximation between 0-80 km, considering the absorption due to oxygen and ozone and scattering due to air molecules. The intensity of solar radiation (I) reaching an altitude level z for a particular solar zenith angle (χ) is obtained by using Beer-Lambert's law and can be represented as

$$\begin{aligned} I(z,\chi,\lambda) &= I_\infty(\lambda) exp[-sec(\chi)(\sigma_{O_2}(\lambda)N_{O_2}(z) \\ &\quad +\sigma_{O_3}(\lambda)N_{O_3}(z) + \sigma_{air}(\lambda)N_{air}(z))] \end{aligned} \tag{3.5}$$

where σ_{O_2} and σ_{O_3} are the photo absorption cross sections of O_2 and O_3, respectively. The molecular scattering cross section of air, σ_{air}, is calculated using the formula given by *Nicolet* [1984]. The vertical column density for the molecule *i* is given by $N_i = \int_z^\infty n_i(z)dz$. Air densities are taken from an empirical reference atmosphere for the equatorial zone given by *Sasi and Sen Gupta* [1986], based on rocket and balloon measurements. Subsequently, the photolysis rates (J) are calculated from the expression

$$J_i(z,\chi) = \sum_{\lambda_{start}}^{\lambda_{end}} \epsilon_i(\lambda_j)\sigma_i(\lambda_j)I(z,\chi,\lambda_j)\Delta\lambda_j \tag{3.6}$$

Quantum efficiencies, $\epsilon(\lambda)$, are taken to be unity for this calculation. $\Delta\lambda$s are the wavelength (λ_j) intervals at which the absorption cross sections are available within the wavelength range λ_{start} and λ_{end}. The temperature dependent reaction rates and the photo absorption cross sections used in the calculation of photolysis rates are taken from *DeMoore et al.* [1992]. Spectral intensities of solar irradiances are incorporated from *Nicolet* [1989], which corresponds to minimum solar activity conditions in the most important wavelength region (200-300 nm) in this study. A local noon time solar zenith angle, χ, has been assumed for this calculation. The integrated loss of these gases together with other parameters are used in equation (3.4) to estimate K_z at each 1 km height interval, for each gas separately.

3.1.3 Formulation of average N_2O and CFC-12 profiles

The vertical distributions of N_2O and CFC-12 were measured from Hyderabad, a tropical station, on March 27, 1987, April 9, 1990 and April 16, 1994 using balloon-borne cryogenic air sampling and gas chromatographic analysis techniques (§2.2; see also *Lal et al.,* [1996]). Mean reference profiles of these gases observed from Southern France are also used to estimate K_z for midlatitude region. These reference profiles are based on a number of measurements made over a period of several years from Southern France (44^0N) [*Fabian et al.,* 1996]. These distribution profiles obtained from Hyderabad and Southern France have been smoothed and extrapolated up to 40 km and mixing ratios at each 1 km are interpolated. These mixing ratio profiles of N_2O and CFC-12 are shown in Figure 3.1a and 3.1b, respectively. Vertical profiles of N_2O measured in 1987 and 1994 agree fairly well in the troposphere and also at a few altitudes in the stratosphere (Figure 3.1a), however, Figure 3.1b clearly indicates a high growth of CFC-12 during this period, but the essential features are similar to that of N_2O, which has been

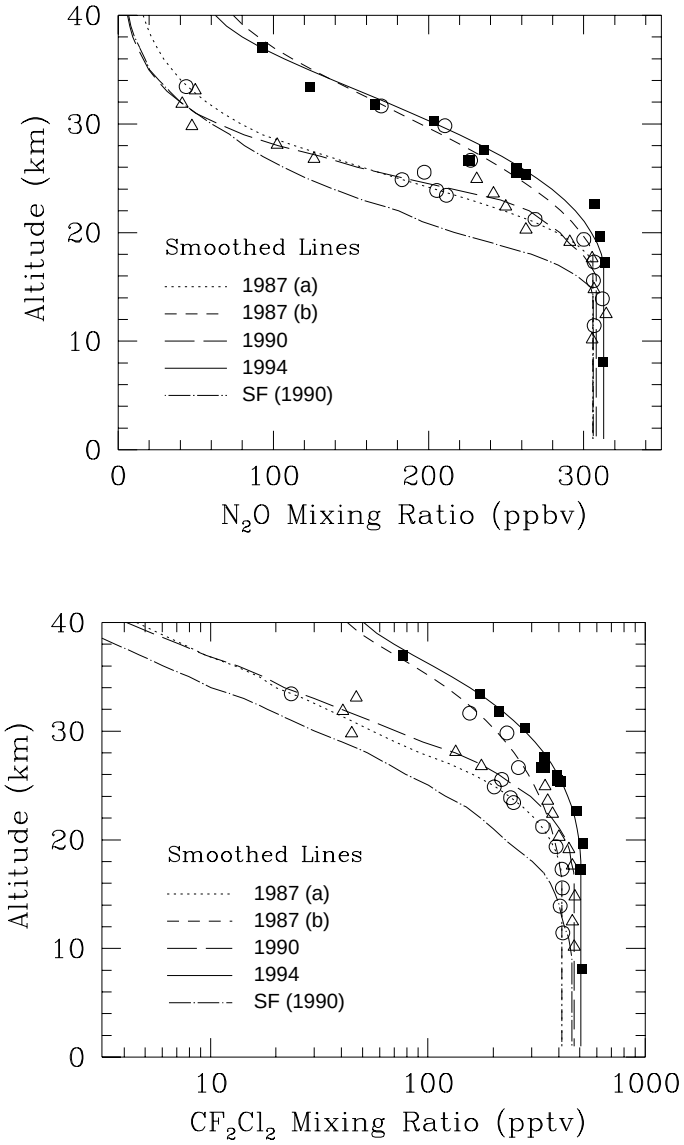

Figure 3.1: *Vertical profiles of N_2O (a: upper panel) and CFC-12 (b: lower panel) are smoothed for calculating the mixing ratio gradients to use in equation 3.4. Symbols are same as used in Figure 2.6. Southern France reference profiles [Fabian et al., 1996] are referred to as "SF".*

discussed in detail in section 2.3. The 1987 measurements over Hyderabad show a perturbation at around 25 km altitude. These divergences caused by atmospheric dynamics (any possibility of chemical sources is ruled out as these characteristics have been observed for all the long-lived species in the stratosphere) are subtle. In view of the later measurements in 1990 and 1994 two extreme cases have been chosen for the 1987 profiles, one with a higher gradient of mixing ratios in the stratosphere and the other with a lower gradient to provide an envelope of two mixing ratio profiles. Hereafter, the profile with the higher gradient will be referred as (a) and that with the lower gradient as (b). The exercise of interpolation could be carried out with much less ambiguity for the mixing ratio profiles measured during April 1990 and 1994 over Hyderabad and for the Southern France reference profiles.

3.1.4 Eddy diffusion profiles

Vertical eddy diffusion coefficients determined using equation 3.4 are shown in Figures 3.2a-d in comparison with earlier estimates. Inter-comparison of eddy diffusion coefficients measured by various techniques, at different locations and times, show a large variation over the entire height region. The K_z profile used by *McElroy et al.* [1974] shows the largest variation in the stratosphere; it increases from a minimum value of 2×10^3 cm^2s^{-1} at the tropopause and attains a value of 1.3×10^5 cm^2s^{-1} at around 40 km (Figure 3.2). The composite eddy diffusion profile of *Massie and Hunten* [1981] varies from $\approx4\times10^3$ cm^2s^{-1} at 17 km to $\approx4\times10^4$ cm^2s^{-1} at 40 km, with a constant value of $\approx10^5$ cm^2s^{-1} in the troposphere. The *NAS* [1979] values are embedded by these two profiles in the stratosphere. The estimated K_z profiles from N_2O and CFC-12 distributions during different balloon flight days from Hyderabad (tropics) and reference midlatitude profiles are discussed below.

K_z on March 27, 1987: A comparison of the calculated altitude profiles of eddy diffusion from the mixing ratio profiles of March 27, 1987 are also shown in Figure 3.2 [(a) and (b)]. These eddy diffusion coefficients obtained from mixing ratio profiles (a) are very close to those of *NAS* [1979] over most of the altitude range, but much higher than the composite profile of *Massie and Hunten* [1981] in the altitude region of 28 km and above, and lower than those of *McElroy et al.* [1974]. The altitude corresponding to the minimum K_z is observed at 20 km. In contrast, the other extreme case (b) produces almost a steady diffusion coefficient of about 7×10^4 cm^2s^{-1} throughout the altitude region of 19 to 38 km. The present estimates are close to the values measured *in situ*, in the height range of 15-28 km, using the expansion of

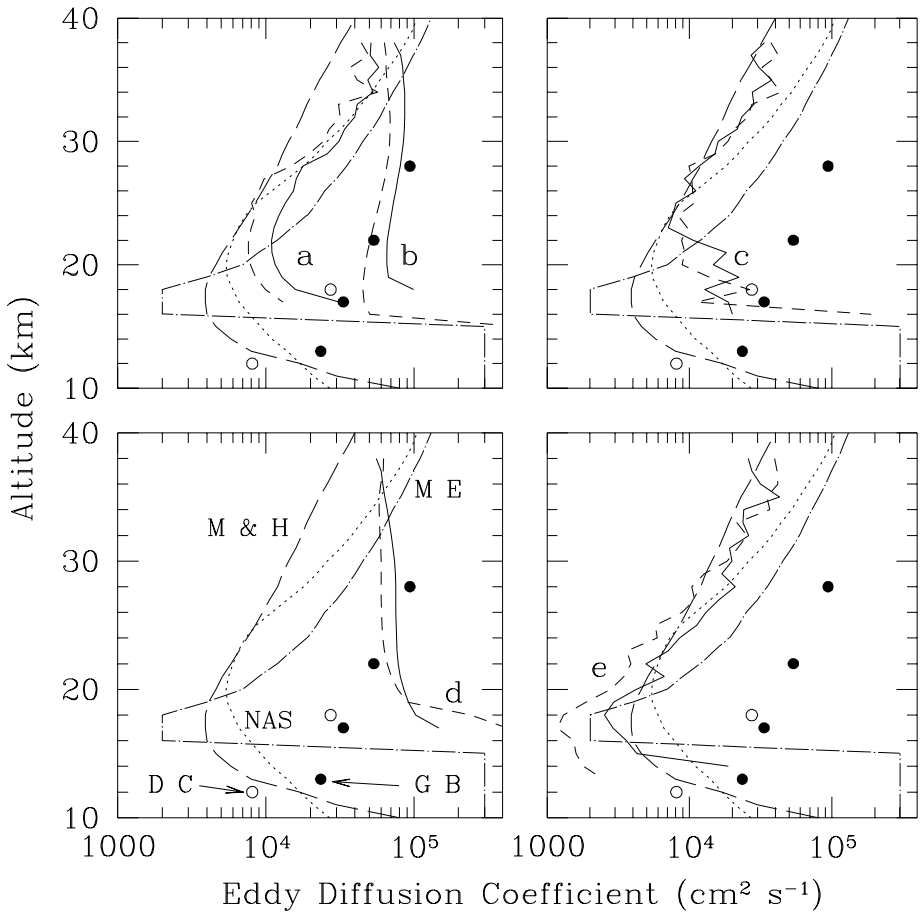

Figure 3.2: *Altitude profiles of eddy diffusion coefficients deduced from the mixing ratio profiles of N_2O (continuous line) and CFC-12 (small dashed line). Two profiles [(a) and (b)] are obtained using the extrema of mixing ratio gradients for the year 1987 as described in the text. Sets (c), (d) and (e) are calculated from the vertical profiles for the years 1990 and 1994 over Hyderabad and reference profiles over midlatitude, Southern France (44^0N), respectively. The present results are also compared with earlier studies (see Figure 3.2d) [M E (dashed-dot line): McElroy et al., 1974; NAS (dotted line): NAS, 1979; M & H (long dashed line): Massie and Hunten, 1981; D C (open circle): Chakrabarty et al., 1987; G B (filled circle): Beig, 1989].*

chemical puffs released at different heights over the same location during March 1985 and 1988 [*Chakrabarty et al.,* 1987; *Beig,* 1989] but the vertical trends are different. However, these results evaluated from N_2O and CFC-12 vertical distribution profiles show similar behaviour. They do not prohibit Holton's proposition of lifetime dependencies; the K_z values obtained from the N_2O profile are about ∼20% more than those obtained from the CFC-12.

K_z on April 9, 1990: Vertical eddy diffusion coefficients calculated from the 1990 measurements are also depicted in Figure 3.2 (c). These results are well within the limits of other measurements and their characteristics are in good agreement with NAS [1979] in the altitude region of 23 to 35 km. The transport gradient changes its sign at 23 km, which is high compared with previous results which are commonly observed at around 17-20 km. But it is apparent from the N_2O and CFC-12 profiles that there should have been higher transport coefficients in the altitude range of 22-25 km and below to sustain such high mixing ratios as shown in Figure 3.1a and 3.1b for April 9, 1990. There is no appreciable difference between the two K_z profiles obtained from both constituents. The small structures are observed due to inadequate smoothing of the altitude profiles.

K_z on April 16, 1994: The eddy diffusivity on April 16, 1994 shows a high (see Figure 3.2 (d)) and constant value ($\approx 7\times10^4$ cm^{2}s^{-1}) compared to previous results over the entire altitude region (20-38 km) and almost follows the characteristics of Figure 3.2 (b). However, these results do not exceed the maximum measured by *Chakrabarty et al.* [1987] and *Beig* [1989] over the same location.

K_z over midlatitude: All the above mentioned results are deduced using the vertical distributions measured over the equatorial region during different years. In order to investigate the latitudinal dependencies, eddy diffusion coefficients are also calculated using the reference mixing ratio profile of CFC-12 proposed by *Fabian et al.* [1996] and the vertical profile of N_2O [*Borchers et al.,* 1989] over Southern France (44^0N), which are shown in Figure 3.2e. These K_z profiles clearly indicate that its minimum value and corresponding altitude are in fairly good agreement with previous estimations [*McElroy et al.,* 1974; *Massie and Hunten,* 1981]. Above this altitude K_z values almost follow the results obtained by *Massie and Hunten* [1981], incorporating globally averaged vertical profiles of N_2O and CH_4, and photochemical loss terms, over the complete altitude region except for the minimum value which is also observed at the same altitude (17 km).

It has been noticed that, even after results of the uppermost few km

have been rejected for all the deduced eddy profiles, they show a decreasing tendency in the upper heights (a few km from the top) which could be due to the first term in equation (3.3). The contribution of this term reduces as the range of integration increases. The fluctuations observed in these profiles are also due to the lack of smoothness during interpolation and extrapolation of the mixing ratio profiles. It is also to be noted that the K_z values derived for the period of 1990 are due to the best possible fits to the corresponding mixing ratio profiles. Experiments were carried out by fitting two extreme profiles which take into account the unconventional variabilities in the mixing ratios above about 30 km altitude for N_2O and CFC-12 separately. The highest possible calculated diffusion coefficients, although higher than those shown in Figure 3.2c, remain much less than those calculated for 1987 (b) and 1994. The average of these two K_z (high and low) profiles almost gives rise to the profiles of both the gases presented.

3.1.5 Possible variabilities in K_z profiles

Large variabilities of the eddy diffusion coefficients in the troposphere up to the thermosphere have been reported [*McElroy et al.,* 1974; *Massie and Hunten,* 1981; *Beig,* 1989; *Fukao et al.,* 1994, etc]. Large latitudinal variations have also been observed [*Schmeltekopf et al.,* 1977]. These variabilities are mostly associated with the difference in space (latitude) and time (season) of the measurements and could also be caused by difference in measurement techniques (especially the K_z values deduced from the chemical constituents vary with their lifetimes and distributions). Although the natural variation of eddy diffusivity is unpredictable, the basic characteristics still remain unchanged. The various possibilities for these observed discrepancies and consistencies in comparison with existing results are discussed below.

Measurements of the vertical distributions of N_2O and CFC-12 over Hyderabad were conducted during the spring (March 27-April 16) of the years 1987, 1990 and 1994 and there are no measurements available for different seasons. Eddy diffusivity deduced from chemical tracers is commonly influenced by advection due to the mean horizontal circulations in the stratosphere related to the adiabatic heating rate. Since solar energy, the main source of heating in this part of the atmosphere, changes with solar activity, we look for a temporal correlation of these discrepancies with solar activity. The sunspot numbers were 11 and 16 on March 27, 1987 and April 16, 1994, respectively, near solar minima, and April 9, 1990 was during solar

maximum, with a sunspot number of 88 (Solar-Geophysical Data, NOAA). To incorporate the effects of change in the solar activity, the spectral distribution of the relative variation of solar irradiances has been adopted from *Brasseur and Simon* [1981]. The vertical eddy profiles from the 1990 distribution of mixing ratios are computed using the same photochemical model with enhanced solar intensity. These values are about 10% higher than those calculated earlier at all altitudes (not shown in Figure 3.2 but still not as high as those observed during March 27, 1987 (b) and April 16, 1994 (d).

The redistribution of N_2O in the stratosphere due to planetary-wave mixing in the winter hemisphere tropics to midlatitudes have been observed from satellite measurements [*Rundel et al.,* 1993]. A modeling study also predicts, from the distribution of atmospheric constituents of sufficiently long enough lifetime compared to quasi-horizontal circulation time scales, an upwelling over the tropics. However, we do not have any supporting data except the zonal and meridional winds as depicted in Figure 3.3 which are obtained by analyzing the balloon trajectories. The wind profiles during March 27,

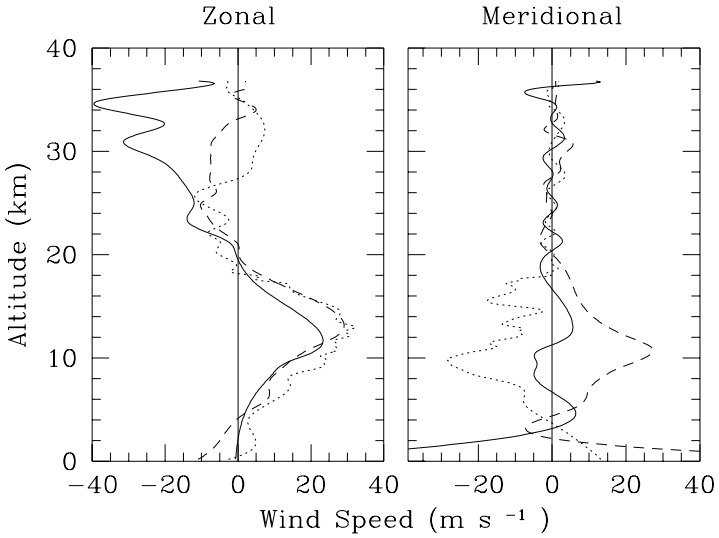

Figure 3.3: *Zonal and meridional winds derived over Hyderabad on the days of the balloon flights (dashed line: March 27, 1987, dotted line: April 9, 1990, and solid line: April 16, 1994). The wind fields on March 27, 1987 and April 9, 1990 are taken from Lal et al. [1994a].*

1987 and 9 April 1990 are taken from *Lal et al.* [1994a]. Horizontal winds show large variations in phase as well as in amplitude (∼0-35 m/s) in the troposphere. In the stratosphere, the meridional winds do not show much variation (0± ∼2 m/s), whereas the zonal winds vary with altitude in both

amplitude and phase. A comparison of the eddy profiles of 1987 (a), 1990, and 1994 with their respective wind fields suggest the requirement for advective motions to satisfy the distributions of the long-lived chemical constituents.

The small-scale turbulence produced in the stratosphere due to gravity wave breaking is well understood [*Weinstock,* 1984]. Stronger vertical wind shear caused by the mean zonal wind does not permit the propagation of waves in the stratosphere which leads to small cellular updrafts corresponding to wave breaking. According to a semi-theoretical approximation, 0.1 to 1 km thick 'gust layers' produced due to breaking of the internal gravity waves and internal inertio-gravity waves which are originated in the troposphere can also give rise to an eddy diffusivity of $\leq 10^5$ cm^{2}s^{-1} [*Yamanaka and Tanaka,* 1986]. This result does not conflict with the eddy coefficients derived from the 1987 (b) or 1994 mixing ratio profiles. The formation of these layers over the whole lower stratospheric height range can be suspected, however, evidences of the occurrence of multiple 'gust layers' have been reported [*Yamanaka and Tanaka,* 1986].

The energy provided by large scale ordered motions (e.g. the atmospheric wind) is directly proportional to the square of the vertical wind shear of the horizontal wind which can produce the largest eddies. The altitude profiles of Richardson number, R_i (a measure of the persistence of turbulent motions) have been calculated for the balloon flight days, using the following expression

$$R_i = \frac{w_B^2}{(\partial u/\partial z)^2 + (\partial v/\partial z)^2} \tag{3.7}$$

where w_B is the Brunt-Väisälä frequency calculated from the altitude profiles of potential temperature Θ(z) and acceleration due to gravity g(z), and $\frac{\partial u}{\partial z}$ and $\frac{\partial v}{\partial z}$ are the velocity shears due to the zonal and meridional winds, respectively. Results showing the height distributions of R_i for March 27, 1987, April 9, 1990, and 16 April 1994 are given in Figure 3.4. It is well accepted that turbulence can persist with the condition, $1 \leq R_i$, once it has been created [*Blix,* 1993], and $R_i \leq \frac{1}{4}$ is suggested as the condition required to develop turbulence. It is seen that the values of R_i satisfy the condition of persistent turbulence on April 16, 1994 at stratospheric altitudes (32-38 km). On April 9, 1990, R_i satisfies the condition for the maintenance of turbulence (at some times, even for its creation) in the troposphere and lower stratosphere. Such turbulence may provide the necessary transport to observe the higher mixing

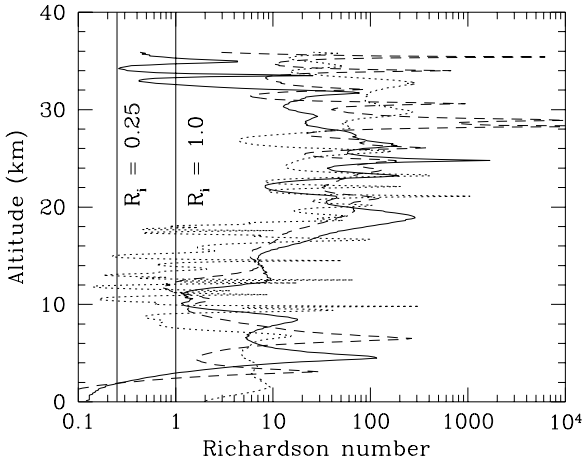

Figure 3.4: *Vertical profiles of Richardson number calculated from the wind and temperature profiles observed over the experimental site during the flights on March 27, 1987 (dashed line), April 9, 1990 (dotted line) and April 16, 1994 (continuous line).*

ratios in the lower stratosphere on April 9, 1990. There has been no significant evidence of turbulence on March 27, 1987. Thus, it appears that the vertical profiles of K_z estimated using the 1987 (a), 1990, and 1994 mixing ratio profiles of N_2O and CFC-12 are feasible.

The latitudinal dependencies of the eddy diffusivity are also very clear from the present results. The altitude corresponding to minimum eddies changes with tropopause height (it varies inversely with latitude), and values of the diffusion coefficients are significantly lower at higher latitudes. Similar results have also been reported by *Schmeltekopf et al.* [1977] based on extensive measurements of N_2O.

Finally, vertical profiles of the eddy diffusion coefficient are suggested [*Patra and Lal,* 1997] to define a range which is most likely be followed in the equatorial region at different times (Figure 3.5).

1) By averaging all the profiles of 1987 (a) and 1990 (c) gives the lower range of the K_z value which increase from a minimum value of $\sim 9\times10^3$ cm^2s^{-1} at around 23 km to $\sim 4.2\times10^4$ cm^2s^{-1} at 38 km. This feature is observed due to the fact that the predominant vertical wavelength of the gravity wave also increases with altitude, which has been shown using radar measurements [*Fukao et al.,* 1994, and references therein].

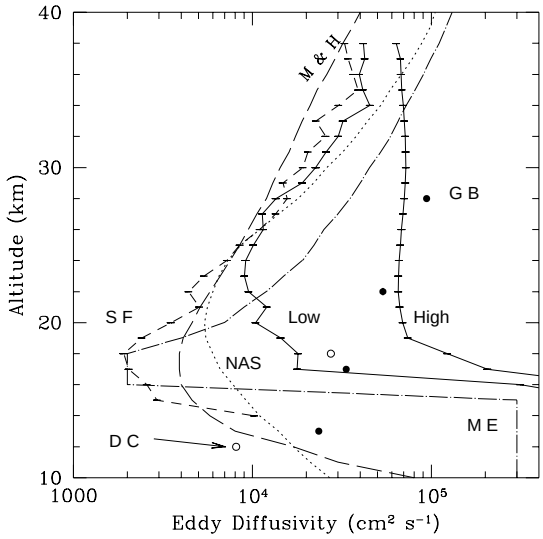

Figure 3.5: *Proposed minimum and maximum of vertical eddy diffusion profiles, K_z in the altitude range of about 17-38 km over a tropical site from 1987 to 1994 (see text for details). The error bars show a spread of $\pm$ 1 σ. A comparison has been made with M E: McElroy et al., 1974; NAS: NAS, 1979; M & H: Massie and Hunten, 1981; $\circ$: Chakrabarty et al., 1987; $\bullet$: Beig, 1989; and S F: average of the present results using the reference mixing ratio profiles over Southern France.*

2) The higher range of eddy diffusivity values is obtained by averaging the profiles of 1987 (b) and 1994 (d), giving an almost constant eddy coefficient of $\approx 7\times10^4$ cm^2s^{-1} throughout the stratosphere. High values of eddy diffusion coefficients have also been observed by others over the tropical region [*Schmeltekopf et al.,* 1977; *Chakrabarty et al.,* 1987; *Beig,* 1989]. The K_z values obtained using the N_2O and CFC-12 mixing ratio profiles over Southern France are smaller than those corresponding to the tropics at lower stratospheric altitudes (Figure 3.5).

3.1.6 Effect of K_z on model calculation

Figure 3.6 shows the CFC-12 loss rates, estimated by reversing equation 3.4 for the distribution observed on April 16, 1994 from Hyderabad and using the average minimum and maximum K_z values over Hyderabad. It shows large differences between the two calculated loss rates; higher loss rates results due to higher K_z values. The production of Cl atoms can be estimated by multiplying the loss rates by a factor of two as the photo dissociation of

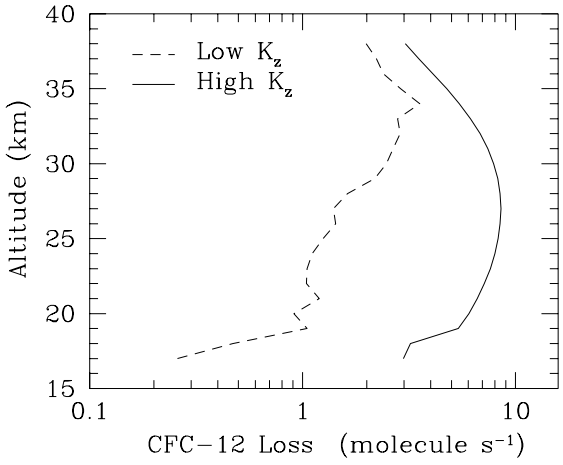

Figure 3.6: *Estimated loss rates of CFC-12 using the eddy diffusion coefficients suggested for a equatorial region and the smoothed mixing ratio profile measured on April 16, 1994 from Hyderabad.*

one CFC-12 molecule produces two Cl atoms. These results indicate that the production of Cl atom is dependent on the value of K_z, i.e. the supply of source gases into these altitude regions. It also plays a critical role in modeling the vertical profiles, thereby in the calculations of the stratospheric ozone loss [*Patra and Lal,* 1997].

3.2 Distributions of SF_6 and "Age" of Stratospheric Air

3.2.1 Introduction

Sulfur hexafluoride (SF_6) is emitted from the Earth's surface, purely due to anthropogenical activities, and is one of the most stable gases in the Earth's atmosphere. Due to its extremely inert nature and high dielectric strength, SF_6 is widely used (≈80% of its production) as an insulator in electrical and electronics equipments such as circuit breakers, transformers, and capacitors. There is almost no photochemical loss of SF_6 in the troposphere and lower stratosphere. Its major loss is considered to be the photodissociation by energetic Lyman α radiation at mesospheric heights leading to a long atmospheric lifetime [*Ravishankara et al.*, 1993]. Its abundance was only 0.03

pptv in the early seventies [*Lovelock*, 1971], however, its long-term measurements showed a global mean abundance of 3.44 parts per trillion by volume (pptv) and a growth rate of 6.9%/year in 1994 [*Maiss et al.*, 1996]. SF_6 is considered to be a better dynamical tracer than the conventional ones such as CO_2, CF_4, and C_2F_6 [*Bischof et al.*, 1985; *Schmidt and Khedim*, 1991; *Harnisch et al.*, 1996] because its sources are solely anthropogenic, it has a high growth rate, and is mostly emitted from the northern hemisphere. Recently, it has also been used as a tool for estimating the "age" of the stratospheric air [*Harnisch et al.*, 1996], which is useful in evaluating the ozone depletion potentials of various source gases [*Pollock et al*, 1992].

Sulfur hexafluoride is one of the most efficient greenhouse warming gases [*Ko et al.*, 1993], and since it has a high rate of increase in concentration and a long atmospheric lifetime, these combine to make SF_6 a possible candidate for future global warming. The atmospheric lifetime of SF_6 (varying from 300 to 3200 years) is still debated to a large extent; however, few attempts have been made to solve this problem [*Ravishankara et al.*, 1993; *Ko et al.*, 1993]. These uncertainties are probably due to the lack of information on reaction rates and photoabsorption cross sections. Proper estimation is needed for realistic evaluation of its impact on global change.

In this section, the vertical distribution of SF_6 measured during the balloon experiment on April 16, 1994 from Hyderabad is described. This profile is used to calculate the "age" of the stratospheric air over an equatorial site and to estimate its atmospheric lifetime [see also *Patra et al.,* 1997a].

3.2.2 Vertical profiles

Sulfur hexafluoride and various other CFCs were separated on a 4 m $\times$ 0.32 cm OD stainless steel column packed with PORASIL-L (80/100 mesh) as shown in the gas chromatogram (Figure 2.7a) during the analysis. The column temperature was varied from -10^0C to 225^0C during the analysis as described in Section 2.3.2. Reproducibility of these analyses was about 4% (at 99.7% confidence level) for SF_6 for samples from any altitude. The absolute concentrations are obtained by calibrating "PRL working standard" as well as a tropospheric sample with respect to a gravimetrically prepared standard [*Maiss et al.*, 1996] at the Institut für Umweltphysik, University of Heidelberg, Germany.

Vertical distribution of sulfur hexafluoride measured over Hyderabad on April 16, 1994 is shown in Figure 3.7. Volume mixing ratio of SF_6 de-

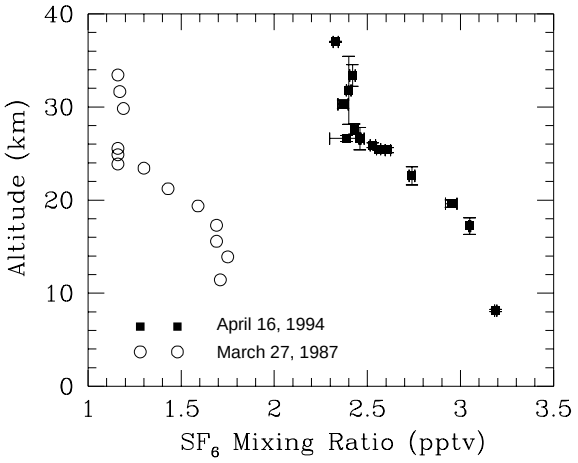

Figure 3.7: *Vertical profile of SF_6 measured over Hyderabad on April 16, 1994 (solid squares). Horizontal error bars are showing 1σ spread of the SF_6 VMRs and the vertical bars are indicating the altitude range of air sampling. The vertical distribution on March 27, 1987 from the same location [from Harnisch et al., 1996] is also shown (open circles) for a comparison.*

creases slowly from a tropospheric value of 3.18±0.006 (1σ) pptv at around 8 km to 3.05±0.005 (1σ) pptv near the tropopause (at 17.2 km). In the lower stratosphere its concentration decreases at a much faster rate (∼0.06 pptv/km), attaining a value of 2.43±0.02 (1σ) pptv at around 27 km. However, the decrease rate is slower (∼0.01 pptv/km) again in the altitude region above 27 km. Hence the stratosphere is divided into two separate regions as suggested by *Bischof et al.* [1985]: the transition layer, which starts immediately after the tropopause and extends up to about 27 km, and the undisturbed upper stratosphere, above the transition layer. At the ceiling altitude of this flight (∼37 km) its concentration is observed to be 2.33±0.05 (1σ) pptv. The decrease in abundance with altitude in the various altitude regions is dependent on the coupled chemical and dynamical processes and has different atmospheric implications.

Measurement on the vertical profile of this gas is very limited in the tropical region; the only other measurement available in the literature is that of *Harnisch et al.* [1996] obtained from the air samples collected on March 27, 1987 over Hyderabad during a collaborative experiment between PRL and MPAE. A comparison (see Figure 3.7) with the present measurement also shows a distinct large increase in its concentration from 1987 to the present at all the altitudes; however, the main features are similar.

Loss mechanisms of SF_6 in the atmosphere are not yet understood clearly. There have been very few efforts to explain its vertical profiles, which were observed mainly in the lower stratosphere. *Ko et al.* [1993] found that the model vertical profile computed assuming a loss rate similar to that of CFC-11 in the stratosphere appears to follow the same trend as the SF_6 mean vertical profile retrieved from the ATMOS/ATLAS 1 occultation spectra observed during March-April 1992 in the latitude range 27.6^0S to 54.2^0S [*Rinsland et al.*, 1993]. But comparisons of the simultaneously measured vertical distributions of CFC-11 (Figure 2.8b) and SF_6 (Figure 3.7) on April 16, 1994, and March 27, 1987, do not seem to support their result.

We have used the NASA/GSFC two-dimensional (2D) photochemistry and transport model to simulate the distribution of sulfur hexafluoride. The GSFC 2D model is described by *Jackman et al.* [1996]. Its vertical range, equally spaced in log pressure, is from the ground to approximately 90 km (0.0024 mbar) with grid spacing of approximately 2-km. Latitudes range from 85^0S to 85^0N with a 10^0 grid spacing. The climatologically based transport consists of a residual circulation and diffusion computed by using a 17-year average (1979-1995) of temperature data from the National Center for Environmental Prediction (NCEP). The transport fields change daily but repeat yearly.

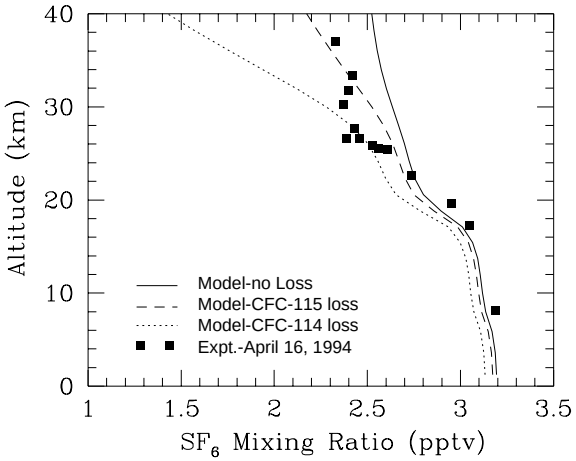

Figure 3.8: *Balloon-borne measurements of SF_6 obtained on April 16, 1994, and two-dimensional model results computed assuming various loss rates (see text for details) at NASA/GSFC.*

Vertical profiles of SF_6 have been computed using the tropospheric inventories proposed by *Maiss et al.* [1996]. In this calculation, three different loss rates are assumed: With no photochemical loss the model results are

in fairly good agreement with the observed abundances; however, because of the limitations of the 2D model, detailed structures observed in the measurements could not be explained. Loss rates identical to those of CFC-115 and CFC-114 have also been used to compute SF_6 vertical distributions. The latter two derived profiles show much larger gradients, particularly above the transition layer. These results are depicted in Figure 3.8 along with the distribution on April 16, 1994. This comparison clearly suggests that the vertical profiles of sulfur hexafluoride follow the no loss type of trend in the vertical distribution and do not show any significant photochemical loss in the stratosphere.

3.2.3 "Age" of the stratospheric air

Because there is no significant chemical loss of SF_6 in the stratosphere, the decrease in volume mixing ratio (VMR) with altitude is attributed to the transport time of the air parcel from the troposphere to the various stratospheric altitudes. Time series measurements of SF_6 at the surface exhibit a quadratic increase in its abundance [*Maiss et al.*, 1996]. This near-linear increasing trend in mixing ratio of an atmospheric constituent with no measurable loss in the troposphere and the stratosphere is appropriate to estimate the "age" of stratospheric air from its vertical profile [*Hall and Plumb*, 1994]. When we correlate the surface VMR of SF_6 as a function of time with stratospheric VMRs, the estimated "age" of the air varies from 4.1 to 4.6 years with an average value of 4.26 ± 0.17 years (1σ) in the altitude region of about 27 to 37 km on April 16, 1994 (Figure 3.9). These "age" values are comparable with the theoretical age estimated using a semi-Lagrangian chemical transport model driven by archived wind data from NCAR MACCM2 (Middle Atmosphere version of NCAR Community Climate Model version 2) general circulation model for 18^0N during March [*Waugh et al.*, 1997]. The time lags between stratospheric and tropospheric air observed by various authors are given in Table 3.1. A mean delay time between tropospheric and stratospheric air (altitude more than 22 km, 44^0N) was reported to be 5 years from the vertical distributions of CO_2 measured over midlatitude [*Bischof et al.*, 1985], a result supported by *Schmidt and Khedim* [1991], who found it to be 5.6 years. Recent observations of SF_6 over midlatitude and arctic polar region inferred an age of air above 19 km altitude to be 3.8 years and 5.7 years, respectively; however, the age of stratospheric air continues to increase above 25 km (8 to 9-year old air was found at 30 km) [*Harnisch et al.*, 1996]. This effect is probably due to the subsidence of high-altitude air inside the polar vortex. Inside the arctic polar lower stratosphere the age of air has been adopted to

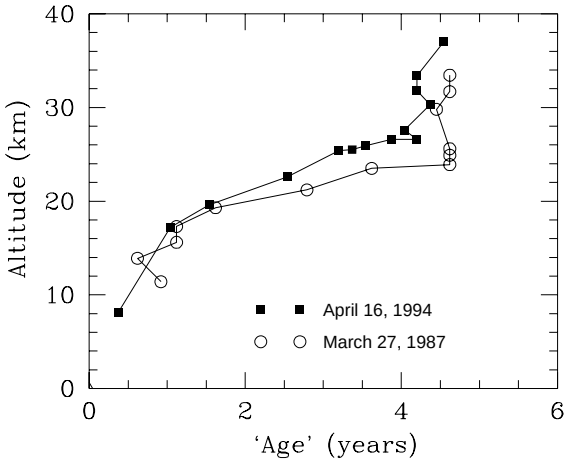

Figure 3.9: *A comparison of "age" of air estimated from the measured vertical profiles of SF_6 on March 27, 1987 [from Harnisch et al., 1996] and on April 16, 1994 over Hyderabad.*

be 4 years in evaluating the ozone depletion potentials [*Pollock et al.*, 1992]. Below 17 and above 27 km the age of air does not change much with altitude. The regions below 17 and above 27 km are mixed much more rapidly than between the two regions.

Table 3.1: *"Age" of stratospheric air calculated from long-lived atmospheric trace gases over various locations over a period of time.*

Location	Period	Gas	Age, years	Reference
44^0N	1979-1984	CO_2	~5	*Bischof et al.* [1985]
44^0N and 52^0N	1976-1988	CO_2	5.6±1.1	*Schmidt and Khedim* [1991]
44^0N and 68^0N	1988-1990	CO_2	2.3±0.3	- do -
62^0N-89^0N	1989	F-115	4.4±1.25	*Pollock et al.* [1992]
44^0N	1983 and 1993	SF_6	3.8	*Harnisch et al.* [1996]
68^0N	1992 and 1995	SF_6	5.7	- do -
17.5^0N	1987	SF_6	4.7	- do -
17.5^0N	1994	SF_6	4.26±0.17	this work

3.2.4 Atmospheric lifetime of sulfur hexafluoride

Nitrous oxide (N_2O) and CFC-12, which have longer photochemical lifetimes than the quasi-horizontal transport timescales, attain 'slope equilibrium' and exhibit a linear relationship that can be related in turn to the ratio of their

atmospheric lifetimes by the following equation [*Plumb and Ko*, 1992]:

$$\frac{\tau_x}{\tau_y} = \frac{dy}{dx} \cdot \frac{\sigma_x}{\sigma_y} \tag{3.8}$$

where the σs are representative of the tropospheric mixing ratios, dy/dx is the slope of the correlation curve, and the τs are atmospheric life times of the gases under study. Similar compact relationships of simultaneously measured N_2O and CFC-12 with SF_6 are investigated here (Figure 3.10). Vertical distribution profiles of N_2O and CFC-12 are taken from *Lal et al.* [1996]. Third-order quadratic fits are found to be in good agreement in the complete altitude range (not shown); however, above the transition layer, where the

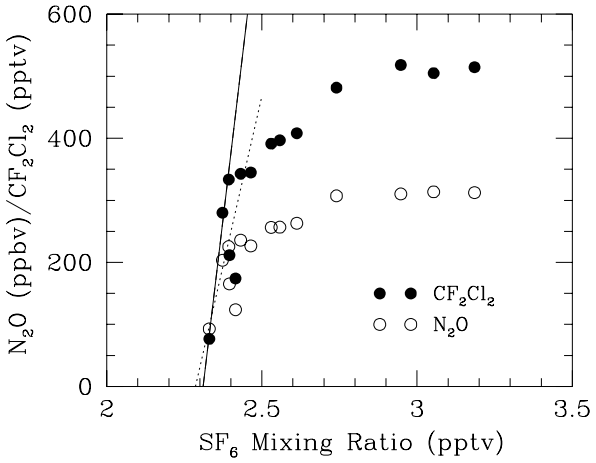

Figure 3.10: *Middle stratospheric intercorrelations of sulfur hexafluoride with N_2O and CFC-12 (CF_2Cl_2). The straight lines can be expressed as (1) dashed line: [N_2O] (ppbv) = 2181.8 [SF_6] (pptv) - 4987 (R^2=0.97) and (2) solid line: [CFC-12] (pptv) = 4195.2 [SF_6] (pptv) - 9693 (R^2=0.99) for SF_6 mixing ratio $\leq$ 2.395 pptv.*

loss of SF_6 due to reactions with OH, O(^1D) are proposed, simple linear fits are apparent. Using equation (3.8) and various probable interrelationships between SF_6 and N_2O and SF_6 and CFC-12 for $SF_6 \leq 2.5$ pptv, we find an average atmospheric lifetimes of SF_6 of 1937$\pm$432 (1σ) years. The best fits for SF_6 VMR $\leq$ 2.395 pptv are only shown in Figure 3.10 (similar correlations of 1987 data have not been used for calculating lifetime, as we have observed a significant effect of dynamical perturbations in the N_2O and CFC-12 vertical profiles). Atmospheric lifetimes of N_2O and CFC-12 are taken to be 120 and 102 years, respectively, for these calculations [*WMO*, 1995]. Lifetimes calculated from the best fits (as shown in Figure 3.10) are in good agreement

with each other. However, this value is much shorter than the best estimate of *Ravishankara et al.* [1993], which is 3200 years. *Ko et al.* [1993] calculated an effective atmospheric lifetime of about 900 years with an extra loss term included due to the photodissociation of SF_6 caused by UV radiation ($\lambda \leq 240$ nm). To check for validity of equation (3.8) for the tropical region, assuming a lifetime of 102 years for CFC-12, we calculated an atmospheric lifetime of 119 years for N_2O, which matches very well with that used in this calculation.

3.3 Vertical Profiles of CH_4 and Quasi-Vertical Mixing in the Tropics

3.3.1 Introduction

Methane is one of the most important greenhouse gases in the earth's atmosphere contributing about 19% to the anthropogenic radiative forcing during 1992 [*IPCC*, 1996]. It also takes an active part in tropospheric and stratospheric O_3 chemistry [*Stolarski and Cicerone*, 1974; *Crutzen*, 1988]. Due to its atmospheric lifetime being longer than the transport mixing time in the stratosphere, CH_4 has been used to study various transport processes, such as the derivation of eddy diffusion coefficients [*McElroy et al.*, 1974] and more recently the subsidence in the polar stratosphere [*Schoeberl et al.*, 1995]. It is well established that the tropical region experiences strong upwelling, thereby, playing an important role in transporting tropospheric constituents into the stratosphere. Recently, mixing of the extra-tropical air with the equatorial air in the stratosphere has been suggested leading to reductions in the mixing ratios of various compounds in the tropical stratosphere from what would be the case without such mixing [*Minschwaner et al.*, 1996]. However, due to much larger vertical gradient compared to the horizontal gradient in the concentrations of some of the long-lived trace gases in the stratosphere (e.g. CFC-12, N_2O, CH_4 etc), downward transport in the tropical stratosphere likewise could lead to such an observation.

In this section we compare vertical profiles of CH_4 measured over a tropical site on April 16, 1994 with those obtained earlier on March 27, 1987 and April 9, 1990. An attempt has also been made to compare these results with HALOE satellite observations of CH_4. Using constituent mixing ratio correlationships, possible dynamical disturbances which explain the observed features in the stratospheric distributions are discussed.

3.3.2 Experimental procedure

Air samples, collected in the altitude range of 8-37 km both during ascent and descent of the balloon during a balloon flight on April 16, 1994 from Hyderabad (17.5^0N, 78.6^0E), are also analyzed for CH_4 and CO using a gas chromatograph equipped with flame ionization detector (GC-FID) within about 3 months of collection. CH_4 and CO were separated on a 0.32 cm OD and 4 m long stainless steel column packed with molecular sieve 13X operated isothermally at 35^0C. A laboratory standard air (PRL-GC-STD 94), calibrated apriori with respect to the synthetic mixtures supplied by NIST and Linde gas, were used for absolute calibration. An analytical precision of about 5 ppbv (1 σ) was achieved in these analyses. However, the errors in absolute concentration could be in the range of 2-3% (1 σ).

The Halogen Occultation Experiment (HALOE) has been measuring the global distribution of CH_4 together with various other constituents, temperature and pressure since its launch on board the Upper Atmospheric Research Satellite (UARS) on September 12, 1991 [*Russell et al.*, 1993; *Schoeberl et al.*, 1995]. CH_4 is measured daily during solar occultations at sunrise and sunset using an optical correlation instrument operating at 3.3 μm wavelength. Here, a few selected profiles measured by HALOE during March-May 1994 for the latitudes nearest to the balloon launching site (17.5^0) are used for comparison.

3.3.3 Results and Discussion

The vertical distribution of methane measured on April 16, 1994 over Hyderabad (17.5^0N, 78.6^0E) is shown in Figure 3.11. The volume mixing ratio (VMR) of CH_4 remain nearly constant (1.71 ppmv) at tropospheric altitudes and decrease slowly in the stratosphere. The VMRs at 26 km and 37 km are 1.53 ppmv and 1.14 ppmv, respectively. For comparison we have also plotted (Figure 3.11) the earlier measurements from the same location on March 26, 1987 [*Borchers et al.*, 1989] and April 9, 1990 [*Lal et al.*, 1994]. These profiles match well in the troposphere. In the stratosphere, they show the following large variations. 1) A prominent kink is observed near 25 km in the profile obtained on March 27, 1987 although the measurements in the 30-32 km region do not considerably deviate from the 1994 profile (the sample from the highest altitude again show a strong deficit). 2) The vertical profile observed on April 9, 1990 shows much faster decrease than that on April 16, 1994 in the altitude range of 20-32 km, returning to normal at 33 km.

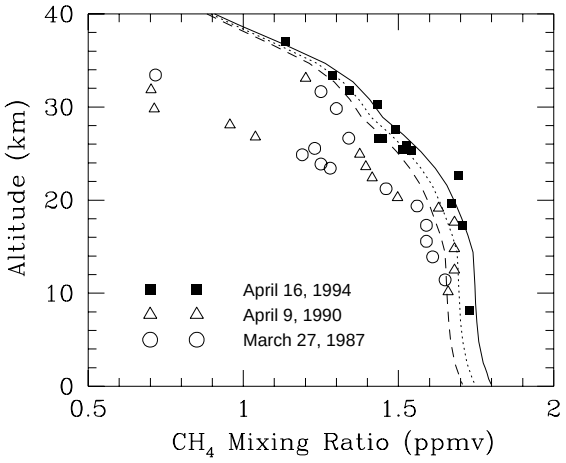

Figure 3.11: *Vertical distribution of CH_4 measured on April 16, 1994 compared with earlier measurements made on March 27, 1987 and April 9, 1990 from Hyderabad, India. MPIC-2D model results computed for the days of measurements for 15^0N are also shown as lines (continuous line for April 16, 1994; dashed line for April 9, 1990; dotted line for March 27, 1987.*

The CH_4 vertical distributions are also simulated using the MPIC-2D model for the three measurement periods together with the observed distributions are also shown in Figure 3.11. The CH_4 profile on April 16, 1994 follows the model simulated profile and hence represents mean tropical stratospheric conditions. The distributions observed on March 9, 1987 and April 9, 1990 clearly show large deviations from the mean. Such large divergences can only be caused by dynamical processes as discussed earlier in §2.3.

Figure 3.12 shows HALOE measured CH_4 vertical profiles around 17.5^0 during 1994 in both hemispheres (see figure for details). CH_4 concentrations measured on March 30 and April 6, 1994 are consistently lower than the *in situ* measurements of April 16, 1994 in the entire altitude region. A fairly good agreement is seen above 30 km for profiles on May 2, 1994 in the northern hemisphere and on March 26, 1994 in the southern hemisphere. It is well understood that during the spring the core of the tropical upwelling shifts from the equator to higher latitudes in the spring hemisphere. It can also be seen from the global distributions of CH_4 and N_2O [*Roche et al.*, 1996] that the "bulge" observed over $\sim 20^0$S in January, which is a characteristic of upwelling, has crossed the equator during March-April. Our measurement site is located near the edge of the upwelling stream. Therefore, we believe that the balloon measured CH_4 profile on April 16, 1994 and HALOE profiles

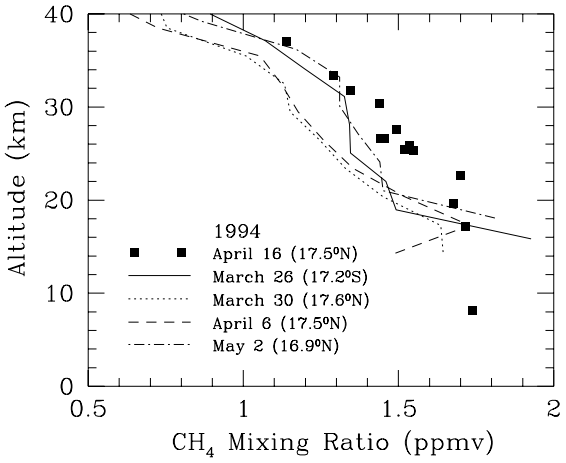

Figure 3.12: *Inter-comparison of balloon measurements on April 16, 1994 from Hyderabad (17.5^{0}N, 78.6^{0}E) and HALOE observations in early 1994 are shown as continuous line: March 26, 1994 (17.2^{0}S, 72.0^{0}E) during sunset; dotted line: March 30, 1994 (17.6^{0}N, 72.0^{0}E) during sunset; dash line: April 6, 1994 (17.5^{0}N, 65.8^{0}E) during sunrise; dash-dot line: May 2, 1994 (16.9^{0}N, 136.8^{0}E) during sunrise. Unpublished HALOE data are obtained from Jim Russell and Patrick Purcell [personal communication, 1996].*

of March 26, 1994 (17.2^{0}S) and May 2, 1994 (16.9^{0}N) are typical of a tropical upwelling region. The vertical distributions obtained on March 30, 1994 (17.6^{0}N) and April 6, 1994 (17.5^{0}N) by HALOE as well as the *in situ* measurements on March 27, 1987 and April 9, 1990 are affected by downward or quasi-horizontal exchange with air from higher latitudes. For instance, *Minschwaner et al.* [1996] found as much as 70% of air entrainment from midlatitude into the tropics.

Transport times from the troposphere to various stratospheric altitudes (also known as the 'age' of stratospheric air) have been calculated, using the vertical profiles of sulfur hexafluoride (SF_6) over the same location on March 27, 1987 [*Harnisch et al.*, 1996] and April 16, 1994 [*Patra et al.*, 1997a]. SF_6 measurements on April 9, 1990 are not available. A comparison (Figure 3.9) of these two 'age' distributions suggests that the 'age' of the stratospheric air at altitudes around 25 km was much higher (about 1.5 years) and was consistently higher at all stratospheric altitudes on March 27, 1987 than on April 16, 1994 with a much faster gradient inside the transition layer [see section 3.2.3 for details]. The transition layer on March 27, 1987 was found to end rather abruptly at around 24 km which is about 4 km lower than on April 16, 1994. It may be explained by stronger quasi-vertical

or horizontal mixing with higher layers around 24 km on March 27, 1987.

Mixing ratio correlations exhibit compact relationships for the species which are in slope/gradient equilibrium [*Plumb and Ko*, 1992]. Figures 4.13 and 4.14 show the correlation plots of CH_4 with N_2O and CFC-12, respectively for three vertical profiles. Although linear relations are apparent, there are significant differences in the slopes that are determined for April 16, 1994 (2.367 and 0.001226 from N_2O vs CH_4 and CFC-12 vs CH_4, respectively) compared to April 9, 1990 (3.452 and 0.002127 from N_2O vs CH_4 and CFC-12 vs CH_4, respectively), and March 27, 1987 (3.259 and 0.002031 from N_2O vs CH_4 and CFC-12 vs CH_4, respectively). However, N_2O vs CFC-12 correlation plots do not show such large differences (not shown here). Lower slopes on April 16, 1994 compared to other two days suggest a phenomenon which would differentially affect the vertical distributions of CH_4 and other two gases.

At stratospheric altitudes CH_4 has lower rate of decrease in mixing ratios with respect to latitude and altitude due to its longer chemical lifetime than N_2O and CFC-12 [see for example *Andrews et al.*, 1987]. Hence, it is suggestive that the difference in the slope can arise due to transport of air parcel from higher to lower altitudes in a quasi-vertical plane and/or due to quasi-horizontal mixing of extra-tropical and tropical air. The zonal mean altitude-latitude maps of CH_4 and N_2O also indicate suppressions of mixing ratio contours in the spring stratosphere [*Russell et al.,* 1993; *Roche et al.*, 1996]. For instance, it has also been seen that the slopes obtained for March 27, 1987 and April 9, 1990 are quite similar to those which can be calculated from the midlatitude distributions [*Fabian et al.*, 1996 and references therein] for these species. It can easily be seen that in normal atmospheric conditions and assuming no mixing (e.g. the distribution obtained on April 16, 1994 and the model simulation), the air at around 25 km on March 27, 1987 corresponds to an air parcel at 35 km and the air at around 30 km on April 9, 1990 corresponds to that of 41 km if the undisturbed stratospheric profiles are considered. Similarly, if only the horizontal mixing is considered the transport of air parcel could come from the latitude range of 55-65^{0}N on the two disturbed days. These altitudes and latitudes can also be consistently determined for N_2O and CFC-12 distributions [*Patra et al.,* 1997d]. As the these atmospheric constituents show concentration gradients with both latitude and altitude, it is not possible to clearly distinguish the source regions with these data sets.

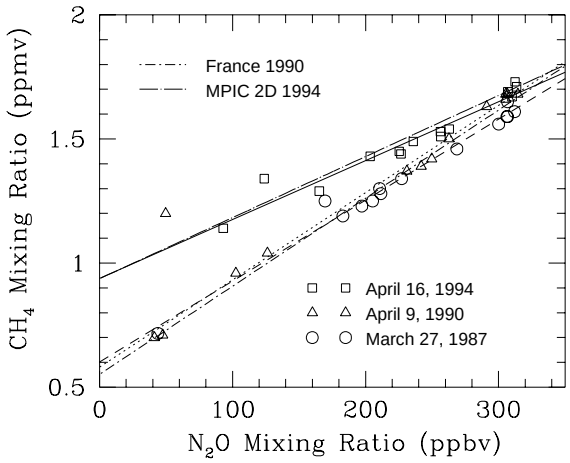

Figure 3.13: *Mixing ratio correlation plots between N_2O and CH_4 measured simultaneously on March 27, 1987, April 9, 1990, and April 16, 1994. The linear inter-relations are $[CH_4]$ (ppmv) = 3.259$[N_2O]$ (ppmv) + 0.60 (coefficient of determination, R^2=0.98), $[CH_4]$ (ppmv) = 3.452$[N_2O]$ (ppmv) + 0.57 (R^2=0.99), and $[CH_4]$ (ppmv) = 2.367$[N_2O]$ (ppmv) + 0.91 (R^2=0.97), respectively. Correlations obtained using MPIC 2D model result (long dash-dotted line) and midlatitude reference profiles (short dash-dotted line) are shown for comparison.*

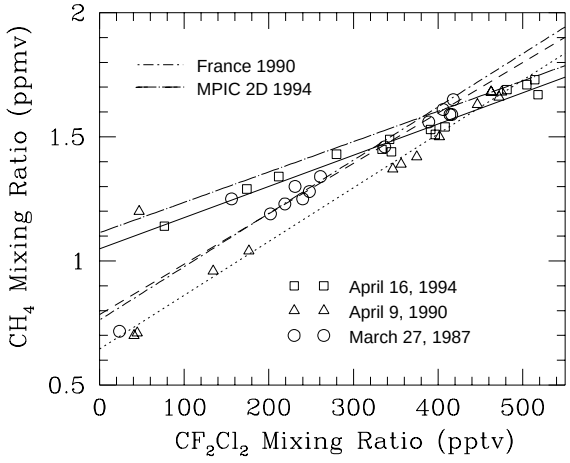

Figure 3.14: *Same as Fig. 4.13 but with CFC-12. The linear fits are $[CH_4]$ (ppmv) = 2031[CFC-12] (ppmv) + 0.78 (R^2=0.95), $[CH_4]$ (ppmv) = 2127[CFC-12] (ppmv) + 0.63 (R^2=0.99), and $[CH_4]$ (ppmv) = 1226[CFC-12] (ppmv) + 1.03 (R^2=0.96), respectively for March 27, 1987, April 9, 1990, and April 16, 1994.*

Chapter 4

Chlorine and Bromine Partitioning in the Stratosphere

4.1 Introduction

Large stratospheric ozone depletion, observed particularly in the high and mid-latitudes, is caused by the chemicals released due to human activities on the Earth's surface [*WMO*, 1995], through the catalytic chemical reactions involving mainly the reactive Cl and Br radicals as discussed in §1.3. A measure of ozone destruction by these specific groups of species are related to the amount of *inorganic* chlorine and bromine (Cl_y and Br_y) present in the stratosphere. They consist of both reactive and non-reactive forms of Cl and Br atoms and are assumed to be formed only in the stratosphere from several species containing Cl and Br atoms (halocarbons), which are transported from the troposphere. The sources of these halocarbons are well known to be located only on the Earth's surface and are transported to the stratosphere mainly through the tropical tropopause. The total abundance of Cl atom weighted halocarbons are referred to as *organic* chlorine (CCl_y) and that of Br atom weighted halocarbons are called as *organic* bromine (CBr_y).

The tropical tropopause is the most active region in transporting the source gases from the troposphere to the stratosphere, it is also important to estimate the amount of organic/inorganic chlorine and bromine explicitly

for this region. Due to the long residence times of both inorganic and organic halogens in the stratosphere, the tropical region can be treated as the source region. Accurate accounts of total chlorine/bromine (Cl_{total}/Br_{total}) in the stratosphere and further assessments of their partitioning in to organic and inorganic chlorine/bromine are often difficult as it requires accurate simultaneous measurements of vertical profiles of halocarbons and determination of "age" of stratospheric air. Only recently such estimations are made for the lower stratosphere (up to about 20 km) using halocarbon distributions obtained during Airborne Arctic Stratospheric Expeditions (AASE) [*Woodbridge et al.*, 1995; *Daniel et al.*, 1996].

It is well recognized that the increase in chlorine and bromine loading leads to larger loss in the total ozone [see for example *WMO,* 1995; *Jackman et al.*, 1996]. Stringent protocols have been signed to phase out halocarbons, which are deleterious to the ozone layer. However, it is demonstrated that the amount of inorganic halogen (defined as chlorine and bromine equivalent to chlorine) to be released in the stratosphere is comparable to that which can be estimated from the CCl_y and CBr_y abundances present in the troposphere 3 to 5 years before [*Montazka et al.*, 1996]. Such delayed response essentially arises because of the time lag that an air parcel takes to reach the specific stratospheric region from the tropical tropopause.

This transport time required for the tropospheric air to move upward is often referred to as 'Age' which is currently being used extensively as an useful diagnostic tool to study the dynamical properties of the stratosphere [e.g., *Patra et al.*, 1997d]. It has always been a difficult task [see *Daniel et al.,* 1996] to choose a suitable species for estimating the age of stratospheric air, with well established tropospheric trends and no measurable loss due to photodissociation and chemical reactions in the stratosphere, to be ideal. Age is traditionally estimated from the spatial distributions of long-lived trace gases, such as CO_2 [*Bischoff et al.*, 1985] and CFC-115 [*Daniel et al.*, 1996] with greater caution. However, it has become easy with the availability of vertical distributions of sulfur hexafluoride (SF_6) [*Harnisch et al.*, 1996; *Patra et al.*, 1997a] to estimate the "age" of the stratospheric air.

In this Chapter, we estimate the amount of chlorine and bromine released from most of the important source gases. The relative efficiencies of chlorine and bromine released in the atmosphere due to various halocarbons has been detailed by *Daniel et al.* [1996]. The main advantage of this study is the simultaneous measurements (three times) of source gases including SF_6 (for "age" determination) up to about 35 km over a period of 1987 to 1994 which covers the time of highest chlorine and bromine loading. The peak in

the ozone mixing ratio profiles is also observed in this height region. Using the reported tropospheric growth rates of individual species and estimated age of air, the vertical profiles of Cl_{total}, CCl_y, and Cl_y have been calculated using the vertical distributions of halocarbons which constitute about 99% of the total atom weighted chlorine at the tropopause level. Distributions of Br_{total}, CBr_y, and Br_y are also derived, using the profiles of three bromine containing gases, viz., halon-1211, halon-1301, and CH_3Br which constitute about 94% of the bromine loading into the stratosphere. Finally, these CCl_y, Cl_y, CBr_y, and Br_y abundances are correlated with chemical tracers like N_2O, CFC-12, CFC-113, and compared with previous estimates and 2D model results.

4.2 Estimation of Vertical Distributions

4.2.1 In situ measurements

Using the balloon-borne cryosampler and subsequent gas chromatographic analyses of the collected air samples, vertical distributions of trace gases have been obtained on March 27, 1987, April 9, 1990, and April 16, 1994 from Hyderabad, India as described in *Chapters 2 and 3. Another set of vertical profiles measured using similar techniques from GAP, France (44^0N) on June 23, 1987 [based on work done at Max Planck Institute for Aeronomy, Lindau, 1987; Borchers et al.,* 1989] and the reference profiles suggested for mid-latitude based on a number of vertical profiles obtained from the same location [*Fabian et al.,* 1996] are used to find the mixing ratio inter-correlations. These data sets are also used to study the latitudinal variations of chlorine loading and its partitioning in the stratosphere. The locations and available profiles for various species are listed in Table 4.1.

4.2.2 Semi-theoretical approach

Since the vertical profiles of some of the important source gases are not available in all sets of measurements, a semi-theoretical approach has been adopted to construct the missing profiles from their mixing ratio correlations with CH_4, CFC-12 or CFC-11 (selected based on their simpler relationships) using the available data sets. Measurements of the long-lived gases on March 27, 1987 and April 9, 1990 are disturbed by the dynamical influences [*Patra et al.*, 1997d] which forced us to check the validity of such correlations in

Table 4.1: *Details of the chemical species used in this calculation. Species those are not measured have been estimated using semi-theoretical approach (discussed in the next section).*

Place and Year	Species measured	Species not measured
Hyderabad (17.5^0N) - March 27, 1987	SF_6, CH_4, N_2O, $CFCl_3$ (CFC-11), CF_2Cl_2 (CFC-12), CF_3CCl_3 (CFC-113), CF_4CCl_2 (CFC-114), CF_5CCl (CFC-115), $CHClF_2$ (HCFC-22), CH_3Cl (methyl chloride), CF_2ClBr (halon-1211), CF_3Br (halon-1301)	CCl_4 (carbon tetrachloride), CH_3CCl_3 (methyl chloroform), CH_3Br (methyl bromide)
Hyderabad (17.5^0N) - April 9, 1990	CH_4, N_2O, carbon tetrachloride, CFC-11, CFC-12, CFC-113, CFC-114, HCFC-22, methyl chloroform, methyl bromide, halon-1211, halon-1301	SF_6, CFC-115, methyl chloride
Hyderabad (17.5^0N) - April 16, 1994	SF_6, CH_4, N_2O, CFC-11, CFC-12, CFC-113, CFC-114, halon-1211, halon-1301	carbon tetrachloride, CFC-115, HCFC-22, methyl chloroform, methyl chloride, methyl bromide
GAP, France (44^0N) - June 23, 1987	CH_4, N_2O, CFC-11, CFC-12, CFC-113, CFC-114, CFC-115, HCFC-22, halon-1211, halon-1301	carbon tetrachloride, methyl chloride, methyl chloroform, methyl bromide
Southern France (44^0N) - Reference 1990	CH_4, N_2O, carbon tetrachloride, CFC-11, CFC-12, CFC-113, CFC-114, CFC-115, HCFC-22, methyl chloroform, methyl chloride, halon-1211, halon-1301, methyl chloride, CFC-115	SF_6, methyl bromide

diverse atmospheric conditions. Inter-correlations of dynamically disturbed species (e.g., CH_4, N_2O, CFC-12 etc.) have been shown in Figures 3.13 and 3.14. Although compact relations are apparent for all the data sets, slopes of the linear fits differ significantly. Mixing ratio correlations obtained on the dynamically disturbed days over Hyderabad can well be compared with those profiles measured and proposed for midlatitude (see Figures 3.13 and 3.14). Whereas the stratospheric distributions on April 16, 1994 appear to represent average stratospheric conditions, and therefore, the correlations are similar to those of the model results of the Max-Planck-Institute for Chemistry 2D transport-chemistry model in this altitude region.

Figure 4.1 shows the mixing ratio correlations plots of CFC-113 and CFC-114 with CFC-12, CCl_4 and CH_3CCl_3 with CFC-11, and CH_3Cl and HCFC-22 with CH_4, exhibiting compact and near linear relations. These relations can be expressed as

$$\begin{aligned} MR_{CFC-113} &= (2.1077 + 0.02588 \cdot MR_{CFC-12} + 0.000211 \cdot MR_{CFC-12}^2 \\ &\quad +1.04 \times 10^{-7} \cdot MR_{CFC-12}^3) \cdot F_{CFC-113} \qquad (4.1) \\ MR_{CFC-114} &= (4.7814 + 0.00734 \cdot MR_{CFC-12} - 3.533 \times 10^{-5} \\ &\quad \cdot MR_{CFC-12}^2) \cdot F_{CFC-114} \qquad (4.2) \\ MR_{CCl_4} &= (-0.3393 + 0.433 \cdot MR_{CFC-11} + 0.000261 \cdot MR_{CFC-11}^2) \\ &\quad \cdot F_{CCl_4} \qquad (4.3) \\ MR_{CH_3CCl_3} &= (-0.766352 + 0.678893 \cdot MR_{CFC-11} - 0.0028151 \cdot MR_{CFC-11}^2 \\ &\quad +7.5859 \times 10^{-6} \cdot MR_{CFC-11}^3) \cdot F_{CH_3CCl_3} \qquad (4.4) \\ MR_{CH_3Cl} &= (338.9 - 784.265 \cdot MR_{CH_4} + 536.997 \cdot MR_{CH_4}^2) \\ &\quad \cdot F_{CH_3Cl} \qquad (4.5) \\ MR_{HCFC-22} &= (28.3676 - 14.9755 \cdot MR_{CH_4} + 24.94 \cdot MR_{CH_4}^2) \\ &\quad \cdot F_{HCFC-22} \qquad (4.6) \end{aligned}$$

where MR_i is the mixing ratio of species under study at any stratospheric altitude. F_i is an adjustable parameter to account for the changes in tropospheric loading, that can be determined from the ratio of tropospheric concentration of a species during which period the mixing ratios are to be calculated to that during which the correlation plots are obtained.

On the basis of available data we have calculated the mixing ratio distributions for CCl_4, CH_3CCl_3, CFC-113, and CFC-114 on March 27, 1987 using correlation plots (Eqns. 5.1-5.4). Vertical distribution of CFC-115 and CH_3Cl were only missing for April 9, 1990 and are calculated using the relations with CFC-12 (second order polynomial fit, not shown in Figure 4.1) and CH_4 (Eqn. 4.5), respectively. Relatively large number of vertical profiles of key chlorine containing species are not measured on April 16, 1994 (Table 4.1). These profiles are assumed to be similar to those which have been simulated using the MPIC 2D transport-chemistry model as it has already been seen that the distributions of measured species in 1994 fit well with the model results. These missing profiles have also been estimated using the mixing ratio correlations obtained in this study.

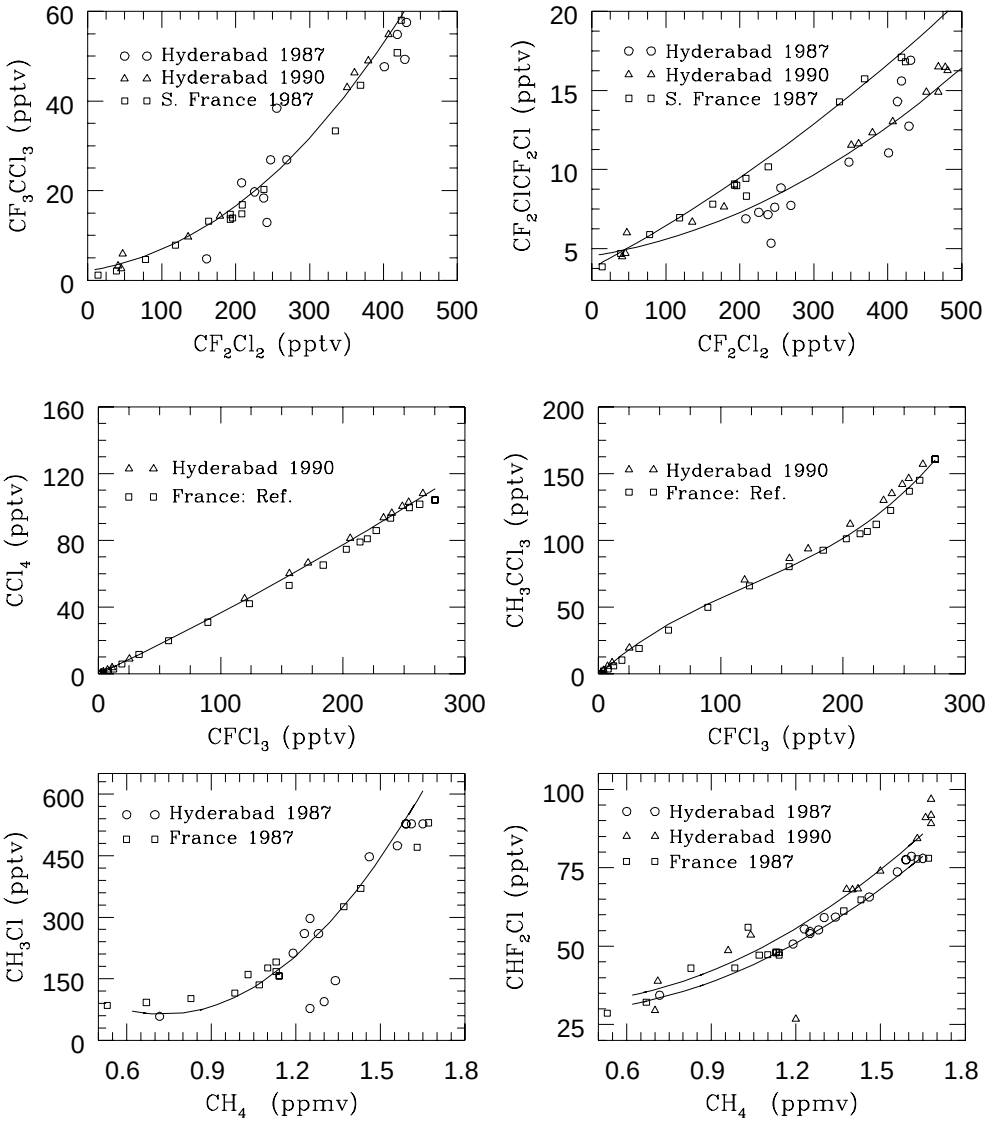

Figure 4.1: *Mixing ratio correlations showing near linear relationships have been used to calculate the vertical distributions of trace gases those are not measured during the balloon flights. Corrections for the increase in tropospheric abundances are applied to the fits.*

4.3 "Age" of Air

It is known that the chemical constituents which originate on the Earth's surface take significant time to reach the stratosphere. The "age" of air essentially indicates the time taken by air parcel to travel from the troposphere to the stratosphere. "Age" of air is about 4 years in the tropical stratosphere, however, it increases significantly with latitude (found up to 8-10 years in the polar region). Therefore, it is important to account for the concentration of the gas under study in an air parcel during its entry to the stratosphere ("age" years before), however, the net effect due to this correction on a species with near zero growth rate (e.g. methyl halides) will be negligible. This correction will be more significant for the chemical species with rapidly changing tropospheric abundances such as CFCs, halons, HCFCs (introduced as substitutes for the CFCs). In this calculation, the correction for such time lag is incorporated using the "age" profiles derived from the vertical distributions of SF_6. Simultaneous "age" profiles are available for March 27, 1987 [*Harnisch et al.*, 1996] and April 16, 1994 from Hyderabad. An "age" profile similar to March 27, 1987 has been used for April 9, 1990 as the mixing ratio correlations of many long-lived trace species (see Figure 3.13 and 3.14) revealed similar behaviour during 1987 and 1990. An average "age" profile is obtained for midlatitude (GAP) based on the reported age distributions [*Harnisch et al.*, 1996]. A comparison shows that the age of air below the tropopause is near zero at latitude of Southern France while it is more than 6 months over Hyderabad region, due to the fact that the major sources of SF_6 are concentrated in the northern hemispheric midlatitude. In general, the stratospheric air over midlatitude is about 1.5 years older when compared to the tropical stratosphere.

4.4 Tropospheric Trends

Global networks are established to monitor the tropospheric concentrations of trace gases at various locations, providing information in relevance to their tropospheric growth rates, effect of phasing out etc. namely, the Atmospheric Lifetime Experiment/Global Atmospheric Gases Experiment (ALE/GAGE) /Advanced GAGE programme, and the National Oceanic and Atmospheric Administration/Climate Monitoring and Diagnostics Laboratory (NOAA/CMDL) programme [e.g., *Fraser et al.,* 1994] Tropospheric concentrations (at the ground level from a tropical and a midlatitude station in NH) are taken mostly from *Fraser et al.* [1994] for 1980-1990 period and from *Montzka et al.,* [1996]

for the period of 1991 to 1996. Abundances of halons during 1980-1990 are taken from *Butler et al.* [1992]. The surface observations of a few key organic chlorine species are shown in Figure 4.2. The symbols show the actual concentrations given in *Fraser et al.* [1994] and *Montzka et al.* [1996], however, to draw continuity with the more recent results, both concentrations are matched at the time boundary (1990-1991). There are also better agreements in few data sets, such as for CFC-11, CFC-12, CH_3CCl_3 etc. Tropospheric growth rates are calculated for each year using these baseline abundances which are to be used in the "age" correction whilst calculating total chlorine/bromine (see Eqn. 4.7).

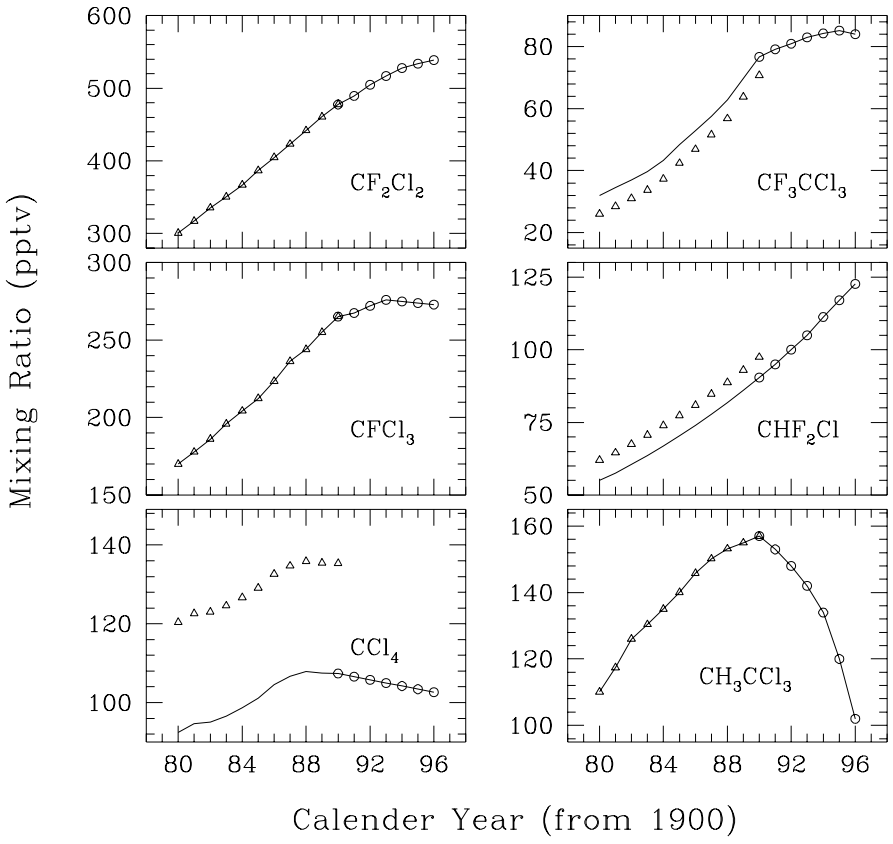

Figure 4.2: *Tropospheric trends of some of the important chlorine containing gases (continuous line). Compiled from Fraser et al. [1994] for the period 1980 to 1990 (△), and from Montzka et al. [1996] during the period of 1991 to 1996 (○) for tropical northern hemisphere. Data obtained from Fraser et al. [1994] are adjusted for a few gases to the later measurements to achieve continuity in the tropospheric trends. These six gases constitute about 85% of CCl_y abundance near the tropopause.*

Tropospheric chlorine and bromine loading due to the halocarbons are calculated using their tropospheric concentrations and compared (not shown here) with the scenario 1 of *WMO* [1995]. A fairly good matching is apparent, indicating the validity of the assumptions employed in evaluating the growth rates as a whole. The decrease after 1994 is observed due to the falling-off production in the ozone depleting substances as per the recommendations of the Montreal Protocol and its amendments, however, it is estimated that the highest loading of halocarbons in the stratosphere will be experienced towards the end of this century.

4.5 Partitioning of Total Chlorine and Bromine

Vertical distributions of Cl_{total}, CCl_y, and Cl_y are shown in Figure 4.3. Total chlorine (bromine) abundances at different altitudes are calculated as the atom weighted mixing ratios of the chlorine (bromine) containing gases CCl_y (CBr_y) at the tropopause with their appropriate age correction applied at particular altitude. In general, a decrease in mixing ratio of Cl_{total} with increasing height is observed as the tropospheric concentration of major CCl_y gases were increasing with time before $\sim$1994. Their increase rate was much faster prior to 1990 (Figure 4.2) which is clearly reflected as larger decrease in Cl_{total} profiles in 1987 and 1990, whereas, the rate of increase was nearing zero after 1990, hence, the Cl_{total} profile estimated for April 1994 does not show any significant decrease with altitude (a case of steady injection to the stratosphere). The mismatch in Cl_{total} profiles from Hyderabad and GAP in 1987 arises due to the difference in the "age" of air profiles.

Partitioning of organic and inorganic chlorine (bromine) in the stratosphere can be estimated from the observed vertical distributions of source gases. Total amount of chlorine/bromine (Cl_{total}/Br_{total}) at the tropopause is transported to the stratosphere in their respective organic forms where they get dissociated either by the solar UV radiation or due to reactions with O^1D and OH in the stratosphere. Dissociation of each compound leads to the formation of inorganic chlorine/bromine. Therefore, at any altitude Cl_{total} (Br_{total}) can simply be represented by the sum of Cl_y (Br_y) and CCl_y (CBr_y) in the stratosphere [see *Woodbridge et al.,* [1995] and *Daniel et al.,* [1996] for further details]. In other words chlorine partitioning can be expressed as

$$Cl_y = Cl_{total,z} - CCl_y$$

$$= \sum_{i=1}^{N} n_{Cl,i} \cdot \mu_{entry,z,i} - \sum_{i=1}^{N} n_{Cl,i} \cdot \mu_{z,i} \quad (4.7)$$

where N is the total number of chlorine containing species under study, $n_{Cl,i}$ is the number of chlorine atoms in species i, $\mu_{entry,z,i}$ is the concentration of a particular species in the air parcel at altitude z while entering the stratosphere, and $\mu_{z,i}$ are the mixing ratios of chlorine containing gases observed at any altitude. Similar equations can be written for bromine compounds also. Both the terms in R.H.S of Eqn. 4.7 are measurable quantities: first from the known age of stratospheric air parcel and tropospheric trends of halocarbons, and second from the vertical distributions of trace gases.

The organic chlorine (CCl_y) in the tropical stratosphere (Figure 4.3a and d) is considerably higher compared to that in the midlatitude (Figure 4.3b) due to the fact that tropical tropopause acts as the source of trace gases that originate in the troposphere. The tropical region transports these constituents most effectively through the strong tropical upwelling from the troposphere to the stratosphere, and concentrations of these gases also decrease from low latitude to high latitude due to their photochemical loss during meridional transport and downward motion in the mid- and high latitudes (see Figure 1.5). Therefore, inorganic chlorine is produced mainly in the tropical stratosphere, due to higher abundances of CCl_y gases, and larger availability of solar radiation and higher abundances of O^1D. Similar are the estimated vertical profiles of Br_{total}, CBr_y and Br_y, but only up to ~32 km as there are no CBr_y gas detected above this altitude from Hyderabad (not shown in figure). Due to inefficient scavenging of Cl and Br atoms from the stratosphere, these radicals and their subsequent transforms (such as HCl, ClO_x, HBr, BrO_x) are transported to the high latitudes and polar stratosphere where they take part efficiently in ozone destruction. It is also apparent from the estimated Cl_y profiles that their abundances in the midlatitude stratosphere (Figure 4.3b) are higher than those in the tropics, particularly in the lower stratosphere (Figure 4.3a) due to the combined effect of transport of inorganic Cl compounds from the tropics and *in situ* production of Cl due to photodissociation and chemical losses of CCl_y gases. Previous estimates of Cl_y and Br_y abundances based on aircraft measurements of trace gases in the lower stratosphere also indicate an increase with increasing altitude and latitude [*Daniel et al.,* 1996].

Two dimensional model results also show fairly good agreement with these calculations. Inorganic chlorine is calculated as (ClO_x + HCl) abundances. The deviations of estimated Cl_y based on observations and the MPIC

2D model derived profiles (see Figure 4.3a and c) are caused by the dynamical perturbations observed in the vertical profiles of some of the chlorine containing organic compounds. For 1994, the vertical profiles of source gases which are not measured have been calculated using: a) the mixing ratio correlations obtained from 1987 and 1990 profiles and b) using the vertical

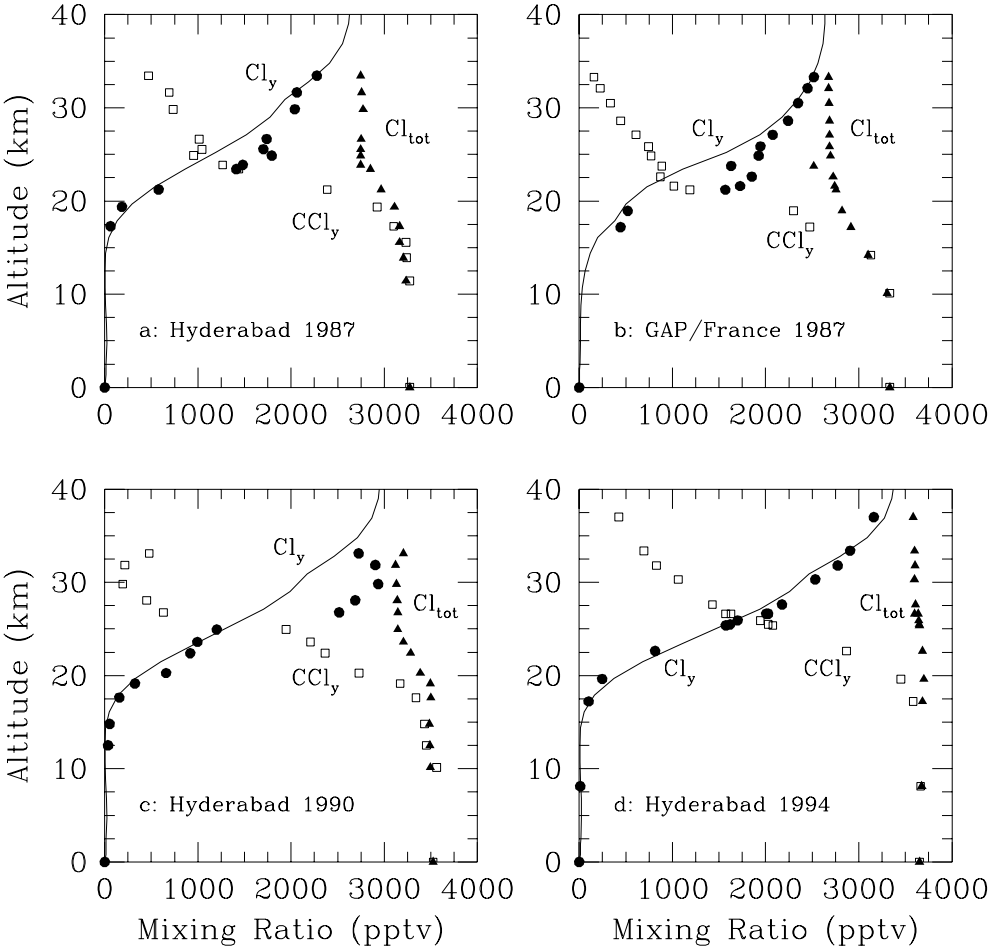

Figure 4.3: *Vertical distributions of Cl_{total} (filled triangle), CCl_y (open square), Cl_y (filled circle) as calculated using the Eqn. 4.7. Estimated Cl_y from MPIC 2D model derived profiles of HCl and ClO_x are shown as continuous line, specified. a: for March 27, 1987. b: estimated using the profiles obtained from GAP, France [Borchers et al., 1989], c: calculated from April 9, 1990 vertical distributions, d: obtained using the 1994 measurements.*

profiles obtained from MPIC 2D model; both these estimates of CCl_y and Cl_y vertical distributions are in close proximity with each other (not shown in the

diagram).

4.6 Correlations of CCl_y and Cl_y with Other Gases

It has already been seen that the vertical distributions of many chemical species like CH_4, N_2O, CFC-12 are dynamically disturbed while compared to their normal stratospheric distributions (e.g. profiles measured on April 16, 1994 or 2D model results). These deviations are also propagated in the CCl_y and Cl_y profiles. Hence, inter-correlations of these chemical species (as tracers/proxy altitude) with organic and inorganic chlorine/bromine species for the individual set of results are expected to eliminate the dynamical influences to a large extent. Compact relations of CCl_y and Cl_y with N_2O are apparent in the stratosphere (Figure 4.4 and 4.5, respectively). It has also been observed in this analysis that CCl_y-N_2O relations tend towards linearity (not shown here) if CFC-113 is used as chemical tracer instead of N_2O. Correlations with CFC-12 can be treated at the juxtaposition with those obtained using N_2O. More importantly, there is no systematic departure of these estimates of CCl_y (and also their correlations with N_2O) for Hyderabad and GAP compared to the best fit obtained by *Woodbridge et al.* [1995]. In addition, Figure 4.4 does not indicate significant increase in chlorine abundances in the stratosphere with time. We calculate organic chlorine abundances to be approximately 3100, 3355, and 3645 pptv, respectively, on March 1987, April 1990, and April 1994 over Hyderabad near the tropopause ($\sim$17 km). These results are in fairly good agreement with the CCl_y concentration of 3449 during 1991-1992 near the tropopause (corresponding to N_2O=310 ppbv) calculated using the "best fit" curve of *Woodbridge et al.,* [1995] and somewhat out of range from that estimated (CCl_y=3667 pptv) by *Daniel et al.* [1996] for the same period.

However, correlations between Cl_y and N_2O suggest rapid increase in the inorganic chlorine mixing ratio in the lower and middle stratosphere, corresponding to N_2O abundance of $\approx$300-100 ppbv in the tropical region. This feature suggests that although there is no distinct growth rate of organic chlorine in the stratosphere, its inorganic component is accumulating with time, which implies that the production of Cl_y from the CCl_y gases is higher than the removal rate of the former. Higher the altitude (lower N_2O concentration) higher is the Cl_y accumulation rate. The correlation of estimated Cl_y with N_2O obtained for GAP shows similar behaviour while compared to that obtained from Airborne Arctic Stratospheric Expedition II (AASE II) flights

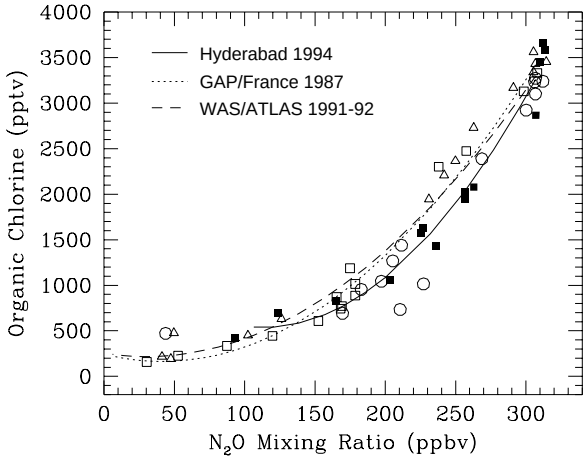

Figure 4.4: *Estimated organic chlorine abundances versus simultaneously measured N_2O mixing ratio correlations obtained on March 27, 1987 (◯), April 9, 1990 (△) and April 16, 1994 (□) from Hyderabad and on June 23, 1987 (□) from GAP compared with the "best fit" of Woodbridge et al. [1995].*

during 1991-1992 period and the difference in concentrations is apparent. But correlation characteristics appear to differ for the tropical region (Hyderabad), particularly on April 16, 1994 which is assumed to represent the normal stratospheric conditions. Steeper gradient can be seen with decreasing N_2O which suggests larger production of inorganic chlorine in the tropics compared to the midlatitude region. The N_2O correlation with Cl_y on April 9, 1990 also shows similar features. Abundances of Cl_y in the tropical stratosphere (at N_2O=100 pptv corresponding altitude) are estimated to be about 2200, 2700, and 3000 pptv, respectively, on March 27, 1987, April 9, 1990, and April 16, 1994. However, we believe Cl_y concentration on March 27, 1987 was higher than this estimate - the error is associated with inadequate measurements in the altitude region of low N_2O concentration. These estimates are again in better agreement with *Woodbridge et al.* [1995] compared to that estimated from *Daniel et al.* [1996] for N_2O=100 pptv. The quadratic fits for GAP in 1987, and Hyderabad in 1994 can be expressed as:

$$\begin{aligned} Cl_y &= 2803.3 + 1.51671(N_2O) - 0.0339448(N_2O)^2 \qquad GAP\ 1987 \\ Cl_y &= 2244.3 + 14.3213(N_2O) - 0.0658306(N_2O)^2 \quad Hyderabad\ 1994 \end{aligned} \tag{4.8}$$

These relations are compared with that (Eqn. 4.9), obtained by *Daniel et al.* [1996] using global measurements in the lower stratosphere indicating much higher gradient of Cl_y with first order in N_2O mixing ratio over Hyderabad on

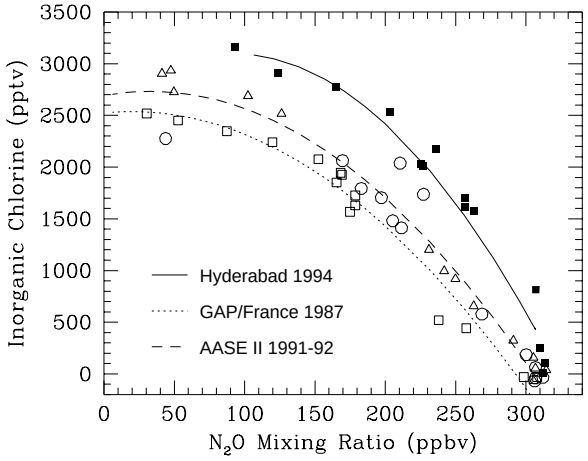

Figure 4.5: *Cl_y versus N_2O correlation plots showing the quadratic fits: dashed line is the best fit for Daniel et al. [1996]; dotted line is obtained from the Southern France reference profiles; continuous line is obtained on April 16, 1994 for Hyderabad.*

April 1994 compared to those which have been obtained for GAP and AASE II.

$$Cl_y = 2691.4 + 2.4359(N_2O) - 0.0368334(N_2O)^2 \quad AASE\ II \tag{4.9}$$

Figure 4.6 shows the mixing ratio correlations of estimated Br_y with CFC-12. Correlations on March 27, 1987 and April 16, 1994 exhibit second order quadratic relations in the lower stratosphere. The maximum Br_y abundance are reached in the lower stratosphere (height below ~32 km), and these abundances are estimated to be about 11, 12, and 12.8 pptv, respectively, in March 1987, April 1990, and April 1994 from Hyderabad. However, this estimation accounts for only 94% of the CBr_y compounds entering the stratosphere. These estimations show a fairly good agreement with the previous study in the lower stratosphere ($\geq$13 pptv for N_2O = 115 ppbv), however, due to lack of accurate measurements of vertical profiles of CBr_y gases these results are not discussed further.

Therefore, it is possible that the amount of organic and inorganic chlorine or bromine abundances causing stratospheric ozone depletion can be well estimated only if prior information on 1) distributions of chemical tracers like CH_4, N_2O, and some of the key organic chlorine- and bromine-containing gases e.g. CFC-12, CFC-11 are available (remaining can be semi-theoretically obtained); 2) well established tropospheric trends of CCl_y and

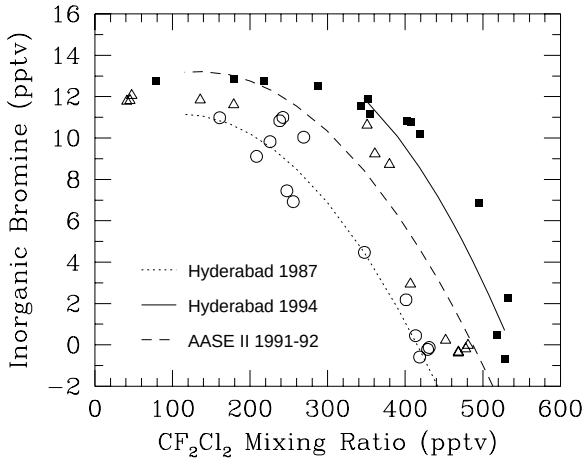

Figure 4.6: *Correlations of estimated inorganic bromine with CFC-12 and compared with only previous estimation [Daniel et al., 1996]. Symbols are same as used in Figure 4.4. The quadratic fit obtained for March 27, 1987 (dotted line) can be given as:* Br_y *= 9.62514 + 0.0271351 (CFC-12) - 0.000121028 (CFC-12)*^{2} *and that on April 16, 1994 can be written as:* Br_y *= 7.93534 + 0.0597514 (CFC-12) - 0.000139101 (CFC-12)*^{2}*.*

CBr_y species from their time-series measurements at a number of ground-based sites. Other additional information ("age" of stratospheric air) will be obtained from the vertical profiles of long-lived gases like SF_6, CFC-115, CO_2 etc.

Chapter 5

N_2O and CH_4 Emissions from the Arabian Sea

Atmospheric budgets of anthropogenically produced gases have been fairly well estimated from the extensive surface measurements or knowing their tropospheric emission scenarios, particularly, for those gases having well known loss processes, e.g. inventories and tropospheric trends of CFCs [*Elkins et al.,* 1993; *Cunnold et al.,* 1997], halons [*Butler et al.,* 1992], HCFCs [*Oram et al.,* 1995], SF_6 [*Maiss et al.,* 1996] etc. On the other hand, the annual budgets and tropospheric trends of atmospheric constituents with both natural and anthropogenical sources are not yet clearly understood; as a result the explanation of observed anomalous growth rates of CH_4 [*Dlugokencky et al.,* 1994], N_2O source distributions and its annual emission budget etc. still remain uncertain [*Bouwman et al.,* 1996]. Major uncertainty in these estimations mainly arise due to the lack of understanding in the source strengths and their global distributions. In this Chapter, we have dealt with ocean as a natural source of many atmospheric gases produced during various biogeochemical processes. Measurements of the two important biogenic gases N_2O and CH_4 have been made both in the water column and in air of the Arabian sea under various possible sea conditions, controlling the production and transport under water, and affecting the exchange across the air-sea interface. In this chapter, annual estimations of ocean-atmosphere fluxes of these two gases are made and their associated uncertainties are discussed.

5.1 Introduction

Study of nitrous oxide (N_2O) has drawn special attention because of its impact on the stratospheric ozone layer and also due to its high greenhouse warming potential to contribute significantly to the global warming as discussed in §1.3. Atmospheric N_2O has both natural and anthropogenical sources, thus accurate information about its sources and their budgets still remain quite uncertain [*Bouwman et al.*, 1996]. World oceans contribute up to about 20% of annual N_2O input to the atmosphere [*IPCC*, 1996]. It is now well recognized that the ocean-to-atmosphere exchange depends primarily on the degree of saturation in the surface water and the transfer velocity of the gas under study, across the air-sea interface. A recent comprehensive analysis shows that the budget of N_2O emission can get affected significantly depending on the choice of gas transfer model used in calculating the fluxes [*Nevison et al.*, 1995]. Despite the sustained uncertainty, it is important to realize that the range in global N_2O budget has reduced considerably over the past decade due to extensive measurements and critical analysis of available results [e.g. *Bouwman et al.*, 1996].

Available data suggest that the Arabian sea is one of the high N_2O flux producing areas among the world oceans [*Law and Owens*, 1990; *Naqvi and Noronha*, 1991; *Lal et al.*, 1996a; *Bange et al.*, 1996] due to large production below the mixed layer, in the intense oxygen minimum zone, and rapid transport of this N_2O rich water to the surface layer by the prevailing advective and diffusive processes. These measurements also indicate large variability in the N_2O emissions as the Arabian Sea experiences extreme physico-chemical changes round the year. However, detailed measurements covering various seasons were not available for the Arabian Sea prior to the measurements undertaken by various groups as a part of *Joint Global Ocean Flux Study (JGOFS), India* programme.

Methane (CH_4) is also a radiatively important gas (about 20 times more effective in radiative forcing than CO_2 on per mole basis) and actively involved in atmospheric photochemical processes which influence the abundance of hydroxyl and other radicals which are primary oxidants in the global atmosphere. In the stratosphere, CH_4 is one of the major sources of water vapour but is a sink of atomic chlorine. Its atmospheric concentration has been increasing at a much faster rate ever since the industrialization has started, however, a dramatic decrease in the growth rate has been observed recently [*Dlugokencky et al.*, 1994; *Khalil and Rasmussen*, 1995]. The causes for such deceleration in concentration increase are speculative by virtue of

the unrealistic representation of its sources as its atmospheric losses are well recognized. Most of CH_4 is produced in the natural wet lands, paddy fields, and by ruminants [*Khalil and Rasmussen*, 1995; *Reeburgh.* 1996]. It is broadly recognized that oceans are one among several minor global sources, however, the processes involved in its production and its distributions below the air-sea interface which control the emission rate, particularly in the Arabian Sea is limited to only one earlier measurement campaign [*Owens et al.,* 1991].

5.2 Experimental Procedure

5.2.1 Analysis of air and water samples

Measurements were made on board ORV Sagar Kanya in the Arabian Sea in different seasons, viz. inter monsoon (April-May 1994; Cruise no. SK 91), northeast monsoon (February-March 1995; Cruise no. SK 99), and two southwest monsoons (July-August 1995; Cruise no. SK 104 and August 1996; Cruise no. SK 115). The water sampling stations established following the approximate cruise track (see Figure 5.2) are shown in Figure 5.1 which cover a latitude and longitude ranges of 10^0N to 22^0N and 64^0E to 75^0E, respectively.

Air samples were collected in 60 ml B-D plastic syringes from the bow of the ship while cruising (i.e. between stations). Samples were injected onto the GC column after passing through a moisture trap (glass bulb filled with magnesium perchlorate [$Mg(ClO_4)_2$)] and using a 4 ml loop connected to a 6 port valve. Both these were flushed with adequate (about 25 ml) sample before final injection. Water samples were collected using 12 GoFlo bottles (General Oceanics) of capacity 1.8/12/30 liters attached to a conductivity-temperature-density (CTD) rosette. The CTD instrument (Sea-Bird Electronics, Inc.) was used to obtain online information of depth, temperature and salinity of the water samples. Samples were drawn from these bottles into 100 ml stoppered glass bottles and stored in a refrigerator until analysis. Most of the sample analyses were completed within 24 hours of collection using standard techniques. Water sub-samples and marine air were analyzed on board the ship using a HP 5890 series II (Varian Vista series was used during SK 91 only) gas chromatograph equipped with an electron capture detector (ECD) following a similar procedure as described in §2.3.1. Each sample of 25 ml volume is equilibrated for about 7 min using a wrist shaker

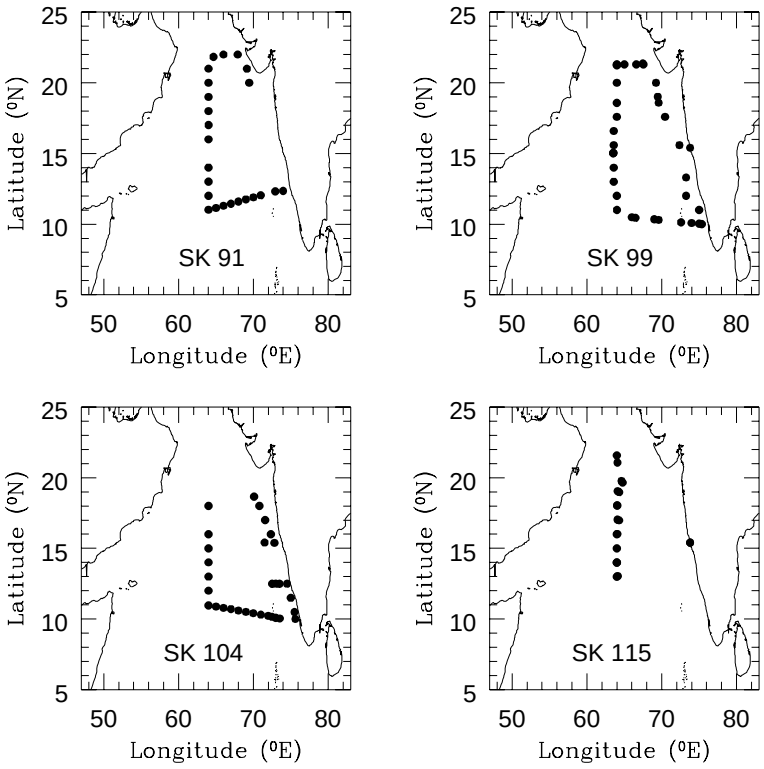

Figure 5.1: *Map of study area in the Arabian Sea, showing the cruise tracks of Indian Joint Global Ocean Flux Study programme. CTD stations (•) were occupied each degree change in latitude or longitude (whichever occurred first) and water samples were collected for the analysis of various chemical and biological parameters. Analyses of marine air samples were made at regular intervals along the cruise track.*

with equal amount of N_2O free He up to 2-3 times. The zeroth order equilibrium concentration of N_2O was determined from the intercept of log-normal (linear) plots of dry N_2O mixing ratio vs the equilibration number based on the principle of multiple phase equilibrium [*McAullife*, 1971]. The precision of our measurements is found to be better than 1% (1 SD). Errors in the absolute N_2O concentrations are estimated to be about 3-5% from multiple analyses of the same water sample.

The water samples, stored in refrigerator, were also analyzed simultaneously for CH_4 on board by making multiple equilibrium and using a Shimadzu (Mini GC 3) gas chromatograph equipped with a flame ionization detector (FID). Multiple phase equilibrium was achieved by equilibrating 20 ml of pure helium with 30 ml of sea-water in 60 ml B-D plastic syringe for 7

minutes with the help of a wrist shaker at room temperature. Each sample was equilibrated twice to ensure complete stripping. About 80-90% of the dissolved methane was found to be extracted in the first equilibrium itself and in the third equilibration the amount of CH_4 was always below the detection limit of the instrument. Equilibrated helium was passed through a moisture trap filled with anhydrous magnesium perchlorate and injected on to the GC column head by means of a sample loop of 4 ml volume. Similar molecular sieve packed column is used as discussed in §3.3.2 for separation of CH_4 from the air peak, but GC oven temperature was maintained isothermally at 70^0C for faster elution of methane. The accuracy of CH_4 measurements (1 SD) in marine air is found to be better than 2-3%, estimated based on the precision (much less than 1%) of the analyses for replicate samples and the errors in the calibration gases supplied by NIST (USA) and Linde Gas (UK). Errors involved in the water analyses can be greater but do not exceed 5-7%, estimated by analyzing duplicate water samples.

5.2.2 Estimations of dissolved gases and sea-to-air fluxes

Concentrations of N_2O and CH_4 in air are calculated by comparing the GC response with the response obtained from the laboratory standard as described earlier (§2.2 and §3.3 respectively). The mole concentrations of dissolved gases in sea water are calculated based on the principle of multiple phase equilibrium as given by *McAullife* [1971]. For example, the concentration of N_2O in sea water in nmol[1] can be expressed as

$$N_2O\ [nmol] = 0.0409 \cdot \frac{1}{H_x} \cdot P_L \cdot \frac{298}{T_L} \cdot N_2O\ [ppbv] \tag{5.1}$$

where H_x is Henry's law constant for solute gas x (a function of temperature and salinity), P_L and T_L are the laboratory pressure (atm) and temperature (^{0}K) respectively, N_2O (ppbv) is the mixing ratio of nitrous oxide in the zeroth order equilibrated air with sea water, and the constant (0.0409) is the conversion factor from mixing ratio (ppbv) to concentration (nmol) at STP. Similar transformation equation can be written for CH_4. This concentration is defined as observed concentration (C_{obs}).

Saturation concentrations (C_{sat}) of the respective gases in water are calculated by multiplying their partial pressure in the ambient marine air with their solubility in sea water at the appropriate temperature and salinity. The solubilities of N_2O and CH_4 in sea water are calculated by using the

[1] 1 nmol = (10^{-9}) mole per liter, is also referred to as nM

relations of *Weiss and Price* [1980] and *Atkinson and Richards* [1967], respectively. Solubility of both these gases decrease with increasing temperature, suggesting possibilities of low surface saturation and the higher escape rate from surface water in summer (inter monsoon). The flux (F) in nmol cm^{-2} s^{-1} between air and water is calculated by using the wind speed dependent transfer velocities and can be expressed as

$$F = k \cdot \Delta C \tag{5.2}$$

where ΔC is the difference in concentrations (= C_{obs} - C_{sat}). $\Delta C > 0$ implies oceans are sink of the solute gas and otherwise ($\Delta C < 0$) a source of the solute gas. k is the gas transfer velocity in cm hr^{-1}. The value of k depends on wind velocity which can be evaluated using one of the following models:

1) *Liss and Merlivat* [1986] wind speed dependent gas transfer model using three linear relationships for three different ranges of wind speed.

$$\begin{aligned} k_{600} &= 0.17 \cdot U_{10} && U_{10} \leq 3.6 \\ k_{600} &= 2.85 \cdot U_{10} - 9.65 && 3.6 < U_{10} \leq 13 \\ k_{600} &= 5.9 \cdot U_{10} - 49.3 && U_{10} > 13 \end{aligned} \tag{5.3}$$

U_{10} is the wind speed (m s^{-1}) at 10 m height from the sea surface.

2) *Wanninkhof's* [1992] gas transfer model shows a quadratic relation with the wind speed (it results in higher k compared to the former particularly in the low wind speed regime).

$$k_{660} = 0.31 \cdot U_{10}^2 \tag{5.4}$$

and

3) Using the stability dependent theory of *Erickson* [1993]

$$k_{885} = 9.58 \cdot (1 - W) + 475.07 \cdot W \tag{5.5}$$

where W is the area covered by white caps. In the present calculations W is taken to be zero as the wind speed exceeding 13 m s^{-1} were observed only rarely, which is the condition of formation of white caps on the sea surface.

We use here the *Liss and Merlivat* [1986] model most widely and the main discussion is based on this gas exchange model, however, other two models will be utilized mainly for calculating extreme annual emission rates.

The numbers indicated as the subscript to k are the Schmidt numbers (S_c, ratio of kinematic viscosity ν to molecular diffusivity D of any gas) associated to a reference gas such as S_c=600 correspond to Schmidt number of CO_2 in freshwater, S_c=660 to that of CO_2 in sea-water, and S_c=885 to that of radon in freshwater at 20^0C. Therefore, a scaling is made for N_2O and CH_4 transfer velocities using the relation as discussed in *Liss and Merlivat* [1986] and references therein.

$$k_{gas} = k_{ref} \left[\frac{S_{c,\ gas}}{S_{c,\ ref}} \right]^n \tag{5.6}$$

where n=-1/2 for U>3.6 m s^{-1} and n=-2/3 for U<3.6 m s^{-1} except that *Wanninkhof* [1992] used n=-1/2 for all U.

The scaling factors (equation 5.7 and 5.8) increases with increasing temperature which can be seen from the expressions to calculate Schmidt numbers

$$S_{c_{N2O}} = 2301.1 - 151.1 \cdot t + 4.7364 \cdot t^2 - 0.059431 \cdot t^3 \tag{5.7}$$

$$S_{c_{CH4}} = 2039.2 - 120.3 \cdot t + 3.4209 \cdot t^2 - 0.040437 \cdot t^3 \tag{5.8}$$

for N_2O and CH_4 in sea-water, respectively [*Wanninkhof,* 1992], where t is the water temperature in ^{0}C.

5.3 N_2O Emission from the Arabian Sea

5.3.1 N_2O distribution in marine air and in surface water

Average N_2O abundances in marine air during these four cruises are observed to be 311±7 ppbv (inter monsoon, 1994), 315±6 ppbv (northeast monsoon, 1995), 310±6 ppbv (southwest monsoon, 1995), and 313±4 ppbv (southwest monsoon, 1996). An average of these concentrations (313 ppbv) is used in evaluating the saturation concentrations of N_2O in the surface waters [*Lal and Patra,* 1997].

For convenience, a generalized cruise track is constructed as shown in Figure 5.2. Based on the prevailing physical conditions in the Arabian sea, the study area is segregated in four zones to understand the regional and seasonal variations in N_2O surface saturations and its evasion rates. These are from stations 1 to 10 (region I), stations 11 to 20 (region II), stations 21

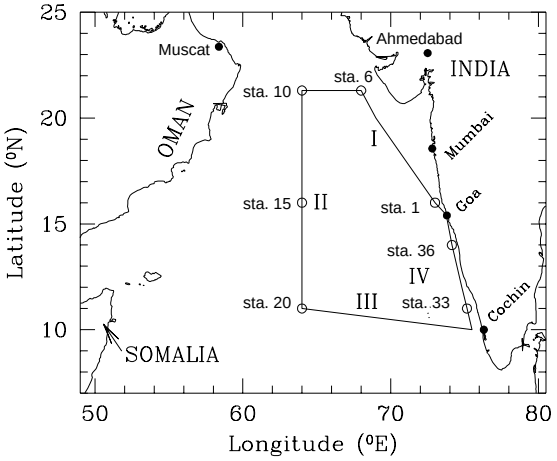

Figure 5.2: *Approximate cruise track followed ORV Sagar Kanya during the JGOFS (India) expeditions in the Arabian Sea.*

to 29 (region III), and stations 30 to 36 (region IV). The regions I and IV, by and large represent the coastal areas whereas the regions II and III are likely to exhibit the characteristics of open ocean.

Surface saturations show significant variations with changing locations. Distributions of N_2O saturations along the cruise track are shown in Figure 5.3. Figure 5.3a indicates higher degree of supersaturations (up to 143%) in the region I, which arise due to enhanced mixing between N_2O rich subsurface and surface water during winter cooling. In this region the mixed layer was deepened to $\sim$100 m [*Kumar and Prasad*, 1996]. The near equilibrium N_2O in the surface water during inter monsoon (Figure 5.3b) was probably due to the combined effect of less vertical mixing caused by the summertime thermal stratification and higher release rates because of higher sea surface temperature (SST). Another physical process which does affect the surface saturations of N_2O and prevalent in the Arabian Sea is the upwelling. Figure 5.3c clearly shows the highest supersaturation (155-175%) occurring in the region IV (Indian west coast off Cochin; 10-13^{0}N, 74-76^{0}E) due to intense coastal upwelling as discussed in *Patra et al.* [1997c]. However, the intensity of upwelling is much weaker compared to those observed off Oman and Somalia [*Law and Owens*, 1990; *Bange et al.*, 1996].

Nitrous oxide in surface waters of the Arabian Sea is found to be supersaturated with respect to that in the marine air during all the seasons (Figure 5.3). The intensity of average supersaturations do not show much

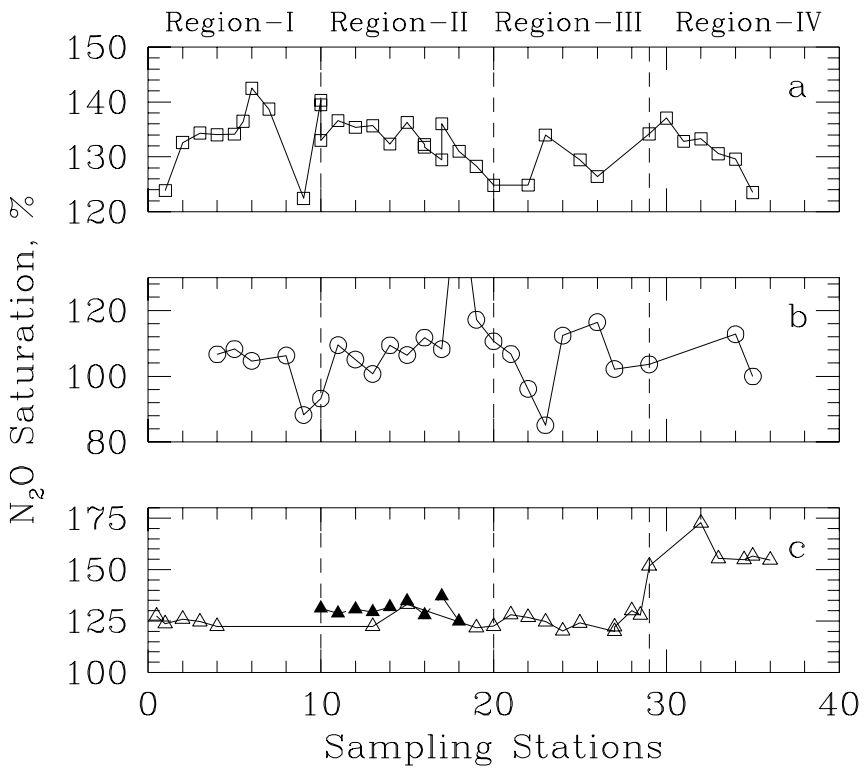

Figure 5.3: *Distributions of N_2O saturation in the surface water observed during (a) northeast monsoon, (b) inter monsoon, and (c) southwest monsoon (open triangles are for 1995 and filled triangles are for 1996).*

variations during northeast and southwest monsoons, however, very low supersaturation (near equilibrium) was observed during inter monsoon period. Average N_2O supersaturations were found to be 132±5% (1 σ spread) during northeast monsoon, 105±8% during inter monsoon, and 133±15% and 130±3% respectively during southwest monsoon periods in 1995 and 1996.

5.3.2 Seasonal and spatial variations of N_2O fluxes

The gas exchange model [*Liss and Merlivat,* 1986] has been used to calculate transfer velocities, using the *in situ* wind speeds. The estimated velocities show wide variations with largest values during the southwest monsoon periods. They lie in the range of 0.2 to 22 cm h^{-1}, 0.2 to 14 cm h^{-1}, and 0.5 to 39 cm h^{-1} and 8 to 44 cm h^{-1} in northeast monsoon, inter monsoon, and southwest monsoon of 1995 and 1996, respectively. Using these transfer velocities and estimated ΔN_2O values, the N_2O fluxes have been computed

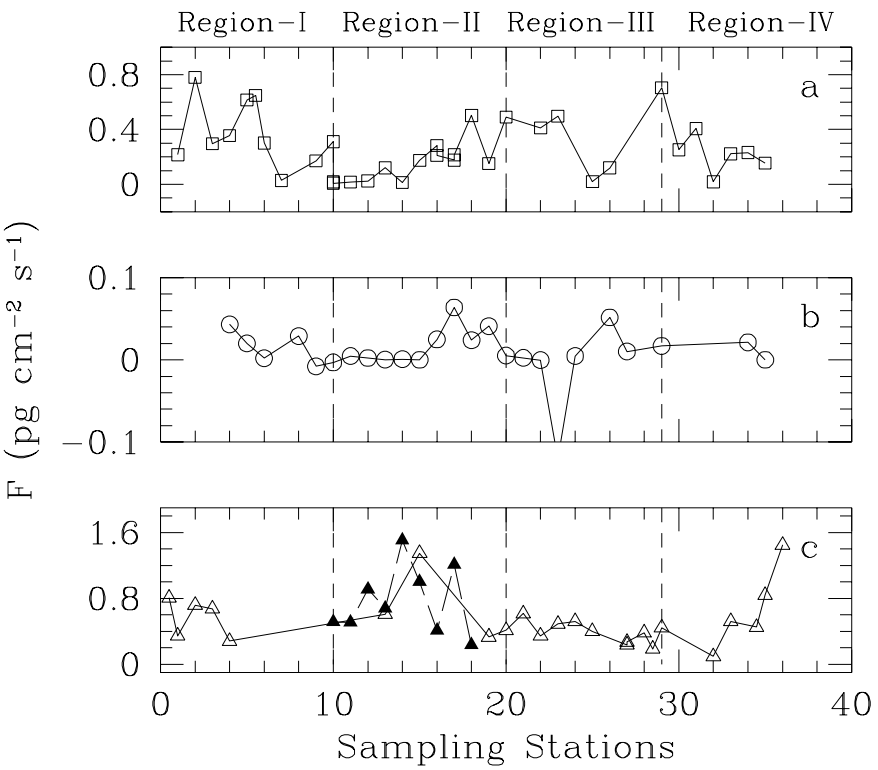

Figure 5.4: *Spatial distributions of N_2O fluxes from the Arabian Sea during (a) northeast monsoon, (b) inter monsoon, and (c) southwest monsoon (open triangles are for 1995 and filled triangles are for 1996).*

for all the seasons and are depicted in Figure 5.4. The effect of high wind speed during southwest monsoon period can be seen in Figure 5.4c (region II), in spite of lower supersaturations, the evasion rates are comparable to those which have been estimated for the highest surface supersaturations (region IV). Spatial distributions of N_2O fluxes do not show any discernible differences between the coastal and open ocean regions for normal sea conditions due to their near uniform surface saturations unless disturbed by the localized intense mixing or strong upwelling. Seasonally averaged values of the fluxes are estimated to be 0.003 $\pm$ 0.04 pg[2] cm^{-2} s^{-1}, 0.26 $\pm$ 0.21 pg cm^{-2} s^{-1}, and 0.51 $\pm$ 0.34 and 0.75 $\pm$ 0.39 pg cm^{-2} s^{-1} in inter monsoon, northeast monsoon, and southwest monsoons (1995 and 1996), respectively (Table 5.1).

The observed flux during the northeast monsoon (February-March

[2] 1 pg (pico gram) = 10^{-12} gram

1995) agrees well with that observed (0.23 pg cm^{-2} s^{-1}) in December 1988 [*Naqvi and Noronha*, 1991]. The extremely low emission rate of N_2O from the Arabian Sea observed during inter monsoon (April-May 1994) was reported for the first time [*Lal et al.,* 1996] in spite of large N_2O production below the mixed layer. Latter measurements made in May 1995 as a part of JGOFS (Germany) expedition in this oceanic region also showed very small flux of 0.02 pg N_2O cm^{-2} s^{-1} [*Bange et al.*, 1996]. These low fluxes are mainly arising due to reduced N_2O supply to the surface water through the underneath stably stratified layers, formed by the intense solar heating and extremely low wind speeds observed during this period. The estimated flux in the first southwest monsoon period (July-August 1995) is significantly lower than the flux estimated by *Bange et al.* [1996] as the intensity of the upwelling observed off Oman and Somalia are much stronger compared to what is experienced off Cochin. However, these fluxes during southwest monsoon are higher than the average flux of 0.44 pg N_2O cm^{-2} s^{-1} observed by *Law and Owens* [1990] during September-October, in spite of similar surface supersaturations. This discrepancy is caused by higher winds prevailing during southwest monsoon than the average value used in their calculation.

Table 5.1: *Average N_2O fluxes and its annual emissions using Liss and Merlivat [1986] gas transfer model from the Arabian Sea.*

Period of study	Flux density pg N_2O cm^{-2} s^{-1}	Net emissions Tg N_2O yr^{-1}	Reference
September-October 1986	0.44±0.22	0.22-0.39*	*Law and Owens*, 1990
December 1988	0.23±0.13	0.44	*Naqvi and Noronha*, 1991
May 1995 and	0.017		*Bange et al.*, 1996
July-August 1995	0.79**	0.8	- do -
February-March 1995	0.26±0.21		this work
April-May 1994	0.003±0.04		- do -
July-August 1995	0.51±0.34		- do -
August 1996	0.78±0.39		- do -
Annual minimum		0.56	- do -
Annual maximum		0.76	- do -

* only upwelling region (1.56×10^6) of the Arabian Sea is considered.

** area weighted average flux ($=\frac{44}{10^4}\cdot\frac{731\times1.47+10.6\times4.7}{6.23}$).

5.3.3 Variations and uncertainties in annual emission

To estimate the annual emission of N_2O, we have assumed four distinct seasonal grids (December-February, March-May, June-August, and September-November) which show discernible ranges of wind speeds and surface supersaturations throughout a year in the Arabian Sea. Due to limited observations during southwest monsoon of 1996, the average flux for this season is calculated using the data obtained in southwest monsoon 1995 and 1996. The fluxes during September-November (post monsoon) have been interpolated between the fluxes observed during the southwest and northeast monsoon periods due to lack of measurements by this group. This average flux is comparable with the value obtained by *Law and Owens* [1990] for the same season. These seasonal fluxes which have been used in estimating N_2O annual emission are shown in Figure 5.5 (dashed line), and we believe that this

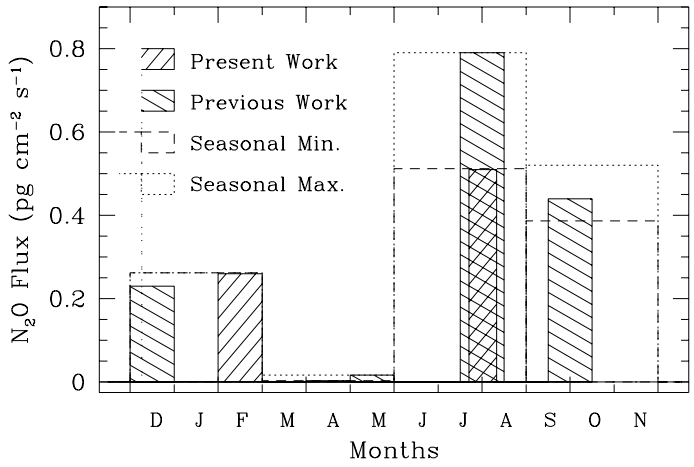

Figure 5.5: *Measured N_2O fluxes during various months by different research groups in Arabian Sea. Seasonal variations over four seasons as used in the estimations of annual emissions are also shown (dashed line: to estimated the lower limit and dotted line: to estimate the upper limit).*

estimation will provide the lower limit of annual emission. The total emission from the Arabian Sea is found to be 0.56 Tg[3] N_2O $year^{-1}$. Similarly, we have calculated an upper limit of the evasion flux from the Arabian Sea. In this case, the average flux during southwest monsoon is taken from *Bange et al.* [1996]. The interpolated flux for the post monsoon season is slightly higher than the flux observed by *Law and Owens* [1990]. The seasonal fluxes

[3] 1 Tg (tera grams) = 1 million million (10^{12}) grams which is equivalent to 1 million tones

assumed in this estimation are also shown in Figure 5.5 (dotted line) which leads to an annual emission of 0.76 Tg N_2O yr^{-1}.

The annual emissions of N_2O as inferred by various groups are also given in Table 5.1 for a better comparison. *Law and Owens* [1990] calculated a net evasion of 0.22-0.39 Tg N_2O yr^{-1} from the upwelling area of the Arabian Sea during the decline of the southwest monsoon (August-September) which would probably be comparable if total area is considered. The present estimated range of annual emission is higher compared to that of 0.44 Tg N_2O yr^{-1} based on the measurements in December only by *Naqvi and Noronha* [1991]. A net emission of about 0.8 Tg N_2O yr^{-1}, based on two seasons (inter monsoon and southwest monsoon), has been suggested by *Bange et al.* [1996] which is in fairly good agreement with our maximum annual emission rate. However, it appears to be an overestimation as about ~97% of the total emission of *Bange et al.* [1996] is contributed by the highest flux producing monsoon season (July-August) in six months and the rest is the contribution from the lowest flux producing summer season (May) in another six months. This study also shows that the Arabian Sea contributes significantly to the N_2O emission by 13-17% of the net global oceanic contribution of about 4.4 Tg N_2O yr^{-1} [*Nevison et al.*, 1995], despite the fact that it covers only about 1.7% of the total oceanic surface area.

Since the estimated emissions can vary with the selection of the gas transfer model, flux rates are also estimated using the transfer velocities calculated from other two proposed models [*Wanninkhof*, 1992; *Erickson*, 1993]. The calculated average N_2O fluxes for all the seasons and the estimated annual emissions are shown in Table 5.2. The relative contribution of the Arabian Sea to the total oceanic emission of N_2O remains nearly the same if its global sources are also calculated using a similar gas transfer model. Both these models give higher fluxes (up to about a factor of 1.8) than those computed using the model of *Liss and Merlivat* [1986]. As it is not clear which model would provide the realistic estimation, these results may indicate the probable ranges of the annual flux. However, such budgets need more refinements, because such variations/differences in the total oceanic source would change the global inventory of N_2O sources and its atmospheric budget quite significantly.

Table 5.2: *Average seasonal fluxes and annual emissions of N_2O from the Arabian Sea as calculated using various gas transfer models (LM 86: Liss and Merlivat [1986]; W 92: Wanninkhof [1992]; E 93: Erickson [1993]). In E 93 model, no whitecap coverage is considered due to its seldom occurrence and lack of proper information. The annual emissions are estimated using the four seasonal grids.*

Season	Average flux density (pg cm^{-2} s^{-1})		
	(LM 86)	(W 92)	(E 93)
Northeast Monsoon	0.26	0.45	0.50
Inter Monsoon	0.003	0.02	0.12
Southwest Monsoon 1995	0.51	0.92	0.56
Southwest Monsoon 1996	0.78	1.34	0.45
Annual Emission (Tg N_2O yr^{-1})	0.56	1.0	0.83
Global Emission (Tg N_2O yr^{-1}) [*Nevison et al.*, 1995]	4.4	8.0	6.0
% of Global Emission	12.7	12.5	13.9

5.4 CH_4 Emission from the Arabian Sea

5.4.1 Spatial and temporal variations in CH_4 distributions

Seasonal average of the CH_4 abundances in the marine air, at about 10 m height above the air-sea interface, are estimated to be 1.66±0.03, 1.74±0.1, 1.69±0.03, 1.72±0.08 (1 σ) ppmv during northeast monsoon, inter monsoon, southwest monsoon 1995, and southwest monsoon 1996, respectively. However, an average atmospheric abundance of 1.7 ppmv for CH_4 is used in the calculations of surface saturations for all the seasons. Surface water was found to be supersaturated with methane at most of the locations in all the seasons, despite the large spatial as well as seasonal variabilities. To study these variabilities, we distinguish four spatial regimes: I (from stas. 1 to 10; coastal), II (from stas. 11 to 20; open ocean), III (from stas. 21 to 29; open ocean), and IV (from stas. 30 to 36; coastal upwelling) like for N_2O as shown in Figure 5.2. The regional averages of surface saturations, ΔCH_4, transfer velocity, and estimated fluxes are given in Table 5.3.

The extent of supersaturation was lowest in inter monsoon and highest in southwest monsoon at all the locations except in regime II (open ocean) which exhibited a reverse trend. The average surface saturations are 140 ±

Table 5.3: *Seasonal and spatial distribution of methane fluxes and other related parameters estimated during April-May 1994 (SK 91), February-March 1995 (SK 99), July-August 1995 (SK 104), and August 1996 (SK 115).*

Stas.	Region	% Sat. (avg ± sd)	Δ CH_4 (avg ± sd)	K_w (cm h^{-1}) (avg ± sd)	Flux (pg cm^{-2} s^{-1}) (avg ± sd)	No. of obs.
Northeast monsoon: SK 99 (1995)						
4-10	I	187 ± 77	1.64 ± 1.3	6.87 ± 6.0	0.08 ± 0.087	8
11-20	II	138 ± 26	0.65 ± 0.5	6.27 ± 5.9	0.017 ± 0.019	12
22-29	III	196 ± 27	1.49 ± 0.4	11.5 ± 7.5	0.078 ± 0.063	5
30-35	IV	202 ± 19	1.58 ± 0.3	6.99 ± 3.4	0.048 ± 0.023	6
Mean		173 ± 54	1.12 ± 1.1	7.41 ± 6.1	0.049 ± 0.069	
Inter monsoon: SK 91 (1994)						
4-10	I	108 ± 26	0.13 ± 0.4	2.85 ± 2.2	-0.001 ± 0.004	5
15-11	II	166 ± 3	1.01 ± 0.1	0.41 ± 0.3	0.002 ± 0.001	5
34	III	192	0.82	0.82	0.005	1
Mean		140 ± 37	0.61 ± 0.6	1.59 ± 1.8	0.0006 ± 0.003	
Southwest monsoon: SK 104 (1995)						
0-4	I	205 ± 29	1.66 ± 0.5	24.24 ± 7.4	0.188 ± 0.095	5
15-20	II	96	-0.07	34.70	-0.01	2
21-29	III	222 ± 96	1.94 ± 1.5	13.43 ± 5.5	0.114 ± 0.083	7
32-35	IV	202 ± 19	1.62 ± 0.3	5.23 ± 3.1	0.036 ± 0.02	5
Mean		200 ± 74	1.59 ± 1.2	16.96 ± 10.8	0.093 ± 0.085	
Southwest monsoon: SK 115 (1996)						
10-14	IIA	325 ± 14	3.32 ± 2.3	23.3 ± 6.1	0.28 ± 0.004	5
15-17	IIB	147 ± 49	0.79 ± 0.8	16.6 ± 0.9	0.08 ± 0.099	3
Mean		234 ± 121	2.23 ± 2.0	24.8 ± 9.1	0.25 ± 0.25	

37, 173 ± 54, 200 ± 74, and 234 ± 121, respectively for northeast monsoon, inter monsoon, southwest monsoon 1995, and southwest monsoon 1996. Analogous to very low supersaturation of N_2O during inter monsoon, CH_4 surface saturations are also quite low, particularly in the coastal region compared to other two seasons (Table 5.3), indicating that the CH_4 concentrations in the surface water are also affected by diffusion/transport inhibition induced by summertime thermal stratification, in addition, a loss mechanism due to its oxidation is plausible to maintain such undersaturation. On the other hand, location II clearly reveals open ocean behaviour; considerably less %saturation compared to other regions in northeast monsoon and a negative/low supersaturation in southwest monsoon are observed, particularly, in southern part of the study area. The undersaturation during southwest monsoon is mainly arising due to the southwest monsoon wind pattern that

causes a local gradient in the wind stress resulting in the convergence of surface waters (downwelling) to the right of the Findlater Jet (FLJ) (south of $\approx 17^0$N) and partially caused by 'net' consumption of CH_4 due to its oxidation [*Ward et al.,* 1987] in presence of highest dissolved oxygen compared to those in other two seasons. This process can be even better understood by dividing the region II in two parts, one being the north of FLJ (IIA) and other being the south of FLJ (IIB), during southwest monsoon 1996 which has larger latitudinal coverage. The flux estimated from the region IIA is extremely high whilst that from region IIB is quite low, even though the gas transfer velocities are fairly comparable (see Table 5.3).

5.4.2 Seasonal variation and annual emission of CH_4

Average sea-to-air fluxes of 0.052 $\pm$ 0.049 (1 SD), 0.093 $\pm$ 0.085, and 0.25 $\pm$ 0.25 pg cm^{-2} s^{-1} are calculated, respectively, for northeast monsoon, southwest monsoon 1995, and southwest monsoon 1996, and almost no flux was experienced during inter monsoon for the whole Arabian Sea. The lower emission rates for inter monsoon result mainly due to very small transfer velocities and partly due to low surface supersaturation compared to those in northeast monsoon and southwest monsoons. During inter monsoon a net negative flux (-0.001 pg cm^{-2} s^{-1}) was observed in region I, in spite of being a coastal region which emanates highest ocean to atmosphere fluxes of 0.08$\pm$0.087 and 0.19$\pm$0.09 pg cm^{-2} s^{-1} in northeast monsoon and southwest monsoon, respectively. These flux values are, in general, lower than those calculated by *Owens et al.* [1991] which ranged from 0.085 to 0.26 pg cm^{-2} s^{-1}, however, they are comparable in the upwelling and coastal region, particularly during the northeast and southwest monsoons. High fluxes observed by *Owens et al.* [1991] are combined effect of higher supersaturations of methane in the surface water (average = 192$\pm$34%) and apparently higher average transfer velocity of 16.9 cm h^{-1}. Transfer velocities (the average $\pm$ 1σ) calculated from the *in situ* wind speeds during the present measurements are 7.4 $\pm$ 6.1, 1.6 $\pm$ 1.8, 16.9 $\pm$ 10.8, and 24.8 $\pm$ 9.1 cm h^{-1} in northeast monsoon, inter monsoon, and southwest monsoon 1995 and 1996, respectively.

Based on the spatial distributions of CH_4 fluxes obtained during these measurements, and previous assessmentas, it is apparent that coastal regions are the main sources of this gas to the atmosphere, about 75% of its global oceanic flux arising from the coastal regions [*Bange et al.,* 1994]. Therefore, the annual emissions of CH_4 are estimated by considering the

surface area of northern Arabian Sea (1.56×10^6) and the average of fluxes (see Figure 5.6) from the continental self/upwelling regions; 0.069, 0.008, and 0.114 pg cm^{-2} s^{-1}, respectively, during northeast monsoon, inter monsoon, and southwest monsoon 1995. As the average flux observed during southwest monsoon 1995 is much less (about a factor of 2.7) compared to southwest monsoon 1996, hence it is suggested that this estimation would result in a conservative annual emission of CH_4 to the atmosphere. A calculation of annual emission using the average flux value during southwest monsoon 1996 can be made to estimate the upper limit. The seasonal fluxes used in both the calculations are also shown in Figure 5.6. Large difference in CH_4 fluxes during the two southwest monsoons is essentially caused by the difference in transfer velocities in these periods.

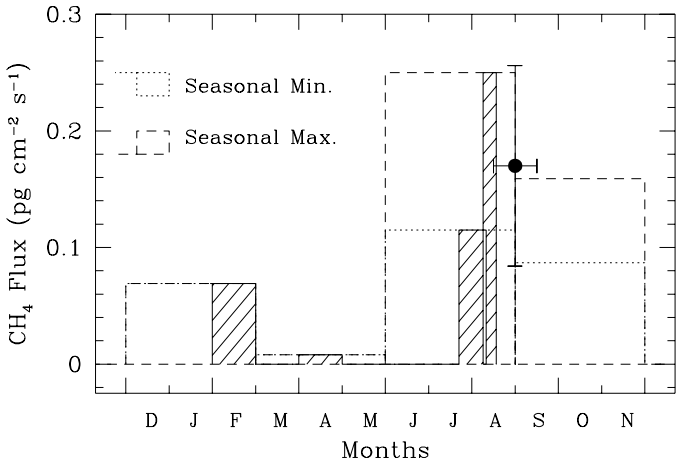

Figure 5.6: *Estimated seasonal fluxes of CH_4 used in the calculation of annual emissions (dashed line: to estimate the lower limit and dotted line: to estimate the upper limit). The only other available measurement of its sea-to-air fluxes [Owens et al., 1991] is also shown (filled circle) for better comparison (horizontal and vertical bars are representing the period of measurement and spread of the observed fluxes, respectively).*

Having four physico-chemically distinguished seasons in a year, viz. northeast monsoon (December-February), inter monsoon (March-May), southwest monsoon (June-August) and post monsoon (October-December), the annual emission of methane from the Arabian Sea can be estimated to be about 0.03 Tg yr^{-1} using the gas transfer model of *Liss and Merlivat* [1986]. In this assessment we interpolated a flux value for post monsoon period from those of southwest monsoon and northeast monsoon. This estimate is slightly lower than the only previous emission rate of 0.04 Tg yr^{-1} for the

Arabian Sea available during September-October 1986 [*Owens et al.*, 1991] using the same gas exchange model. Coastal region of the Arabian Sea covers about 0.43% of the total oceanic area and this estimate shows that it contributes about 0.3-0.5% to the total emission of 11 Tg CH_4 yr^{-1}, estimated using a similar gas transfer model from the global oceans [*Bange et al.,* 1994], suggesting this region to be a normal oceanic source of methane compared to Bay, Bight, river estuary and gulf regions [see *Bange et al.,* 1994 for details]. As seen from equations (5.3), (5.4), and (5.5), the gas transfer rates depend quite differently on the wind speeds and sea surface conditions which prompted us to estimate the annual CH_4 emissions using the latter two gas exchange models. Table 5.4 (see next page) shows the annual emissions of CH_4 estimated using different gas transfer models leading to variation in its evasion rates, however, such variations cannot significantly influence the global budget of CH_4 [*Patra et al.,* 1997b].

Table 5.4: *Average seasonal fluxes and annual emissions of CH_4, from the northern Arabian Sea (1.56×10^6 km^2, 0.43% of the total surface area of oceans) representing mainly the upwelling area, calculated using various gas transfer models: LM 86 [Liss and Merlivat, 1986], W 92 [Wanninkhof, 1992], and E 93 [Erickson, 1993].*

Season	Average flux density (pg cm^{-2} s^{-1})		
	(LM 86)	(W 92)	(E 93)
Northeast Monsoon	0.069	0.093	0.098
Inter Monsoon	0.008	0.006	0.04
Southwest Monsoon 1995	0.114	0.192	0.123
Southwest Monsoon 1996	0.252	0.425	0.137
Annual Emission (Tg CH_4 yr^{-1})	0.034-0.059	0.053-0.095	0.045-0.048
Gobal Emission (Tg CH_4 yr^{-1}) [*Bange et al.*, 1994]	11		18
% of Global Emission	0.3-0.5		0.25-0.27

Chapter 6

Summary and Future Scope

Vertical distributions of atmospheric trace gases have been measured with the help of balloone-borne cryogenic air sampler and detailed study of various chemical and dynamical parameters has been carried out utilizing a number of theoretical frame works. Assessments of the fluxes of N_2O and CH_4 from the Arabian Sea is also made based on extensive measurement in three seasons (four cruises).

Ambient air samples, collected during a balloon flight on April 16, 1994 carrying the cryogenic whole air sampler, are analyzed at PRL for large number of trace gases which include CH_4, N_2O, SF_6, and various halocarbons. Analyses are made by using various gas chromatographic techniques like GC-FID, GC-ECD and GC-MS, and IR absorption technique. The vertical distribution profiles of chemical tracers such as CH_4, N_2O, and CFC-12 compare quite well with theoretical simulations using the MPIC 2D chemistry-transport model, and exhibit discernible and intriguing features in the stratosphere while compared to the earlier measurements on March 27, 1987 and April 9, 1990 carried out in collaboration with MPAE. However, due to smaller photochemical lifetimes, the vertical profiles of CFC-11 and halons on April 16, 1994 do not show any characteristic difference from the previous measurements over the same location, despite the increase in their loading into the stratosphere. It is, in general, observed that the tropospheric growth rates of gases such as CFCs and halons during the period 1990-1994 are lower than those were estimated during 1987-1990. This reduction in the growth rates is the effect of curtailed use of ozone depleting substances under regulation by the Montreal Protocol and its amendments.

Stratospheric distributions of the long-lived (photochemical lifetime

of the order of or higher than that of dynamical lifetime) gases such as N_2O, CFC-12 observed over Hyderabad and reference profiles for the midlatitude have been used to estimate vertical eddy diffusion coefficients. These eddy profiles showed large variations on the balloon flight days. Richardson numbers are calculated using the *in situ* horizontal winds to study the formation and persistence of turbulent layers leading to eddy mixing. Based on these estimates two k_z profiles giving lower and higher ranges have been proposed for the equatorial region. The lower k_z values range from $\sim 9\times10^3$ cm^2s^{-1} at around 23 km to $\sim 4.2\times10^4$ cm^2s^{-1} at 38 km, and the upper limit is nearly constant at a value of $\approx 7\times10^4$ cm^2s^{-1} in the entire stratosphere.

Vertical distribution of SF_6 is measured on April 16, 1994. Its very small atmospheric loss, which has been shown by using improved NASA/GSFC 2D model results, in contrast to the previous studies. In addition, rapid increase in its atmospheric burden combine to make sulphur hexafluoride extremely useful to study the tropospheric and stratospheric dynamical processes. The vertical distribution measured from Hyderabad shows a transition layer between the tropopause and 27 km height. Above the transition layer the age of the air is found to vary from 4.1 to 4.6 years which are the least for this altitude region compared to any other latitude and suggests an efficient transport from the troposphere to the stratosphere through the tropical tropopause. An atmospheric lifetime of about 1937 years has been calculated from stratospheric mixing ratio interrelationships of SF_6 with simultaneously observed vertical distributions of N_2O and CFC-12.

An inter comparison of in situ measurements of CH_4 with the MPIC 2D model results show that while the April 16, 1994 profile is "normal", previous measurements made on 27 March, 1987 and April 9, 1990 are dynamically disturbed. The satellite-borne HALOE observations of CH_4 profiles also show large changes in stratospheric concentrations near this location. Estimated "age" of stratospheric air (inferred from SF_6 measurements) on March 27, 1987 and April 16, 1994 indicate the presence of older air around 25 km on March 27, 1987 than on April 16, 1994. Inter-correlations of simultaneously measured mixing ratios of CH_4 with N_2O and CFC-12 also suggest that the chemical constituents which are in slope equilibrium are affected more due to mixing. These two results strongly support intrusion of air at lower stratospheric heights from the extra-tropical regions on March 27, 1987 and April 9, 1990.

Acquired knowledge about the vertical profiles from the simultaneous *in situ* measurements of most of the trace constituents and accurate estimations of the transport time required for an air parcel to reach any

stratospheric altitude region are used to study the partitioning of chlorine and bromine compounds into their organic and inorganic forms due to their photochemical losses in the stratosphere. This estimate shows a large increase in inorganic chlorine (Cl_y) in the stratosphere from 1987 to 1994. The Cl_y abundances are estimated to be about 2200, 2700, and 3000 pptv in 1987, 1990, and 1994, respectively, at an altitude corresponding to N_2O mixing ratio of 100 ppbv ($\approx$35 km under normal stratospheric conditions in the tropics). Abundances of Cl_y increases with increasing latitude and altitude.

Estimation of fluxes of N_2O, and CH_4 from one of their natural source is also important as it can reduce the uncertainty prevailing in their atmospheric budgets. To identify the relative strength of the sources in question measurements of these gases are made during four ship cruises in different seasons in the Arabian Sea. Annual emission of N_2O is found to vary from 0.56 to 0.76 Tg N_2O per year from the Arabian Sea which constitute about 13-17% of the total oceanic contribution to the atmosphere, although it covers only about 1.47% of the world oceanic area. Emission of CH_4 from the Arbian Sea is estimated to be 0.3-0.5% (only from the coastal region) of the global oceanic source into the atmosphere. Natural sources of CH_4 from the oceans can be neglected without any significant perturbation to its annual budgets as this particular source constitute less than a percent to its total.

In spite of its important role, the tropical region is least probed for atmospheric measurements. There is a need for better understanding of the physical and chemical processes in the equatorial troposphere and stratosphere. The impact of phase out of several CFCs and introduction of new substitutes demands a long term study of this region. Some of the specific problems are described below.

- Climatology of the vertical profiles of atmospheric trace gases is still sparse in the tropical region. In addition, to study the modulations in the vertical profiles due to the phasing out of ozone depleting substances as per the Montreal protocol and its amendments, regular balloon experiments at suitable intervals should be conducted from Hyderabad. Present estimate indicates that the net stratospheric abundance of effective inorganic halogen would peak by the end of this century. Extremely high tropospheric growth rates of the CFC-substitutes also underscore the need for stratospheric observations to study their atmospheric impact.
- It will be extremely useful to construct eddy diffusion profiles using different technique e.g. Indian Mesosphere-Stratosphere-Troposphere

(MST) radar, established at Gadanki near Tirupati (13.5^0N, 79.2^0E), to overcome some of the existing uncertainties in k_z profiles. It is further advantageous that this system can also provide comprehensive measurements of vertical and horizontal winds. A simple 1 D model can be developed which will be capable of handling both eddy diffusion and vertical wind. These ST mode measurements are also suggested to provide useful informations on troposphere-stratosphere exchange processes.

- Although it is difficult to envisage a downward transport in the tropical stratosphere, there are evidences of descent of air relative to the mean stratospheric circulation over the equatorial region, e.g. in the westerly shear zone of the quasi-biennial oscillation (QBO). The quasi-vertical mixing discussed in §3.3 needs to be studied in greater detail in the light of the zonal wind variations over Hyderabad.

- MPIC 2D model can be used to study the heterogeneous chemistry near the cold tropical tropopause region. The temperature of tropical tropopause ($\sim 190^0$K) is comparable to that of the polar winter, hence, there can also be significant depletion of ozone due to heterophase chemistry in the presence of larger amount of halogen atoms released in the upper troposphere from the CFC substitutes, mainly HCFC-141b and HCFC-142b which exhibit large tropospheric increase in the last couple of years.

- Satellite measurements are providing global coverage of a number of atmospheric parameters (e.g. scientific payloads on UARS and ADEOS) and long-term trends of various changing constituents, particularly in the stratosphere and above. There is also a need to make global tropospheric measurements to study the troposphere-stratosphere coupling, trends for greenhouse gases, transport and transformations of various pollutants emitted from the Earth's surface etc.

Bibliography

Andrews, D.G., J.R. Holton, and C.B. Leovy, *Middle Atmosphere Dynamics*, Academic Press, San Diego, Calif., 498 pp., 1987.

Anderson, J.G., W.H. Brune, and M.H. Proffitt, Ozone destruction by chlorine radicals within the Antarctic vortex: The spatial and temporal evolution of ClO-O_3 anticorrelation based on in situ ER-2 data, *J. Geophys. Res., 94*, 11,465-11,479, 1989.

Atkinson, L.P., and F.A. Richards, The occurrence and distribution of methane in the marine environment, *Deep-Sea Res., 14*, 673-684, 1967.

Bange, U.H. Bartell, H.W., S. Rapsomanikis, and M.O. Andrae, Methane in the Baltic and North Seas and a reassessment of the marine emissions of methane, *Global Biogeochem. Cycles, 8*, 465-480, 1994.

Bange, H.W., S. Rapsomanikis, and M.O. Andrae, Nitrous oxide emissions from the Arabian Sea, *Geophys. Res. Lett., 23*, 3175-3178, 1996.

Bates, D.R, and M. Nicolet, The photochemistry of atmospheric water vapor, *J. Geophys. Res., 55*, 301-327, 1950.

Beig, G., Some experimental and theoretical studies of electrical and dynamical parameters of the middle atmosphere, *Ph.D. Thesis*, Physical Research Laboratory, Sukhadia University, India, 103-124, 1989.

Bischof, W., R. Borchers, P. Fabian, and B.C. Krüger, Increased concentration and vertical distribution of carbon dioxide in the stratosphere, *Nature, 316*, 708-710, 1985.

Blix, T.A. In-situ studies of turbulence and mixing: problems and questions, *Coupling Processes in the Lower and Middle Atmosphere,* Ed. E. V. Thrane, T. A. Blix and D. C. Fritts, Kluwer Acad. Pub., 329-344, 1993.

Borchers, R., P. Fabian, O.N. Singh, S. Lal, and B.H. Subbaraya, The vertical distribution of source gases at tropical latitudes, *Proc. of the Quadrennial Ozone Symposium 1988 and Tropospheric Ozone Workshop*, Ed., R.D. Bojkov and P. Fabian, A. Deepak Publishing, 290-293, 1989.

Bouwman, A.F., C. Kroeze, and J.A. Taylor, On sources and atmospheric concentrations of nitrous oxide, *Global Change: IGAC newsletter, 6*, 10-12, 1996.

Brasseur, G., and S. Solomon, *Aeronomy of the middle atmosphere,* D. Reidel Publishing Co., Dordrecht, 2nd Ed., 452 pp., 1986.

Brasseur, G., and P.C. Simon, Stratospheric chemical and thermal response to long-term variability in solar UV irradiance, *J. Geophys. Res., 86,* 7343-7362, 1981.

Brewer, A.W., Evidence for a world circulation provided by measurements of helium and water vapor distribution in the stratosphere, *Quart. J. Roy. Meteorol. Soc., 75*, 351-360, 1949.

Brühl, C., and P.J. Crutzen, Scenarios of possible changes in atmospheric temperatures and ozone concentrations due to man's activities, estimated with a one-dimensional coupled photochemical climate model, *Climate Dynamics, 2,* 173-203, 1988.

Brühl, C., and P.J. Crutzen, On the disproportionate role of tropospheric ozone as a filter against solar UV-B radiation, *Geophys. Res. Lett., 16*, 703-706, 1989.

Butler, J.H., and J.W. Elkins, An automated technique for the measurement of dissolved N_2O in natural water, *Mar. Chem., 34*, 47-61, 1991.

Butler, J.H., J.W. Elkins, B.D. Hall, S.O. Cummings, and S.A. Montzka, A decrease in the growth rates of atmospheric halon concentrations, *Nature, 359,* 403-405, 1992.

Chakrabarty, D.K., G. Beig, J.S. Sidhu, H. Chakrabarty, R. Narayanan, N.K. Modi, S.R. Das, and P. Chakrabarty, Measurement of the eddy diffusion coefficient of the middle atmosphere from a balloon at low latitude, *J. Atmos. Terr. Phys., 49*, 975-980, 1987.

Chapman, S., A theory of upper atmospheric ozone, *Quart. J. Roy. Meteorol. Soc., 3,* 103-125, 1930.

Cicerone, R.J., L. E. Heidt, and W. H. Pollock, Measurements of atmospheric methyl bromide and bromoform, *J. Geophys. Res., 93*, 3745-3749, 1988.

Crutzen, P.J., The influence of nitrogen oxide on the atmospheric ozone content, *Quart. J. Roy. Met. Soc., 96*, 320-325, 1970.

Crutzen, P.J., and F. Arnold, Nitric acid cloud formation in the cold Antarctic atmosphere: A major cause for springtime 'ozone hole', *Nature, 324,* 651-655, 1986.

Crutzen, P.J., Tropospheric ozone: an overview, in *Tropospheric ozone*, I.S.A. Isaken, editor, Reidel Dordrecht, 3-32, 1988.

Cunnold, D.M., R.F. Weiss, R.G. Prinn, D. Hartley, P.G. Simmonds, P.J. Fraser, B. Miller, F.N. Alyea, and L. Porter, GAGE/AGAGE measurements indicating reduction in global emissions of $CFCl_3$ and CF_2Cl_2 in 1992-1994, *J. Geophys. Res., 102*, 1259-1269, 1997.

Damle, S.V., G.S. Gokhale, and R.T. Redkar, Present status and new trends in scientific ballooning in India, *Adv. Space Res., 3*, 101-104, 1983.

Daniel, J.S., S.M. Schauffler, W.H. Pollock, S. Solomon, A. Weaver, L.E. Heidt, R.R. Garcia, E.L. Atlas, and J.F. Vedder, On the age of stratospheric air and inorganic chlorine and brimone release, *J. Geophys. Res., 101*, 16,757-16,770, 1996.

Danilov, A.D., and U.A. Kalgin, Seasonal and latitudinal variations of eddy diffusion coefficient in the mesosphere and lower thermosphere, *J. Atmos. Terr. Phys., 54*, 1481-1489, 1992.

DeMoore, W.B., S.P. Sander, D.M. Golden, R.F. Hampson, M.J. Kurylo, C.J. Howard, A.R. Ravisankara, C.E. Kolb, and J.J. Molina, Chemical kinetics and photochemical data for use in stratospheric modeling, *JPL Publication, 92-20*, Jet Prop. Lab., Pasadena CA, USA, 1992.

Dlugokencky, E.J., K.A. Masarie, P.M. Lang, P.P. Tans, L.P. Steele, and E.G. Nisbet, A dramatic decrease in the growth rate of atmospheric methane in the northern hemisphere during 1992, *Geophys. Res. Lett., 21*, 45-48, 1994.

Dobson, G.M.G., Origin and distribution of polyatomic molecules in the atmosphere, *Proc. Roy. Soc. Lond. A, 236*, 187-199, 1956.

Ehhalt, D.H, *In situ* observations, *Phil. Trans. R. Soc. Lond. A, 296*, 175-189, 1980.

Elkins, J.W, T.M. Thompson, T.H. Swanson, J.H. Butler, B.D. Hall, S.O. Cummings, D.A. Fisher, and A.G. Raffo, Decrease in growth rates of atmospheric chlorofluorocarbons 11 and 12, *Nature, 364*, 780-783, 1993.

Erickson, D.J, A stability dependent theory for air-sea gas exchange, *J. Geophys. Res., 98*, 8471-8488, 1993.

Fabian P., Atmospheric Sampling, *Adv. Space Res, 1*, 17-27, 1981.

Fabian, P., R. Borchers, S.A. Penkett, and N.D. Prosser, Halocarbons in the stratosphere, *Nature, 294,* 733-735, 1981.

Fabian, P., R. Borchers, H. Duscha, B.C. Krüger, S. Lal, and B.H. Subbaraya, $CHClF_2$ (CFC-22): distribution, budget and environmental impact, *Proc. of the Quadrennial Ozone Symposium 1988 and Tropospheric Ozone Workshop*, Ed., R.D. Bojkov and P. Fabian, A. Deepak Publishing, 294-297, 1989.

Fabian, P., R. Borchers, and U. Schmidt, Proposed reference models for CO_2 and halogenated hydrocarbons, *Adv. Space Res., 18,* (9/10)145-153, 1996.

Farman, J.C., B.G. Gardiner and J.D. Shanklin, Large losses in total ozone in Antarctica reveals ClO_x/NO_x interaction, *Nature, 315*, 207-210, 1985.

Fraser, P., M. Gunson, S. Penkett, F.S. Rowland, U. Schmidt, and R. Weiss, Measurements (Chapter 1), in *Report on concentrations, lifetimes, and trends of CFCs, Halons, and related species, NASA Ref. Pub. 1339,* 1994.

Fukao, S., M.D. Yamanaka, N. Ao, W.K. Hocking, T. Sato, M. Yamamoto, T. Nakamura, T. Tsuda, and S. Kato, Seasonal variability of vertical eddy diffusivity in the middle atmosphere 1. Three-year observations by the middle and upper atmosphere radar, *J. Geophys. Res., 99*, 18,973-18,987, 1994.

Garcia, R.R., and S. Solomon, A numerical model of the zonally averaged dynamical and chemical structure of the middle atmosphere, *J. Geophys. Res., 88*, 1379-1400, 1983.

Gidel, L.T., P.J. Crutzen, and J. Fishman, A two-dimensional photochemical model of the atmosphere 1: chlorocarbon emissions and their effect on stratospheric ozone, *J. Geophys. Res., 88*, 6622-6640, 1983.

Goldan, P.D., W.C. Kuster, D.L. Albritton, and A.L. Schmeltekopf, Stratospheric $CFCl_3$, CF_2Cl_2, and N_2O height profile measurements at several latitudes, *J. Geophys. Res., 85*, 413-423, 1980.

Hall, T.M, and R.A. Plumb, Age as a diagnostic of stratospheric transport, *J. Geophys. Res., 99*, 1059-1070, 1994.

Hanson, D.R., A.R. Ravishankara, and S. Solomon, Heterogeneous reactions in sulfuric acid aerosols: A framework for model calculations, *J. Geophys. Res., 99*, 3615-3629, 1994.

Harnisch, J., R. Borchers, P. Fabian, and M. Maiss, Tropospheric trends for CF_4 and C_2F_6 since 1982 derived from SF_6 dated stratospheric air, *Geophys. Res. Lett., 23*, 1099-1102, 1996.

Hofmann, D.J., The 1996 Antarctic ozone hole, *Nature, 383,* 129, 1996.

Holton, J.R., A dynamically based transport parameterization for one-dimensional photochemical models of the stratosphere, *J. Geophys. Res., 91*, 2681-2686, 1986.

Holton, J.R., P. H. Haynes, M.E. McIntyre, A.R. Douglass, R.B. Rood, and L. Pfister, Stratosphere-troposphere exchange, *Rev. Geophys., 33*, 403-439, 1995.

Intergovernmental Panel on Climate Change (IPCC), *Climate Change 1995,*, University Press, Cambridge, Great Britain, 1996.

Jackman, C.H., E.L. Fleming, S. Chandra, D.B. Considine, and J.E. Rosenfield, Past, present, and future modeled ozone trends with comparisons to observed trends, *J. Geophys. Res., 101*, 28,753-28,767, 1996.

Joshi, M.N., Balloon flight operations, *Indian J. Radio Space Phys., 20*, 176-181, 1991.

Khalil, M.A.K., R.A. Rasmussen, and R. Gunawardena, Atmospheric Methyl Bromide: Trends and Global Mass Balance, *J. Geophys. Res., 98*, 2887-2896, 1993.

Khalil, M.A.K., and R.A. Rasmussen, The changing composition of the Earth's atmosphere, in *Composition, Chemistry, and Climate of the Atmosphere*, edited by H. B. Singh, Van Nostrand Reinhold, New York, 50-87, 1995.

Ko, M.K.W., N.D. Sze, W.C. Wang, G. Shia, A. Goldman, F.J. Murcray, D.G. Murcray, and C.T. Rinsland, Atmospheric sulfur hexafluoride: Sources, sinks, and greenhouse warming, *J. Geophys. Res., 98*, 10,499-10,507, 1993.

Kourtidis, K., R. Borchers, and P. Fabian, Dibromomethane (CH_2Br_2) measurements at the upper troposphere and lower stratosphere, *Geophys. Res. lett., 23*, 2581-2583, 1996.

Krueger, A.J., and R.A. Minzner, A mid-latitude model for the 1976 U.S. Standard atmosphere,, *J. Geophys. Res., 81*, 4477-4480, 1976.

Kumar, S. P., and T. G. Prasad, Winter cooling in the northern Arabian Sea, *Curr. Sci., 71*, 834-841, 1996.

Lal, S., R. Borchers, and B.C. Krüger, Increasing abundance of $CBrClF_2$ in the atmosphere, *Nature, 316*, 135-136, 1985.

Lal, S., R. Borchers, P. Fabian, P.K. Patra and B.H. Subbaraya, Vertical distribution of methyl bromide over Hyderabad, India, *Tellus, 46B*, 373-377, 1994.

Lal, S., B.H. Subbaraya, P. Fabian, and R. Borchers, Vertical distribution of CH_4 and N_2O over the tropical site Hyderabad, *Proc. of the Quadrennial Ozone Symposium 1992*, Virginia, 823-826, 1994a.

Lal, S., Y.B. Acharya, P.K. Patra, P. Rajaratnam, B.H. Subbaraya, and S. Venkataramani, Balloon-borne cryogenic air sampler experiment for the study of atmospheric trace gases, *Indian J. Radio Space Phys., 25*, 1-7, 1996.

Lal, S., P.K. Patra, S. Venkataramani, and M.M. Sarin, Distribution of nitrous oxide and methane in the Arabian Sea, *Curr. Sci., 71*, 894-899, 1996a.

Lal, S., and P.K. Patra, Variability in the fluxes of nitrous oxide in the Arabian Sea, submitted to *Global Biogeochem. Cycle*, 1997.

Law, C.S. and J.P. Owens, Significant flux of atmospheric nitrous oxides from the northwest Indian ocean, *Nature, 346*, 826-828, 1990.

Liou, K.N., An introduction to atmospheric radiation, Academic Press, Inc., San Diego, pp. 392, 1980.

Liss, P.S., and L. Merlivat, Air_sea gas exchange rates: introduction and synthesis. In: *The Role of Air_Sea Exchange in Geochemical Cycling*, P Baut-Menard, editor, N.A.T.O.A.S.I Series, vol. 185, pp. 113-128, 1986.

Lobert, J.M., J.H. Butler, S.A. Montzka, L.S. Geller, R.C. Myers, and J.W. Elkins, A net sink for atmospheric CH_3Br in the east Pacific Ocean, *Science, 267*, 1002-1005, 1995.

London, J., In *Proc. of the NATO Advance Study Institute on Atmospheric Ozone: its variation and human influences (Portugal), FAA-EE-80-20*, M. Nicolet and A.C. Aikin (Eds.), Washington, D.C., 1980.

Lovelock, J.E., Atmospheric fluorine compounds as indicator of air movements, *Nature, 230*, 379, 1971.

Lueb, R.A., D.H. Ehhalt, and L.E. Heidt, Balloon-borne low temperature air sampler, *Rev. Sci. Insrtum., 41*, 702-705, 1975.

Maiss, M., L.P. Steele, R.J. Francey, P.J. Fraser, R.L. Langenfelds, N.B.A. Trivett, and I. Levin, Sulfur hexafluoride: A powerful new atmospheric tracer, *Atmos. Environ., 30*, 1621-1629, 1996.

Massie, S.T., and D.M. Hunten, Stratospheric eddy diffusion coefficients from tracer data. *J. Geophys. Res., 86*, 9859-9868, 1981.

McAullife, C., GC determination of solutes by multiple phase equilibrium, *Chem. Technol., Jan.*, 46-51, 1971.

McElroy, M.B., S.C. Wofsy, J.E. Penner, and J. McConnell, Atmospheric ozone : Possible impact of stratospheric aviation, *J. Atmos. Sci., 31*, 287-300, 1974.

McElroy, M.B., R.J. Salawitch, S.C. Wofsy, and J.A. Logan, Reduction of Antarctic ozone due to synergictic interactions of chlorine and bromine, *Nature, 321*, 759-762, 1986.

McGrath, W.D., and R.G.W. Norrish, Influence of water on the photolytic decomposition of ozone, *Nature, 182,* 235, 1958.

Minschwaner, K., A.E. Dessler, J.W. Elkins, C.M. Volk, D.W. Fahey, M. Loewenstein, J.R. Podolske, A.E. Roche, and K.R. Chan, Bulk properties of isentropic mixing into the tropics in the lower stratosphere, *J. Geophys. Res., 101*, 9433-9439, 1996.

Molina, J.S., and F.S. Rowland, Stratospheric sink for chlofluoromethanes: Chlorine atom-catalized destruction of ozone, *Nature, 249*, 810-812, 1974.

Montzka, S.A., J.H. Butler, R.C. Myers, T.M. Thompsom, T.H. Swanson, A.D. Clarke, L.T. Lock, and J.W. Elkins, Decline in the tropospheric abundance of halogen from halocarbon: implications of stratospheric ozone depletion, *Science, 272*, 1318-1322, 1996.

Naqvi, S.W.A. and R.J. Noronha, Nitrous oxide in the Arabian Sea. *Deep Sea Res., 38*, 871-890, 1991.

NAS, Stratospheric ozone depletion by halocarbons: Chemistry and Transport, National Academy of Sciences, Washington D C, 1979.

Nevison, C.D., R.F. Weiss, D.J. Erickson III, Global oceanic emissions of nitrous oxide, *J. Geophys. Res., 100*, 15,809-15,820, 1995.

Nicolet, M., Stratospheric ozone: An introduction to its study, *Rev. Geophys. Space Phys., 5,* 593-636, 1975.

Nicolet, M., On the molecular scattering in the terrestrial atmosphere: An empirical formula for its calculation in the homosphere, *Planet. Space Sci., 32*, 1467-1468, 1984.

Nicolet, M., Solar irradiances with their diversity between 120 and 900 nm, *Planet. Space Sci., 37*, 1249-1289, 1989.

Oram, D.E., C.E. Reeves, S.A. Penkett, and P.J. Fraser, Measurements of HCFC-141b and HCFC-142b in the Cape Grim air archive: 1978-1993, *Geophys. Res. lett., 22*, 2741-2744, 1995.

Owens, N.J.P., C.S. Law, R.F.C. Mantoura, P. Burkill, and C.A. Llewellyn, Methane flux to the atmosphere from the Arabian Sea, *Nature, 354*, 293-296, 1991.

Patra, P.K., and S. Lal, Variability of eddy diffusivity in the stratosphere deduced from vertical distributions of N_2O and CFC-12, *J. Atmos. Terr. Phys., 59*, 1149-1157, 1997.

Patra, P.K., S. Lal, B.H. Subbaraya, C.H. Jackman, and P. Rajaratnam, Observed vertical profile of sulphur hexafluoride (SF_6) and its atmospheric applications, *J. Geophys. Res., 102*, 8855-8859, 1997a.

Patra, P.K., S. Lal, S. Venkataramani, M. Gauns, and V.V.S.S. Sarma, Seasonal variability in distribution and fluxes of methane in the Arabian Sea, Submitted to *J. Geophys. Res.,* 1997b.

Patra, P.K., S. Lal, S. Venkataramani, S.N. de Sousa, V.V.S.S. Sarma, and S. Sardesai, Seasonal and spatial variability in N_2O distribution in the Arabian Sea, Submitted to *Deep-Sea Res.*, 1997c.

Patra, P.K., S. Lal, P.J. Crutzen, and C. Brühl, Vertical profiles of CH_4: evidence of quasi-vertical exchange in the tropical stratosphere, Unpublished manuscript, 1997d.

Plumb, R.A., and M.K.W. Ko, Interrelationships between mixing ratios of long-lived stratospheric constituents, *J. Geophys. Res., 97*, 10,145-10156, 1992.

Plumb, R.A, A "tropical pipe" model of stratospheric transport, *J. Geophys. Res., 101*, 3957-3972, 1996.

Pollock, W.H, L.E. Heidt, R.A. Lueb, J.F. Vedder, M.J. Mills, and S. Solomon, On the age of stratospheric air and ozone depletion potentials in polar regions, *J. Geophys. Res., 97*, 12,993-12,999, 1992.

Ramachandran, S., A. Jayaraman, Y.B. Acharya, and B.H. Subbaraya, Balloon-borne photometric studies of the stratospheric aerosol layer after Mt. Pinatubo eruption, *J. Geophys. Res., 99*, 16,771-16,777, 1994.

Ramaswamy, V., M.D. Schwarzkopf, and K.P. Shine, Radiative forcing of climate from halocarbon-induced global stratospheric ozone loss, *Nature, 355*, 810-812, 1992.

Ravishankara, A.R., S. Solomon, A.A. Turnipseed, and R.F. Warren, Atmospheric lifetimes of long-lived halogenated species, *Science, 259*, 194-199, 1993.

Reeburgh, W.S., Global methane budget studies, *Global Change: IGAC newsletter, 6*, 6-9, 1996.

Reeves, C.E. and S.A. Penkett, An estimate of the anthropogenic contribution to methyl bromide, *Geophys. Res. Lett., 20*, 1563-1566, 1993.

Rinsland, C.P., M.R. Gunson, M.C. Abrams, L.L. Lowes, R Zander, and E. Mathieu, ATMOS/ATLAS 1 measurements of sulphur hexafluoride (CF_6) in the lower stratosphere and upper troposphere, *J. Geophys. Res., 98*, 20,491-20,494, 1993.

Roche, A.E., J.B. Kumer, R.W. Nightingale, J.L. Mergenthaler, G.A. Ely, P.L. Bailey, S.T. Massie, J.C. Gille, D.P. Edwards, M.R. Gunson, M.C. Abrams, G.C. Toon, C.R. Webster, W.A. Traub, K.W. Jucks, D.G. Johnson, D.G. Murcray, F. H. Murcray, A. Goldman, and E. C. Zipf, Validation of CH_4 and N_2O measurements by the cryogenic limb array etalon spectrometer instrument on the Upper Atmosphere Research Satellite, *J. Geophys. Res., 101*, 9679-9710, 1996.

Rundel, W.C., J.C. Gille, A.E. Roche, J.B. Kumar, J.L. Mergenthaler, J.W. Waters, E.F. Fishbein, and W.A. Lahoz, Stratospheric transport from the tropics to middle latitudes by planetary-wave mixing, *Nature, 365*, 533-535, 1993.

Russell, J.M., L.L. Gordley, J.H. Park, S.R. Drayson, W.D. Hesketh, R.J. Cicerone, and P.J. Crutzen, The Halogen Occultation Experiment, *J. Geophys. Res., 98*, 10,777-10,979, 1993.

Sander, R., and P.J. Crutzen, Model study indicating halogen activation and ozone destruction in polluted air masses transported to the sea, *J. Geophys. Res., 101*, 9121-9138, 1996.

Sasi, M.N., and K. Sen Gupta, A reference atmosphere for indian equatorial zone from surface to 80 km - 1985, *Scientific Report*, *SPL:SR:006:85*, 1986.

Schmeltekopf, A.L., D.L. Albritton, P.J. Crutzen, P.D. Golda, W.J. Harrop, W.R. Henderson, J.R. McAfee, M. McFarland, H.I. Schiff, T.L. Thompson, D.J. Hofmann, and N.T. Kjome, Stratospheric nitrous oxide altitude profiles at various latitudes, *J. Atoms. Sci., 34*, 729-736, 1977.

Schmidt, U., and A. Khedim, In situ measurements of carbon dioxide in the winter arctic vortex and at mid latitudes: An indicator of the 'age' of stratospheric air, *Geophys. Res. Lett., 18*, 763-766, 1991.

Schoeberl, M.R., L.R. Lait, P.A. Newman, and J.E. Rosenfield, The structure of the polar vortex, *J. Geophys. Res., 97*, 7859-7882, 1992.

Schoeberl, M.R., M. Luo, J.E. Rosenfield, An analysis of the Antarctic Halogen Occultation Experiment trace gas observations, *J. Geophys. Res., 100*, 5159-5172, 1995.

Singh, H.B., and M. Kanakidou, An investigation of the atmospheric sources and sinks of methyl bromide, *Geophys. Res. Lett., 20*, 133-136, 1993.

Solomon, S., Progress towards a quantitative understanding of Antarctic ozone depletion, *Nature, 347*, 347-354, 1990.

Solomon, S., J.B. Burkholder, A.R. Ravishankara and R.R. Garcia, Ozone depletion and global warming potentials of CH_3I, *J. Geophys. Res., 99*, 20,929-20,935, 1994.

Stolarski, R.S. and R.J. Cicerone, Stratospheric chlorine: possible sink for ozone, *Cand. J. Chem., 52*, 1610, 1974.

Subbaraya, B.H., Vertical distribution of minor constituents in the tropical middle atmosphere, *Ind. J. Radio Space Phys., 16,* 25-25, 1987.

Wang, C., P.J. Crutzen, V. Ramanathan, S.F. Williams, The role of a deep convective storm over the tropical Pacific Ocean in the redistribution of atmospheric chemical species, *J. Geophys. Res., 100*, 11,509-11,516, 1995.

Wanninkhof, R., Relationship between wind speed and gas exchange over the ocean, *J. Geophys. Res., 97*, 7373-7382, 1992.

Ward, B.B., K.A. Kilpatrick, P.C. Novelli, and M.I. Scranton Methane oxidation and methane fluxes in the ocean surface layer and deep anoxic waters, *Nature, 327*, 226-229, 1987.

Waugh, D.W., T.M. Hall, W.J. Randel, P.J. Rasch, B.A. Boville, K.A. Boering, S.C. Wofsy, D.C. Daube, J.W. Elkins, D.W. Fahey, G.S. Dutton, C.M. Volk, and P.F. Vohralik, Three-dimensional simulations of long-lived tracers using winds from MACCM2, *J. Geophys. Res., in press*, 1997.

Weiss, R.F. and B.A. Price, Nitrous oxide solubility in water and seawater. *Mar. Chem., 8*, 347-359, 1980.

Wennberg, P.O, R.C. Cohen, R.M. Stimpfle, J.P. Koplow, J.G. Anderson, R.J. Salawitch, D.W. Fahey, E.L. Woodbridge, E.R. Keim, R.S. Gao, C.R. Webster, R.D. May, D.W. Toohey, L.M. Avallone, M.H. Profitt, M. Loewenstein, J.R. Podolske, K.R. Chan, and S.C. Wofsy, Removal of stratospheric O_3 by radicals: In situ measurements of OH, HO_2, NO, NO_2, ClO, and BrO, *Science, 266*, 398-404, 1994.

Weinstock, J., Gravity wave saturation and eddy diffusion in the middle atmosphere, *J. Atmos. Terr. Phys., 46*, 1069-1082, 1984.

Wofsy, S.C., M.B. McElroy, and Y.L. Yung, The chemistry of atmospheric bromine, *Geophys. Res. lett., 2*, 215-218, 1975.

Woodbridge, E.L., J.W. Elkins, D.W. Fahey, L.E. Heidt, S. Solomon, T.J. Baring, T.M. Gilpin, W.H. Pollock, S.M. Schauffler, E.L. Atlas, M. Loewenstein, J.R. Podolske, C.R. Webster, R.D. May, J.M. Gilligan, S.A. Montzka, K.A. Boering, and R.J. Salawitch, Estimates of total organic and inorganic chlorine in the lower stratosphere from in situ and flask measurements during AASE II, *J. Geophys. Res., 100*, 3057-3064, 1995.

Woodman, R.F. and P.K. Rastogi, Evaluation of effective eddy diffusive coefficients using radar observations of turbulence in the stratosphere, *Geophys. Res. Lett., 11*, 243-246, 1984.

World Meteorological Organization (WMO), Scientific assessment of ozone depletion: 1994, *Rep. 37*, Global Ozone Res. and Monit. Proj., Geneva, Switzerland, 1995.

Yamanaka, M.D., H. Tanaka, Multiple "Gust Layers" observed in the middle atmosphere, *Dynamics of the Middle Atmosphere*, Ed. J.R. Holton and T. Matsuno, Terra Sci. Pub. Co., 117-140, 1986.

Yvon-Lewis, S.A., and J.H. Butler, The potential effect of oceanic biological degradation on the lifetime of atmospheric CH_3Br, *Geophys. Res. lett., 24*, 1227-1230, 1997.

Zander, R., E. Mathieu, P.H. Demoulin, C.P. Rinsland, D.K. Weisenstein, M.K.W. Ko, N.D. Sze and M.R. Gunson, Secular evolution of the vertical column abundances of $CHClF_2$ (HCFC-22) in the earth's atmosphere inferred from ground-based IR solar observations at the Jungfraujoch and at Kit Peak, and comparison with model calculations, *J. Atmos. Chem., 18*, 129-148, 1994.

List of Publications

Lal, S., R. Borchers, P. Fabian, **P.K. Patra** and B.H. Subbaraya, Vertical distribution of methyl bromide over Hyderabad, India, *Tellus, 46B*, 373-377, 1994.

Lal, S., Y.B. Acharya, **P.K. Patra**, P. Rajaratnam, B.H. Subbaraya, and S.Venkataramani, Balloon-borne cryogenic air sampler experiment for the study of atmospheric trace gases, *Ind. J. Radio and Space Phys., 25*, 1-7, 1996.

Lal S., **P.K. Patra**, S. Venkataramani, and M.M. Sarin, Distribution of nitrous oxide and methane in the Arabian Sea, *Curr. Sci., 71*, 894-899, 1996.

Patra, P. K., S. Lal, B. H. Subbaraya, C. H. Jackman, and P. Rajaratnam, Observed vertical profile of sulphur hexafluoride (SF_6) and its atmospheric applications, *J. Geophys. Res., 102*, 8855-8859, 1997.

Patra, P. K., and S. Lal, Variability of eddy diffusivity in the stratosphere deduced from vertical distributions of N_2O and CFC-12, *J. Atmos. Terr. Phys., 59*, 1149-1157, 1997.

Patra, P. K., S. Lal, S. Venkataramani, S. N. de Sousa, V. V. S. S. Sarma, and S. Sardesai, Seasonal and spatial variability in N_2O distribution in the Arabian Sea, Under revision for *Deep-Sea Res.*, 1997a.

Patra, P. K., S. Lal, S. Venkataramani, S. P. Kumar, M. Gauns, and V. V. S. S. Sarma, Seasonal variability in distribution and fluxes of methane in the Arabian Sea, Accepted for publication in *J. Geophys. Res.*, 1997b.

Patra, P. K., S. Lal, P. J. Crutzen, and C. Brühl, Vertical profiles of CH_4: evidence of quasi-vertical exchange in the tropical stratosphere, Unpublished manuscript, 1997c.

Lal, S., and **P. K. Patra**, Variability in the fluxes of nitrous oxide in the Arabian Sea, Under revision for *Global Biogeochem. Cycle*, 1997.

Patra, P. K., S. Lal et al., Partitioning of Organic/inorganic chlorine and bromine in the tropical atmosphere, under preparatichlorine and bromine in the tropical atmosphere, under preparation.